

Electronic Thesis and Dissertation Repository

4-12-2012 12:00 AM

Vibration of Carbon Nano-Structures

Sina Arghavan
The University of Western Ontario

Supervisor
Professor Anand V. Singh
The University of Western Ontario

Graduate Program in Mechanical and Materials Engineering
A thesis submitted in partial fulfillment of the requirements for the degree in Doctor of
Philosophy
© Sina Arghavan 2012

Follow this and additional works at: <https://ir.lib.uwo.ca/etd>



Part of the [Computational Engineering Commons](#), and the [Nanoscience and Nanotechnology Commons](#)

Recommended Citation

Arghavan, Sina, "Vibration of Carbon Nano-Structures" (2012). *Electronic Thesis and Dissertation Repository*. 417.
<https://ir.lib.uwo.ca/etd/417>

This Dissertation/Thesis is brought to you for free and open access by Scholarship@Western. It has been accepted for inclusion in Electronic Thesis and Dissertation Repository by an authorized administrator of Scholarship@Western. For more information, please contact wlsadmin@uwo.ca.

**VIBRATION OF CARBON
NANO-STRUCTURES**

(Spine title: Vibration of Carbon Nano-Structures)
(Thesis format: Integrated Article)

by
Sina Arghavan

Graduate Program in Engineering Science
Department of Mechanical and Materials Engineering

A thesis submitted in partial fulfillment
of the requirements for the degree of
Doctor of Philosophy

The School of Graduate and Postdoctoral Studies
The University of Western Ontario
London, Ontario, Canada

© Sina Arghavan 2012

THE UNIVERSITY OF WESTERN ONTARIO
SCHOOL OF GRADUATE AND POSTDOCTORAL STUDIES

CERTIFICATE OF EXAMINATION

Chief Advisor

Dr. A. V. Singh

Advisory Committee Members

Dr. S. F. Asokanthan

Dr. R. Kelassen

Examiners

Dr. S. F. Asokanthan

Dr. O. R. Tutunea-Fatan

Dr. M. Singh

Dr. K. Behdinin

The thesis by

Sina Arghavan

entitled:

Vibration of Carbon Nano-Structures

is accepted in partial fulfillment of the

requirements for the degree of

Doctor of Philosophy

Date

Chair of the Thesis Examination Board

ABSTRACT

In this thesis, first the fundamental characterizations of carbon nano-structures and basic atomistic models of the carbon nanotubes and graphitic sheets are reviewed extensively. Different simulation methods used in this field of study are discussed critically. Advantages and shortfalls of each method are reported in detail. A new structural approach based on the lattice atomic structure is selected as an accurate and efficient model for simulating carbon nano-structures. This method is used comprehensively in the present work along with continuous shell and plate theories to study the mechanical and vibrational characteristics of single-walled carbon nanotubes and single and multi-layered graphene sheets. Covalent bonds are modeled using three-dimensional frame elements in finite element simulation. Nucleus of each carbon atom is considered as a node with concentrated mass and six degrees of freedom. Highly nonlinear van der Waals interactions between adjacent layers of graphitic sheets are modeled successfully and their true nonlinear nature is preserved. Free and forced vibrations are studied accordingly to investigate the natural frequencies and frequency spectrums. Mode shapes are obtained from eigen-analyses and results are compared with other methods available in the literature. Effects of size, atomic structure and boundary conditions on vibrational behaviors of these structures are studied in detail. Static analysis of single-layered graphene sheets is also carried out to obtain the Young's modulus of elasticity of graphitic sheets under various loading conditions. Two different continuous models are proposed for simulating the in-plane and transverse vibrations of graphene sheets. Results of the continuous models are compared with the lattice structure approach for rectangular, skewed and circular graphenes to show the accuracy of the models. Forced nonlinear vibration of multi-layered graphenes is investigated subsequently to study the effects of van der Waals interactions on the vibrational characteristics. Time-histories and fast

Fourier transforms are obtained for in-plane and transverse vibrations and effects of inter-layer interactions are studied in detail.

Keywords: Carbon nanotubes, graphene sheets, covalent bonds, van der Waals forces, lattice structure, frame element, vibration, natural frequency, mode shape.

CO-AUTHORSHIP

The articles presented in this thesis are published, presented or submitted in part or in full in the technical journals or conferences with the co-authorship of Professor Anand V. Singh. All the research, development, simulation and manuscript preparation were performed by Sina Arghavan under the supervision of Professor Anand V. Singh.

To my parents, Hengameh and Hassan,

for their patience, understanding and unconditional love;

and to my brother, Soroush, for being a better half.

*Though words have built this thesis that I dedicate to you, they cannot express my
gratitude enough.*

ACKNOWLEDGMENTS

I am heartily thankful to my supervisor, Professor Anand V. Singh, whose supervision, guidance and support from the initial to the final level enabled me to develop an understanding of the subject. He has supported me throughout my thesis with his patience and knowledge whilst allowing me the room to work in my own way. I attribute the level of my PhD degree to his encouragement and effort and without him this thesis, too, would not have been completed or written. One simply could not wish for a better or friendlier supervisor.

TABLE OF CONTENTS

CERTIFICATE OF EXAMINATION	ii
ABSTRACT	iii
CO-AUTHORSHIP	v
DEDICATION	vi
AKNOWLEDGEMENTS	vii
TABLE OF CONTENTS.....	viii
LIST OF TABLES	xi
LIST OF FIGURES	xii
LIST OF NOMENCLATURE.....	xvi

CHAPTER 1

1. Introduction to the Thesis	1
1.1. General introduction.....	1
1.2. Objective and scopes of this thesis.....	2
1.3. Outline of the thesis.....	3

CHAPTER 2

2. Vibration of Carbon Nano-Scale Structures: A Critical Review	6
2.1. Introduction	6
2.2. Structural and mechanical parameters of graphitic sheets	9
2.3. Mechanical properties of carbon nanotubes.....	14
2.4. Vibration of carbon nanotubes	20
2.4.1. Atomic scale simulations	20
2.4.2. Shell theories.....	22
2.4.3. Beam theories.....	24
2.4.4. Nonlocal theory of elasticity.....	26
2.5. Vibration of graphitic sheets	26
2.6. Concluding remarks	29
References	30

CHAPTER 3

3. On the Vibrations of Single-Walled Carbon Nanotubes.....	42
3.1. Introduction	42
3.2. Modeling procedure	46
3.3. Results and discussion.....	48
3.3.1. Case i: clamped-free zigzag single-walled carbon nanotube	50
3.3.2. Case ii: clamped-clamped zigzag single-walled carbon nanotube	57
3.3.3. Case iii: clamped-free armchair single-walled carbon nanotube	63
3.3.4. Case iv: clamped-clamped armchair single-walled carbon nanotube.....	67
3.4. Concluding remarks	71
Acknowledgement	72
References	72

CHAPTER 4

4. Mechanical Properties and Vibrational Characteristics of Graphenes.....	77
4.1. Introduction	77
4.2. Lattice structure method.....	79
4.3. Equivalent continuum plate method.....	81
4.4. Results and discussion.....	82
4.5. Concluding remarks	89
References	90

CHAPTER 5

5. Free Vibration of Single-Layered Graphene Sheets: Lattice Structure versus Continuum Plate Theories.....	94
5.1. Introduction	94
5.2. Methods of analysis.....	97
5.2.1. Lattice structure method of analysis	97
5.2.2. Equivalent continuum plate method	98
5.3. Results and discussion.....	100
5.4. Concluding remarks	107
References	110

CHAPTER 6

6. Nonlinear Vibration of Multi-Layered Graphene Sheets.....	114
6.1. Introduction	114
6.2. Governing equation and the solution	118
6.3. Numerical results for a double-layered graphene sheet and discussions	121
6.4. Concluding remark	127
Acknowledgement	128
References.....	128

CHAPTER 7

7. Conclusions, Contributions and Future Works.....	132
7.1. Introduction	132
7.2. Conclusions	133
7.3. Contributions.....	136
7.4. Future works.....	137

APPENDIX.....	139
---------------	-----

CURRICULUM VITAE.....	143
-----------------------	-----

LIST OF TABLES

Table 2.1 Properties of the space frame elements.....	17
Table 3.1 Frequencies in THz of a zigzag single-walled carbon nanotube (8, 0) with diameter = 0.626 nm and length = 5.826 nm	51
Table 3.2 Frequencies in THz of a armchair single-walled carbon nanotube (6, 6) with diameter = 0.814 nm and length = 5.66 nm	52
Table 4.1 Equivalent Young's modulus and the mass density for different sizes of single-layered graphene sheets	83
Table 4.2 Natural frequencies of single-layered graphene sheets (THz), $a = 30.0$ nm	85
Table 6.1 Natural frequencies of single-layered graphene sheet	122

LIST OF FIGURES

Fig. 2.1 Schematic diagram of a graphene sheet.....	11
Fig. 2.2 Nondimensional van der Waals force between two carbon atoms versus the distance	12
Fig. 2.3 carbon nanotubes: (a) Chiral, (b) Zigzag, and (c) Armchair	13
Fig. 3.1 Fundamental natural frequencies (GHz) of clamped-free carbon nanotubes with different aspect ratios, o:(5, 0) Reference [35], *(5, 0) Present, Δ:(4, 4) Reference [35], +:(4, 4) Present.....	49
Fig. 3.2 Fundamental natural frequencies (GHz) of clamped-clamped carbon nanotubes with different aspect ratios, o:(5, 0) Reference [35], *(5, 0) Present, Δ:(4, 4) Reference [35], +:(4, 4) Present	50
Fig. 3.3 First eight mode shapes of the (6, 0) zigzag single-walled carbon nanotube, clamped-free boundary condition	52
Fig. 3.4 First four mode shapes of the (6, 0) zigzag single-walled carbon nanotube with cross sectional distortion, clamped-free boundary condition.....	53
Fig. 3.5 Cross sectional deformation as circumferential wave-forms.....	54
Fig. 3.6 Time history and fast Fourier transformation plot of the (6, 0) zigzag single-walled carbon nanotube, clamped-free boundary condition, load and response are in axial direction	56
Fig. 3.7 First five extensional mode shapes of the (6, 0) zigzag single-walled carbon nanotube, clamped-free boundary condition.....	56
Fig. 3.8 Time history and fast Fourier transformation plot of the (6, 0) zigzag single-walled carbon nanotube, clamped-free boundary condition, load and response are in horizontal plane.....	57
Fig. 3.9 Time history and fast Fourier transformation plot of the (6, 0) zigzag single-walled carbon nanotube, clamped-free boundary condition, torsional load is applied, response is obtained in horizontal plane	57
Fig. 3.10 First four torsional mode shapes of the (6, 0) zigzag single-walled carbon nanotube, clamped-free boundary condition.....	58
Fig. 3.11 First eight mode shapes of the (6, 0) zigzag single-walled carbon nanotube, clamped-clamped boundary conditions	60
Fig. 3.12 First four mode shapes of the (6, 0) zigzag single-walled carbon nanotube with cross sectional distortion, clamped-clamped boundary condition	60
Fig. 3.13 Fast Fourier transformation plot of the (6, 0) zigzag single-walled carbon nanotube, clamped-clamped boundary conditions, load and response are in axial direction	61

Fig. 3.14 First seven extensional mode shapes of the (6, 0) zigzag single-walled carbon nanotube, clamped-clamped boundary condition	61
Fig. 3.15 Time history and fast Fourier transformation plot of the (6, 0) zigzag single-walled carbon nanotube, clamped-clamped boundary condition, load and response are in horizontal plane.....	62
Fig. 3.16 Time history and fast Fourier transformation plot of the (6, 0) zigzag single-walled carbon nanotube, clamped-clamped boundary condition, torsional load is applied, response is obtained in horizontal plane	62
Fig. 3.17 First five torsional mode shapes of the (6, 0) zigzag single-walled carbon nanotube, clamped-clamped boundary condition	63
Fig. 3.18 First eight mode shapes of the (4, 4) armchair single-walled carbon nanotube, clamped-free boundary conditions.....	65
Fig. 3.19 First eight mode shapes of the (4, 4) armchair single-walled carbon nanotube with cross sectional distortion, clamped-free boundary condition	65
Fig. 3.20 Time history and fast Fourier transformation plot of the (4, 4) armchair single-walled carbon nanotube, clamped-free boundary condition, load and response are in axial direction	66
Fig. 3.21 First four extensional mode shapes of the (4, 4) armchair single-walled carbon nanotube, clamped-free boundary condition.....	66
Fig. 3.22 First four torsional mode shapes of the (4, 4) armchair single-walled carbon nanotube, clamped-free boundary condition.....	67
Fig. 3.23 First eight mode shapes of the (4, 4) armchair single-walled carbon nanotube, clamped-clamped boundary condition	68
Fig. 3.24 First five mode shapes of the (4, 4) armchair single-walled carbon nanotube with cross sectional distortion, clamped-clamped boundary condition	69
Fig. 3.25 First four extensional mode shapes of the (4, 4) armchair single-walled carbon nanotube, clamped-clamped boundary condition	69
Fig. 3.26 First five torsional mode shapes of the (4, 4) armchair single-walled carbon nanotube, clamped-clamped boundary condition	70
Fig. 3.27 First 30 natural frequencies of single-walled carbon nanotubes with different atomic structures and boundary conditions, ...: Armchair single-walled carbon nanotube with clamped-free boundary condition, ___: Zigzag single-walled carbon nanotube with clamped-free boundary condition, *: Armchair single-walled carbon nanotube with clamped-clamped bound, o: Zigzag single-walled carbon nanotube with clamped-clamped boundary condition	71
Fig. 4.1 Geometry of a graphene sheet lattice structure.....	80
Fig. 4.2 Out-of-plane natural frequencies of rectangular single-layered graphene sheets of different aspect ratios, CCCC; *, Mode 1; +, Mode 3; ▲, Mode 5; ■, Mode 7; ●, Mode 9	86

Fig. 4.3 In-plane natural frequencies of rectangular single-layered graphene sheets of different aspect ratios, CCCC; *, Mode 1; +, Mode 3; ▲, Mode 5; ■, Mode 7; ●, Mode 9	87
Fig. 4.4 Out-of-plane natural frequencies of square single-layered graphene sheets of different sizes, CCCC; *, Mode 1; +, Mode 3; ▲, Mode 5; ■, Mode 7; ●, Mode 9	87
Fig. 4.5 In-plane natural frequencies of square single-layered graphene sheets of different sizes, CCCC; *, Mode 1; +, Mode 3; ▲, Mode 5; ■, Mode 7; ●, Mode 9	88
Fig. 4.6 First six out-of-plane mode shapes of a nearly square single-layered graphene sheet (4.92 nm×4.97 nm), CCCC.....	88
Fig. 4.7 First six in-plane mode shapes of a nearly square single-layered graphene sheet (4.92 nm×4.97 nm), CCCC.....	89
Fig. 5.1 Geometry of a graphene sheet	98
Fig. 5.2 In-plane Young's modulus of elasticity for different sizes of rectangular single-layered graphene sheets	101
Fig. 5.3 Young's modulus of elasticity of bending modes for different sizes of rectangular single-layered graphene sheets.....	101
Fig. 5.4 Density of different sizes of rectangular single-layered graphene sheets based on number of carbon atoms.....	102
Fig. 5.5 In-plane natural frequencies of 30° skewed single-layered graphene sheets, all edges are clamped	103
Fig. 5.6 In-plane natural frequencies of 60° skewed single-layered graphene sheets, all edges are clamped	104
Fig. 5.7 In-plane natural frequencies of 90° skewed (rectangular) single-layered graphene sheets, all edges are clamped	104
Fig. 5.8 Out-of-plane natural frequencies of 30° skewed single-layered graphene sheets, all edges are clamped	105
Fig. 5.9 Out-of-plane natural frequencies of 60° skewed single-layered graphene sheets, all edges are clamped	105
Fig. 5.10 Out-of-plane natural frequencies of 90° skewed (rectangular) single-layered graphene sheets, all edges are clamped.....	106
Fig. 5.11 In-plane natural frequencies of clamped edge circular single-layered graphene sheets	108
Fig. 5.12 Out-of-plane natural frequencies of clamped edge circular single-layered graphene sheets	108
Fig. 5.13 First 6 in-plane mode shapes of a clamped edge circular single-layered graphene sheet	109
Fig. 5.14 First 6 out-of-plane mode shapes of a clamped edge circular single-layered graphene sheet.....	109

Fig. 6.1 Geometry of one layer of the 3.69 nm × 3.69 nm double-layered graphene sheet	122
Fig. 6.2 Time history and fast Fourier transform plot of two nodes at the centre of the bottom and top layers of the double-layered simply supported graphene sheets in transverse vibration	124
Fig. 6.3 Time history and fast Fourier transform plot of two nodes at the centre of the bottom and top layers of the double-layered clamped graphene sheets in transverse vibration	125
Fig. 6.4 Time history and fast Fourier transform plot of a node at the centre of the top layer of the double-layered clamped graphene sheets in in-plane vibration.....	127

LIST OF NOMENCLATURE

A	Cross section of the frame element
\mathbf{a}	Translational period along the axis of single-walled carbon nanotube
a, b	Length parameters of the graphene sheet
a_0	Length of graphene lattice vectors \mathbf{a}_1 and \mathbf{a}_2
$\mathbf{a}_1, \mathbf{a}_2$	Graphene lattice vectors
C_1, C_2	Parameters used in the stiffness matrix of the frame element
c_0, c_1, c_2	Parameters used in the Newmark's direct integration method
\mathbf{c}	Chirality vector
\mathbf{c}'	Graphene chiral lattice vector
D	Flexural rigidity of the plate
d	Diameter of the single-walled carbon nanotube
E	Young's modulus of elasticity of the frame element
E_x, E_y	In-plane Young's modulus of elasticity of the graphene sheet in x and y directions
E_b	Bending Young's modulus of elasticity of the graphene sheet
$F(r)$	Van der Waals force between two atoms as a function of r

F	Load vector
F_{ext.}	Load vector produced by external loads
F_i	Load vector in the i^{th} time step
F_{vdw}	Load vector produced by van der Waals forces
f_{ij}	Natural frequency of the plate in the classical plate theory
G	Shear modulus of elasticity of the frame element
h	Thickness of the graphene sheet
I	Area moment of inertia of the frame element
J	Polar mass moment of inertia of the frame element
i, j	Number of half waves in the mode shapes of the plate
K	Membrane stiffness of the plate
K	Stiffness matrix of the structure
$\tilde{\mathbf{K}}$	Nondimensional stiffness matrix
K_g	Stiffness matrix of the single-layered graphene sheet
K^G	Stiffness matrix of the frame element in the global coordinate system
K_{vdW}	Stiffness matrix associated with inter-layer van der Waals forces
k_r, k_θ, k_τ	Extensional, bending and torsion stiffness of the frame element
k	Stiffness matrix of the frame element in its local coordinate system

L	Length of the frame element used to simulate the covalent bond
\mathbf{M}	Mass matrix of the structure
$\tilde{\mathbf{M}}$	Nondimensional mass matrix
\mathbf{M}_g	Mass matrix of the single-layered graphene sheet
\mathbf{M}^G	Mass matrix of the frame element in the global coordinate system
m_c	Mass of each carbon atom
\mathbf{m}	Mass matrix of the frame element in its local coordinate system
n	Greatest common divisor of n_1 and n_2
n_1, n_2	Chirality parameters of the single-walled carbon nanotube
P	Force
Q	Parameter used in determining the geometry of the single-walled carbon nanotube
q	Distributed load
R	Radius of the graphene sheet
\mathbf{R}	Transformation matrix for a vector from local to global coordinate systems
\mathbf{R}_α	Transformation matrix for a vector about z axis by angle α
\mathbf{R}_β	Transformation matrix for a vector about y axis by angle β
r	Distance between two carbon atoms used to find the van der Waals interaction

\mathbf{T}	Transformation matrix for a matrix from local to global coordinate systems
t	Time
\tilde{t}	Nondimensional time
$U(r)$	Potential energy of the van der Waals interaction between two atoms as a function of r
u_0, v_0	In-plane and out-of-plane displacements
X, Y, Z	Global coordinate system
x, y, z	Local coordinate system
$\mathbf{x}, \dot{\mathbf{x}}, \ddot{\mathbf{x}}$	Displacement, velocity and acceleration vectors
$\tilde{\mathbf{x}}, \tilde{\dot{\mathbf{x}}}, \tilde{\ddot{\mathbf{x}}}$	Nondimensional displacement, velocity and acceleration vectors
$\mathbf{x}_i, \dot{\mathbf{x}}_i, \ddot{\mathbf{x}}_i$	Displacement, velocity and acceleration vectors in the i^{th} time step
$\ddot{\mathbf{x}}_i^{(\gamma)}, \ddot{\mathbf{x}}_i^{(\delta)}$	Linear approximations of acceleration in the i^{th} time step
α, β	Rotation angles about z and y axes
γ	Parameter used in the Newmark's direct integration method
Δt	Time increment
δ	Parameter used in the Newmark's direct integration method
ε	Parameter used in the Lennard-Jones 6-12 formula to approximate the potential energy of the van der Waals interaction
η	Parameters used to find flexural stiffness of the plate

θ	Chiral angle of the single-walled carbon nanotube
λ_{ij}	Parameters used to find natural frequencies of the plate
ρ	Density
σ	Parameter used in the Lennard-Jones 6-12 formula to approximate the potential energy of the van der Waals interaction
ν	Poisson's ratio
Ω	Nondimensional natural frequency
ψ	Skewed angle
ω	Natural frequency

“Remember that all models are wrong;

The practical question is how wrong do they have to
be to not be useful.”

George E.P. Box

CHAPTER 1

Introduction to the Thesis

1.1. General introduction

Carbon nano-structures attracted many attentions during past two decades because of their exceptional mechanical, physical, chemical, electrical and vibrational properties and hence, new applications are introduced by researchers literally every day. For example, medical laboratories which are working on cancer treatments use nano-devices for injecting drugs to specific cells. Similarly, wireless technology developers are interested in producing ultra high frequency waves in very compact devices. Researchers are tailoring the properties according to the needs by developing new shapes and adding additional substances in the manufacturing process. Carbon nano-devices are used widely in producing nano-sensors, nano-actuators and nano-oscillators due to extremely high stiffness and negligibly small weight. As the technology advances and manufacturing methods are refined, these devices can be produced with high quality and significantly reduced structural defects.

To start designing a new nano-scale device, researchers need detailed information about mechanical and physical properties of the nano-materials. These properties may include Young's modulus, shear modulus, Poisson ratio, density, etc. In contrast to macro-scale design, atomic structure of the nano-structure plays an important role in the mechanical properties. Defining the mechanical properties requires clear understanding of the detailed layout, covalent bonds and other interacting effects in the atomistic scale. On the other hand, producing prototypes without having unambiguous perception of the structural properties might be very misleading, time consuming and very inefficient.

Based on these, many scientists attempted to find analytical and numerical methods to have a good insight of such mechanical behaviors.

1.2. Objective and scopes of this thesis

This thesis deals with the study of the mechanical properties and response behaviours of carbon nanotubes and graphitic sheets. With this into consideration, the scopes and objectives of the present research project can be specified by the following points.

- To get solid understanding of the available analytical and numerical methods which are used in the literature for modeling the mechanical behaviors of carbon nano-structures.
- To study the advantages and disadvantages of different simulation methods and developing an efficient, accurate and state-of-the-art technique for analyzing carbon nanotubes and graphitic sheets.
- To develop comprehensive algorithms for reproducing the geometry and atomic structure of carbon nanotubes and graphitic sheets in C++ environment.
- To investigate mechanical properties of single-walled carbon nanotubes and to get a clear understanding of the effects of atomic structure and boundary conditions on these properties.
- To survey free and forced vibrational analysis of single-walled carbon nanotubes, find natural frequencies, mode shapes and frequency spectrums and study the effects of their atomic structure on vibrational behaviors.
- To understand the in-plane and out-of-plane mechanical properties of graphene sheets and to describe a systematic way for modeling a single-layered graphene sheet as a continuum plate structure.
- To study the in-plane and bending vibrations of single-layered graphene sheets using atomistic methods and continuum plate theory.

- To compare atomic scale model and continuum plate theory in vibrational analyses of graphenes. This includes comparing vibration results for various shapes and sizes with different boundary conditions.
- To develop accurate, efficient and relatively fast techniques for modeling nonlinear van der Waals interactions in multi-layered graphene sheets.
- To study the vibrational behavior of multi-layered graphene sheets and investigate the influence of van der Waals interactions on in-plane and out-of-plane frequency spectra.

1.3. Outline of the thesis

This thesis is written in the integrated form in which each chapter is a standalone article with introductory notes, literature review, problem definition, solution method, results and discussion, conclusions and references. In chapter two, a review study is presented starting with an extensive introductory report on basic definitions of carbon nanotubes and graphitic sheets, their atomic structure, covalent bonds and van der Waals interactions. This chapter contains a critical review on various simulation techniques presented by other researchers. More than 100 papers are cited in order to obtain a deep insight on the subject of the matter. Different molecular dynamic methods, atomic scale and lattice structure approaches, continuous beam, shell and plate theories and nonlocal elasticity assumptions are discussed in detail. In general, this chapter provides some of the very basic concepts to researchers with background in engineering mechanics.

Chapter three aims to study the mechanical properties and vibrational characteristics of single-walled carbon nanotubes. In this chapter, a detailed numerical study on the free and forced vibrations of single-walled carbon nanotubes is presented. A simple and straightforward method is used such that the proximity of the mathematical model to the actual atomic structure of the nanotube is closely retained. Each carbon atom is modeled as a node in finite elements method with concentrated atomic mass and six prescribed degrees of freedom. The covalent bond between adjacent carbon atoms which provides

axial, bending and torsional stiffness is modeled as a three-dimensional frame element. Both zigzag and armchair chiralities of the carbon nanotubes for clamped-free and clamped-clamped boundary conditions are analyzed and their natural frequencies and corresponding mode shapes are obtained. Results pertaining to axial, bending, and torsional modes of vibration are reported with discussions. These modes of vibration appear in the eigen-values and eigen-vectors without any distinction. The direct integration method by Newmark is used extensively along with the fast Fourier transform to identify different types of vibrational modes.

Chapter four aims to introduce a classical plate model for simulating the mechanical behaviors of graphene sheets. Classical plate theories are very well established and closed form solutions are available for various geometries and boundary conditions. Even though such models are presented by other researchers in the literature, no attempt was made to compare the results of the plate theory to those of atomic scale simulations. In this chapter, equivalent mechanical and geometric properties of rectangular single-layered graphene sheets are investigated. Equivalent extensional and flexural rigidities of single-layered graphene sheets are obtained by treating graphene as a plane lattice structure made of tightly packed carbon atoms into an array of honeycomb-shaped cells. Subsequently, the graphene structure is simulated by a classical plate with prescribed geometrical and mechanical properties. The in-plane and out-of-plane free vibration analyses of the rectangular plate provide the natural frequencies and associated mode shapes. Results are compared with eigen-analyses of lattice structure model for different sizes of graphenes. Examples are considered in this chapter to show close agreement in the results from these two methods for different sizes of graphenes with different boundary conditions. When the lattice structure models become too large to handle computationally, this study suggests that well established continuum plate theory can be used for reasonably accurate results using the appropriate Young's moduli.

Chapter five is dealing with free vibrational analyses of skewed and circular graphene sheets. In this chapter, atomic scale lattice structure method and continuum classical plate theory are used for modeling the graphene sheets. This chapter aims to show the effectiveness and accuracy of the equivalent classical plate theory which was introduced

in chapter four. While the equivalent Young's moduli are obtained from static analyses of rectangular plates, it is shown that these mechanical properties can be used for other shapes of graphene sheets. Results are obtained for various skewed angles of the skewed plate and also for circular graphenes with different radii. A very close agreement is observed between results of the plate theory and lattice structure simulations. This chapter concludes that the recommended plate model can be used in modeling graphene sheets of any size and boundary condition.

Chapter six is concerned with the forced vibration of multi-layered graphene sheets by the lattice structure approach. Each layer is modeled at the atomic level using the same mechanical and geometrical assumptions that are made regarding the covalent bonds in chapters three, four and five. The nonlinear van der Waals interaction between adjacent graphene layers is fully incorporated by placing it in the force vector in its direct form. This adjustment significantly reduces the computational hardships due to nonlinearity. Newmark's direct integration method is modified and used for the solution of the matrix equation governing the motion of the multi-layered graphene sheet. Double-layered square graphene with simply supported and clamped boundary conditions are analyzed to examine the out-of-plane and in-plane vibrational characteristics and also to illustrate the applicability of the numerical method developed. Influence of the van der Waals interaction is noticeable in bending modes, but it essentially does not play any role in the in-plane modes.

Finally, a general conclusion is presented in chapter seven that sums up topics of discussion in the thesis and points out main contributions of this research project and possible ideas for the future works.

CHAPTER 2

Vibrations of Carbon Nano-Scale Structures: A Critical Review*

2.1. Introduction

During experiments conducted at Rice University aimed at understanding the formation of long-chain carbon molecules in interstellar space and circumstellar shells, Kroto et al. [1] produced a remarkable stable cluster of 60 carbon atoms. The new carbon structure is formed through the vaporization of carbon species from the surface of a solid disk of graphite into high-density helium flow by a focused pulsed laser. This carbon cluster was suggested to be a truncated icosahedron, a polygon with 60 vertices and 32 faces, out of which 12 were pentagonal and the remaining 20 hexagonal. This form of pure soccer-ball-shaped solid carbon C_{60} had the ‘fullerene’ structure and was studied further by Krätschmer and co-researchers [2]. Considering the potential this material possesses, researchers then raced towards investigating various physical and chemical properties along with the production techniques. Iijima reported preparation technique of a needle-like tubular carbon structure using an arc-discharged evaporation method similar to the one used earlier by other researchers [3]. The needles ranging from 4 to 30 nm in diameter and up to 1 μm in length were grown on the negative end of the carbon electrode in the direct current arc-discharge evaporation in an argon-filled vessel and found through electron microscopy to be formed with coaxial tubes of graphitic sheets. The carbon-

* A version of this chapter is published in the Computational Technology Reviews as: Singh, A. V., and Arghavan, S., 2010, "Vibration of carbon nanoscale structures: a critical review," Computational Technology Reviews, 1, pp. 281-314.

atom-hexagons on each tube were arranged helically about the needle axis. Iijima and Ichihashi demonstrated capillarity in the open tubes and reported the synthesis of single-shell carbon nanotube with one nanometer diameter [4]. They also mentioned the significance of further research to predict accurately the electronic structure and mechanical strength, for which well defined morphologies, length, thickness and number of concentric shells would be needed.

Carbon nanotubes have interesting mechanical properties, such as low density, high stiffness and axial strength due to their seamless cylindrical graphitic structure plus the extraordinary flexibility and resilience, making them useful as nanoscale fibers in strong lightweight composites. Consequently, experimental studies were performed to understand and predict their elastic properties using the transmission electron microscopes. Among such studies is the work of Treacy et al. [5] who estimated the Young's modulus of isolated nanotubes by measuring the amplitude of their intrinsic thermal vibrations. A quantitative relationship between the Young's modulus and the amount of disorder in the atomic structure of the nanotube walls was illustrated by Salvétat et al. [6]. There are some books available containing the basic as well as advanced topics on this subject [7-10].

A large number of researchers got involved in this general area of nanotechnology as graphitic sheets possess outstanding mechanical, physical and electronic properties. Consequently, the information available in the literature grew very rapidly and many review articles were published. Iijima [11] outlined the work done in his laboratories concerning carbon nanotubes and touched upon some ambitious studies and application possibilities regarding the unique nanometric space inside single-walled carbon nanotubes and the special behaviour arising from the ultimately thin wall of a single-layered graphene sheet. He continued with the comment that new phenomena were still being discovered 10 years after the discovery of carbon nanotubes and certainly there were many more attractive phenomena hidden within the tiny, mysterious world inside the carbon nanotubes. From the above, it is readily learnt that carbon nanotubes are among the stiffest and strongest fibres known, with Young's moduli as high as 1 TPa and tensile strengths of up to 63 GPa. There has been great interest in exploiting these properties by

incorporating carbon nanotubes into some form of matrix, e.g. nanotubes in polymer, ceramic or metal matrices. Review article of recent advances in carbon nanotubes and their composites examining in detail on the characterization of the structure, processing and modeling of carbon nanotubes and their composites has been published by Thostenson et al. [12] and Harris [13]. Theoretical predictions and experimental techniques that are most often used for the challenging tasks of visualizing and manipulating these tiny structures are discussed in the paper by Qian et al. [14] by citing nearly 350 published articles. They also outline the computational approaches such as ab initio quantum mechanical simulations, classical molecular dynamics, and continuum models. Their focus has been on the exploration of mechanical properties such as Young's modulus, bending stiffness, buckling criteria, and tensile and compressive strengths. Finally, they discuss several examples including nanoropes, filled nanotubes, nano-electro-mechanical systems, nano-sensors, and nanotube-reinforced polymers.

Modeling and simulation at the nanoscale are seen to be a better way to the understanding of the mechanical behaviours of carbon nanotubes. In this task, the knowledge to incorporate atomic features into the continuum or structural mechanics theories is imperative. Tools have also been developed to effectively link basic scientific research with engineering applications. The paper by Chen and Huang [15] is intended to introduce to the readers, particularly those with traditional civil engineering or engineering mechanics backgrounds, to this relatively new, interdisciplinary and emerging field in engineering mechanics. Gibson et al. [16] cover in their review work the modeling and simulation of vibrating nanotubes, nano-mechanical resonators and oscillators, the use of vibration measurements to characterize nanotube mechanical properties, nanotube augmentation of dynamic structural properties of composites, vibrations of nanotube-based sensors and actuators, sonication of nanotube-reinforced polymer resins, Raman scattering from nanotubes, high frequency wave-nanotube interactions, and others. In a very recent publication, Chou and co-workers [17] reviewed the recent advancements in the science and technology of carbon nanotube based fibres and composites as well as fibres of pure or embedded carbon nanotubes in polymer matrix produced by several spinning techniques. They examined mechanical and physical properties of carbon nanotube/polymer composites.

In the present review article, some historical background, reference to the published textbooks and brief contents of review articles are collected and discussed critically. An attempt is made in this paper to review published articles in the open literature on the vibrations of carbon nanotubes and graphitic sheets from the structural mechanics point of view. Citations of relevant papers are made with brief discussion based on the reported materials by their respective authors. By no account, this paper should be construed as rigorous covering all the details of this new and still emerging field of study. The primary topics covered in the following are: description of the geometries single-walled and multi-walled carbon nanotubes, studies on the mechanical properties, structural mechanics approaches to the vibrations of single-walled and multi-walled carbon nanotubes, and also the vibrations of graphitic sheets. Different simulation techniques which are used in the literature are reviewed here and advantages and disadvantages of each method are discussed.

2.2. Structural and mechanical parameters of graphitic sheets

Before getting into exploring the vast amount of literature created by researchers across the globe, it is worthwhile to briefly introduce some of the essential geometric and material characteristics of graphitic sheets. The mechanical properties of carbon nanotubes and all other graphene-based structures are dependent on the nature of the covalent bonds between carbon atoms. The atomic number for carbon is six which means each carbon atom has six electrons and its electronic structure is $1s^2 2s^2 2p^2$ in atomic physics notation [18]. Each carbon atom has four free electrons which can form bonds with other atoms. In the process of graphene formation, one s-orbital and two p-orbitals combine to form three hybrid sp^2 -orbitals at 120° to each other within a plane. The covalent bonds are formed by sp^2 -orbitals of adjacent carbon atom. These interactions are named σ -bonds. The covalent bond exists between two atoms to keep them connected in each layer of the graphene sheet. To be precise, each carbon atom is covalently bonded to three carbon atoms in a nested cage-like structure. Fig. 2.1 shows a graphene sheet with the carbon atoms arranged such that each atom is shared by three hexagons. The tubes are

usually labeled in terms of the graphene lattice vectors \mathbf{a}_1 and \mathbf{a}_2 at an angle of 60° to each other as shown in the bottom left corner of Fig. 2.1. These vectors contain the unit cell with two carbon atoms positioned at $(\mathbf{a}_1 + \mathbf{a}_2)/3$ and $2(\mathbf{a}_1 + \mathbf{a}_2)/3$ from the intersection point of the vectors. The magnitude of each of these two vectors \mathbf{a}_1 and \mathbf{a}_2 is: $a_0 = 2.461 \text{ \AA}$.

Each carbon atom has one free unhybridized p-orbital which is perpendicular to the plane of the graphene sheet, making them vulnerable to form π -bond networks. These out-of-plane π -bonds get delocalized and the delocalized π -bonds interact with the π -bonds on the neighbouring layer. This atomic interaction is called the van der Waals force and also is rather weak and non-bonding when compared with the covalent bonds between the neighbouring carbon atoms. Multi-layered graphene sheets are called graphite in this context and the stable distance between adjacent layers of graphite is reported to be 0.34 nm [10]. Potential energy of the van der Waals forces are usually modeled using Lennard-Jones 6-12 potential [19], which provides a smooth transition between the attraction and repulsion regions and can be written in the following form.

$$U(r) = 4\varepsilon \left[\left(\frac{\sigma}{r} \right)^{12} - \left(\frac{\sigma}{r} \right)^6 \right] \quad (2.1)$$

where, r is the distance between interacting atoms. Indices σ and ε are the Lennard-Jones parameters given by $\varepsilon = 0.0556 \text{ kcal. mole}^{-1}$ and $\sigma = 0.34 \text{ nm}$ respectively for this case [20]. The potential $U(r)$ is usually truncated at the inter-atomic distance of 2.5σ without a significant loss of accuracy, i.e. no interactions are evaluated beyond this distance. Based on the Lennard-Jones potential, the van der Waals force between interacting atoms can then be written as:

$$F(r) = -\frac{dU(r)}{dr} = 24 \frac{\varepsilon}{\sigma} \left[2 \left(\frac{\sigma}{r} \right)^{13} - \left(\frac{\sigma}{r} \right)^7 \right] \quad (2.2)$$

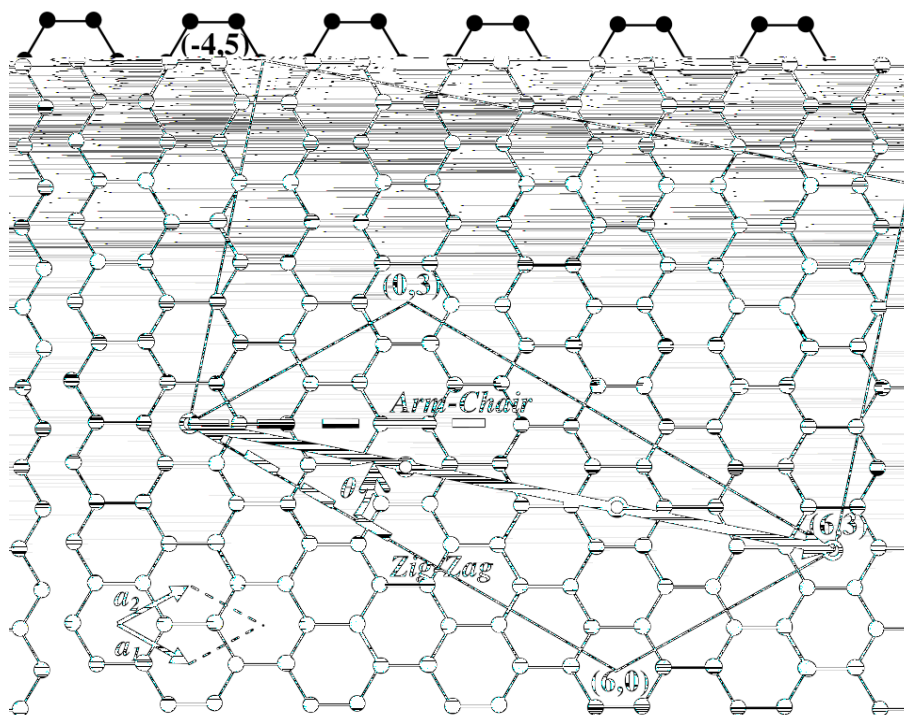


Fig. 2.1 Schematic diagram of a graphene sheet

As known, these interactions can be either attractive or repulsive depending on the distance between the participating atoms. The attraction occurs when a pair of atoms approaches each other within a certain distance. When atoms get very close to each other, van der Waals force is repulsive. Fig. 2.2 shows the variation of nondimensional van der Waals force ($F\sigma/24\epsilon$) between two carbon atoms versus the distance between their nuclei. For a carbon-carbon interaction, van der Waals force becomes zero when atoms are 0.3816 nm apart.

A single-walled carbon nanotube has been described as graphene sheet rolled into a seamless tube with hexagonal cells around the circumference and its quantum properties depend on the diameter and chirality, which is denoted by a pair of integers (n_1, n_2) . The graphene sheet is rolled up such that the chiral vector $\mathbf{c} = n_1 \mathbf{a}_1 + n_2 \mathbf{a}_2$ becomes the circumference of the carbon nanotube from which the magnitude of the chiral vector and diameter can be obtained as follows.

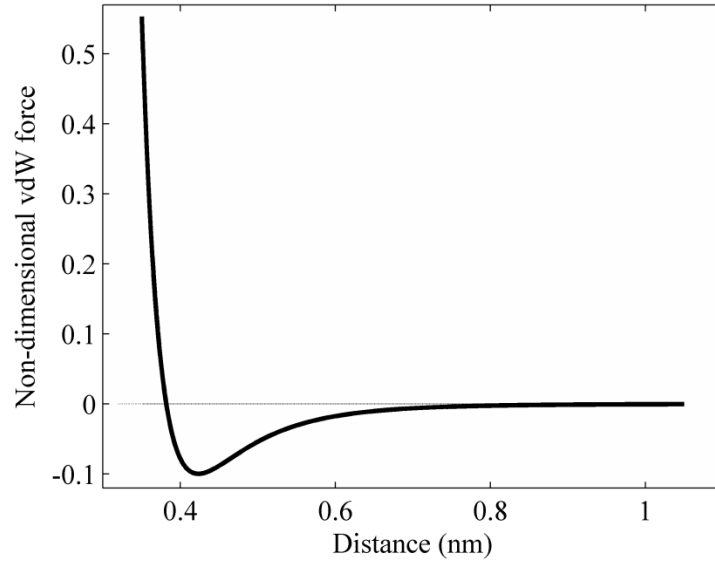


Fig. 2.2 Nondimensional van der Waals force between two carbon atoms versus the distance

$$|\mathbf{c}| = \sqrt{(n_1 + \frac{1}{2}n_2)^2 + (\frac{\sqrt{3}}{2}n_2)^2} = \sqrt{n_1^2 + n_1n_2 + n_2^2} \quad (2.3)$$

$$d = \frac{|\mathbf{c}|}{\pi} = a_0 \sqrt{n_1^2 + n_1n_2 + n_2^2} \quad (2.4)$$

Also, the chiral angle θ is defined by the angle between vectors \mathbf{a}_1 and \mathbf{c} . It is given as:

$$\cos \theta = \frac{\mathbf{a}_1 \cdot \mathbf{c}}{|\mathbf{a}_1| |\mathbf{c}|} = \frac{n_1 + \frac{1}{2}n_2}{\sqrt{n_1^2 + n_1n_2 + n_2^2}} \quad (2.5)$$

For the chiral vector illustrated in Fig. 2.1 by $\mathbf{c} = 6\mathbf{a}_1 + 3\mathbf{a}_2$, or (6, 3), there are three lattice vectors indicated by four circles on it. The first and the last circles coincide if the sheet is rolled up. The number of lattice points on the chiral vector is given by the greatest common divisor n of the (n_1, n_2) , since $\mathbf{c} = n[(n_1/n)\mathbf{a}_1 + (n_2/n)\mathbf{a}_2] = n\mathbf{c}'$ is a multiple of another graphene lattice vector \mathbf{c}' . The chiral angles of 0° and 30° represent the two special forms of carbon nanotubes. For example, tube represented by $(n, 0)$ is known as the “zigzag” (Fig. 2.3.b) as it exhibits a zigzag pattern along the circumference. Similarly,

case by (n, n) is called the “armchair” (Fig. 2.3.c) whose chiral angle is 30° . The smallest graphene lattice vector \mathbf{a} , which is perpendicular to the chiral vector \mathbf{c} , defines the translational period along the axis of the tube and is determined from the chiral indices (n_1, n_2) by:

$$\mathbf{a} = -\frac{2n_2 + n_1}{nQ} \mathbf{a}_1 + \frac{2n_1 + n_2}{nQ} \mathbf{a}_2 \quad (2.6)$$

$$|\mathbf{a}| = \frac{\sqrt{3(n_1^2 + n_1n_2 + n_2^2)}}{nQ} a_0 \quad (2.7)$$

where $Q = 3$ if $(n_1 - n_2)/3n$ is integer and $Q = 1$ otherwise. The above equations along with some others given in the book by Reich et al. [10] are essential in creating the geometry of carbon nanotubes of different diameter and chirality.

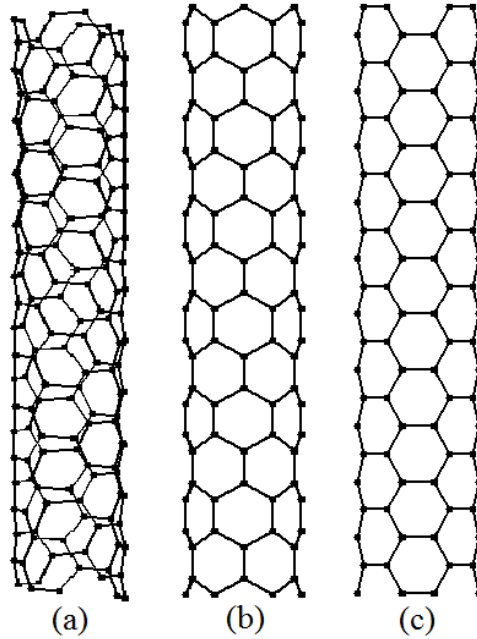


Fig. 2.3 carbon nanotubes: (a) Chiral, (b) Zigzag, and (c) Armchair

Other form of carbon nanotubes which generally has more than one layer of carbon atoms is called multi-walled carbon nanotube. There are different theories available in the literature about its structure. The two main dominant theories out of those are called

Swiss roll and Russian roll [10] respectively. Swiss roll is a theory which suggests a scroll-like structure for carbon nanotubes while Russian roll arrangement consists of discrete tubes composed of a set of coaxially situated single-walled carbon nanotubes. The distance between two neighbouring layers is assumed to be the same as the spacing between adjacent graphene sheets in graphite, i.e., 0.34 nm. Van der Waals forces are helping to keep these layers connected together.

2.3. Mechanical properties of carbon nanotubes

In this section, a selective review on the studies made by researchers on the mechanical and physical properties of carbon nanotubes and composites embedded with such tubes is presented. Molecular dynamic simulations, using realistic many-body inter-atomic potential functions, are mainly used by researchers to model the mechanical behavior of carbon nanotubes. Classical molecular dynamic methods are using predefined potential functions (force fields), either based on empirical data or structural calculations to find the total potential energy of a system [21]. Typically, using some inter-atomic potential functions, total energy of a system of particles can be calculated. Most notably Lennard-Jones 6-12 potential function and the exponential Morse potential, consist of two main functions that are used in this method [22]. When the total potential energy of a system is in hand, one can perform realistic calculations of the properties of a quite large system.

Robertson et al. [23] examined the energetics and elastic properties of graphitic tubules using both empirical potentials and first principles total energy methods and found that the strain energy per carbon atom relative to an unstrained graphite sheet varies inversely with the square of the tubule radius. The elastic constants along the tubule axis were generally found to soften with decreasing tubule radius. Iijima et al. [24] reported atomistic simulations of the bending of single and multi-walled carbon nanotubes under mechanical loading and observed fully reversible single and multiple kinks at high bending angles. They attributed this behavior to the remarkable flexibility of the hexagonal network at large strain. The research area dealing with the elastic properties of carbon nanotubes dominated in the late 1990s and early 2000s and a large number of

studies were reported in the literature. Lu [25] showed that the elastic moduli for single and multi-walled nanotubes were insensitive to the structural details such as the helicity, radius, and number of walls. The tensile Young's modulus and the torsional shear modulus of tubes were comparable to those of the diamond, while the bulk modulus was smaller. Nanoropes composed of single-walled carbon nanotubes demonstrated the ideal elastic properties of high tensile stiffness and light weight. Cornwell [26] investigated the elasticity of the open-ended and free-standing single-walled carbon nanotubes using quenched molecular dynamic simulations and describing inter-atomic interactions by the Tersoff-Brenner potential. The tubes' response to axial compression was examined and typical failure modes as well as stress-strain curves for a number of tube radii were shown. Data collected for the tubes under compression were used to calculate Young's modulus and to develop a simple formula approximating it over a wide range of tube radii. The Young's modulus of carbon nanotubes are quite susceptible to the variation of their size, e.g. the Young's modulus increases significantly with reduction in the diameter and increases slightly with decrease in the helicity [27].

Young's modulus and the effective wall thickness of single-walled carbon nanotubes are obtained from the bending strain energies with various cross sectional radii in the work reported by Xin et al. [28]. Both these properties are independent of the radius and the helicity. The results showed that continuum elasticity theory could serve well to describe the mechanical properties of single-walled carbon nanotubes. Zhou and Shi [29] studied the mechanical properties of zigzag and armchair single-walled carbon nanotubes under tensile loading with and without hydrogen storage. Hydrogen molecules reduced the maximum tensile strength particularly the armchair type. A nanoscale continuum theory is established by Zhang et al. [30] to directly incorporate inter-atomic potentials into a continuum analysis without any parameter fitting. They studied linear elastic modulus of single-walled carbon nanotubes.

Because of the exceptionally superior mechanical and physical properties, the overall properties of the carbon nanotube reinforced composites were studied by researchers with deep interest. Thostenson and Chou [31] developed a fundamental understanding of the structure/size influence of carbon nanotubes on the elastic properties of such composites

by conducting both experimental and numerical studies. Large diameter carbon nanotube showed lower effective modulus and occupied greater volume than the one having small diameter. Odegard and co-workers [32] proposed a method for developing structure-property relationships for nano-structured composites. The aim of their method was to make it serve as a link between chemistry and solid mechanics. They provided further details in another paper [33] on the multi-scale modeling and simulation of materials such as high-performance polymers, composites, and nanotube-reinforced polymers. They highlighted and discussed challenges with verification and validation. The macroscopic elastic properties of carbon nanotube reinforced composites were evaluated through analyzing the elastic deformation of a representative volume element under various loading conditions by Hu et al. [34]. To obtain these properties, they constructed an equivalent beam model based on the force field theory of molecular mechanics.

Modeling and simulation of the effective elastic properties by miscellaneous methods were presented by various researchers [35-37]. A series of formulations for obtaining the equivalent Young's modulus, shear modulus and Poisson's ratio of carbon nanotubes under tensile and bending with small deformation conditions were reported in reference [38]. Similarly, through various methods predicting the mechanical properties were subsequently reported by others [39, 40]. Chang et al. [41] used molecular dynamic to obtain explicit expressions for in-plane elastic properties of single-walled carbon nanotubes including the effects of chirality and diameter. Also, the Young's modulus, shear modulus and coefficient of thermal expansion of single-walled carbon nanotubes and graphene sheets were evaluated numerically by Kirtania and Chakraborty [42] and presented against diameter of the nanotubes and depth of the graphene sheets.

Molecular dynamic methods are very accurate in simulating the mechanical and thermal behaviors of carbon nanotubes. Generally, these methods can predict the behavior of small systems of up to several hundred particles. The computational cost of these methods is very high and special high-performance computational facilities are required to perform the simulation. Because of these limitations, researchers got motivated to study relatively simpler methods for modeling mechanical behaviors of carbon nanotubes. Conventional shell and beam theories as well as more complicated nonlocal theories are

frequently used in this case. A mechanical structural approach is also introduced by researchers [43] to simulate the characteristics of carbon nanotubes. This method has the accuracy of molecular dynamic techniques while it maintains the efficiency of finite element method. Deformation of the carbon nanotubes was investigated by Li and Chou [43] using this approach in which a carbon nanotube was treated as a frame-like structure.

This approach is much faster than molecular dynamic techniques while it can accurately model the behavior of carbon nano-scale structures. The covalent bond is treated as the connecting element characterized by length, cross sectional properties, angular orientation in the three-dimensional space, and mechanical properties. The hexagons on the wall of a tube are, thus, considered to be formed with such connecting elements and each of these can be treated as a space frame element in finite element simulation with longitudinal, bending and torsional stiffness. A carbon atom is taken as a node with six degrees of freedom, three translational and three rotational, with mass concentrated on it. The stiffness parameters of frame elements are derived from the properties of the graphite sheets. For example, the longitudinal, bending and torsional stiffness parameters are: $938 \text{ kcal.mol}^{-1}.\text{\AA}^{-2}$, $126 \text{ kcal.mol}^{-1}.\text{rad}^{-2}$ and $40 \text{ kcal.mol}^{-1}.\text{rad}^{-2}$ respectively and known as the force field constants in molecular mechanics. It should be noted that one kcal.mol^{-1} is equivalent to $6.947700141 \times 10^{-21}$ Joule. Direct relationship between the structural mechanics parameters of a frame element are: extensional stiffness $k_r = EA/L$, bending stiffness $k_\theta = EI/L$, and torsional stiffness $k_\tau = GJ/L$. Table 2.1 shows the mechanical properties of such an element.

Table 2.1 Properties of the space frame elements

Length of the covalent bond, L	1.42 \AA
Cross sectional area, A	1.68794 \AA^2
Polar moment of inertia, J	0.45346 \AA^4
Moment of inertia, I	0.22682 \AA^4
Young's modulus of elasticity, E	$5.488 \times 10^{-8} \text{ N/ \AA}^2$
Shear modulus of rigidity, G	$8.711 \times 10^{-9} \text{ N/ \AA}^2$
Mass of a carbon atom, m_c	$1.9943 \times 10^{-26} \text{ Kg}$

For a frame element in three-dimensional space, stiffness matrix can be defined as follows [44] (x and y are perpendicular directions in the cross section plane and z is the axial direction):

$$\mathbf{k} = \begin{bmatrix} \mathbf{k}_1 & \mathbf{k}_2 \\ \mathbf{k}_3 & \mathbf{k}_4 \end{bmatrix} \quad (2.8)$$

where:

$$\mathbf{k}_1 = \frac{EI}{L^3} \begin{bmatrix} C_1 & 0 & 0 & 0 & 0 & 0 \\ 0 & 12 & 0 & 0 & 0 & 6L \\ 0 & 0 & 12 & 0 & -6L & 0 \\ 0 & 0 & 0 & C_2 & 0 & 0 \\ 0 & 0 & -6L & 0 & 4L^2 & 0 \\ 0 & 6L & 0 & 0 & 0 & 4L^2 \end{bmatrix}, \mathbf{k}_2 = -\frac{EI}{L^3} \begin{bmatrix} C_1 & 0 & 0 & 0 & 0 & 0 \\ 0 & 12 & 0 & 0 & 0 & -6L \\ 0 & 0 & 12 & 0 & 6L & 0 \\ 0 & 0 & 0 & C_2 & 0 & 0 \\ 0 & 0 & -6L & 0 & -2L^2 & 0 \\ 0 & 6L & 0 & 0 & 0 & -2L^2 \end{bmatrix},$$

$$\mathbf{k}_{j4} = \frac{EI}{L^3} \begin{bmatrix} C_1 & 0 & 0 & 0 & 0 & 0 \\ 0 & 12 & 0 & 0 & 0 & -6L \\ 0 & 0 & 12 & 0 & 6L & 0 \\ 0 & 0 & 0 & C_2 & 0 & 0 \\ 0 & 0 & 6L & 0 & 4L^2 & 0 \\ 0 & -6L & 0 & 0 & 0 & 4L^2 \end{bmatrix}, \text{ and } \mathbf{k}_3 = \mathbf{k}_2^T.$$

Here $C_1=AL^2/I$ and $C_2=GJL^2/I$.

Owing to the fact that the electrons of carbon atoms are of negligible mass as compared to the mass of the nuclei and that the radius of the nuclei ($2.75 \times 10^{-5} \text{ \AA}$) is small as well, it is assumed that the mass of carbon atoms are concentrated at the joints of frame elements. From the modeling point of view, lumped mass technique has been used here. Since each carbon atom has been participated in three covalent bonds, for each frame element, one third of the mass of each carbon atom is considered at each end of the element. As a result, mass matrix can be written as follows for each element:

$$\mathbf{m} = \begin{bmatrix} \mathbf{m}_1 & 0 \\ 0 & \mathbf{m}_1 \end{bmatrix} \quad (2.9)$$

$$\text{where: } \mathbf{m}_1 = \frac{m_c}{3} \begin{bmatrix} 1 & 0 & 0 & 0 & 0 & 0 \\ 0 & 1 & 0 & 0 & 0 & 0 \\ 0 & 0 & 1 & 0 & 0 & 0 \\ 0 & 0 & 0 & 0 & 0 & 0 \\ 0 & 0 & 0 & 0 & 0 & 0 \\ 0 & 0 & 0 & 0 & 0 & 0 \end{bmatrix}$$

Since each element has its own orientation in the three-dimensional space, a rotation tensor is needed for each element to transform its mass and stiffness matrices from its local coordinate system to a global coordinate system of the carbon nanotube. In the global coordinate system, X and Y are supposed to be two perpendicular directions in the cross section plane of the carbon nanotube and Z is supposed to be the axial coordinate of the tube. The angle between the axial direction of each element and the cross section of the tube is called β and the angle between the projection of each element on the cross section of the tube and the X direction is called α here. Based on these definitions, the rotation tensor can be defined as follows for each element:

$$\mathbf{T} = \begin{bmatrix} \mathbf{R} & 0 & 0 & 0 \\ 0 & \mathbf{R} & 0 & 0 \\ 0 & 0 & \mathbf{R} & 0 \\ 0 & 0 & 0 & \mathbf{R} \end{bmatrix} \quad (2.10)$$

$$\text{where } \mathbf{R} = \mathbf{R}_\beta \cdot \mathbf{R}_\alpha, \mathbf{R}_\alpha = \begin{bmatrix} \cos(\alpha) & \sin(\alpha) & 0 \\ -\sin(\alpha) & \cos(\alpha) & 0 \\ 0 & 0 & 1 \end{bmatrix} \text{ and } \mathbf{R}_\beta = \begin{bmatrix} \cos(\beta) & 0 & \sin(\beta) \\ 0 & 1 & 0 \\ -\sin(\beta) & 0 & \cos(\beta) \end{bmatrix}.$$

For each element, its mass and stiffness matrices in global coordinate system will be defined by $\mathbf{K}^G = \mathbf{T}^T \cdot \mathbf{k} \cdot \mathbf{T}$ and $\mathbf{M}^G = \mathbf{T}^T \cdot \mathbf{m} \cdot \mathbf{T}$ respectively.

Li and Chou also investigated multi-walled carbon nanotubes by treating them as nested single-walled carbon nanotubes (Russian rolls) [45]. As discussed before, van der Waals forces are acting along the connecting line between two interacting atoms. Li and Chou [45] have suggested simulating these interactions by truss rods with rotatable end joints. Further, they considered van der Waals forces only between the nearest

neighbouring layers and used nonlinear truss element in their studies. It was observed that the Young's modulus and shear modulus of multi-walled carbon nanotubes were in the ranges of 1.05-0.05 and 0.40-0.05 TPa, respectively. The tube diameter, chirality and number of layers showed noticeable effects on the elastic properties of multi-walled carbon nanotubes.

2.4. Vibration of carbon nanotubes

Carbon nanotubes are used in numerous nano-devices such as sensors, oscillators, and actuators. The structural and elastic properties of single and multi-walled nanotubes were used by many to investigate the vibrations of these nanoscale structures. Scientists are eager to find vibrational characteristics of carbon nanotubes such as natural frequencies and mode shapes. Different theories are used in the literature on vibrational study of carbon nanotubes. Atomic scale simulations and continuum models such as beam and shell theories are widely used here. In this section, a brief review is brought which covers outstanding literatures in this area.

2.4.1. Atomic scale simulations

Li and Chou studied the vibrational behavior of carbon nanotubes by applying the atomistic modeling technique as mentioned above. They further studied the vibrational characteristics of carbon nanotubes used as resonators [46, 47]. They obtained the fundamental frequencies of cantilevered or bridged single-walled nanomechanical resonators and observed that the frequencies could reach the level of 10 GHz-1.5 THz and were influenced by the tube diameter and length [46]. Their results also showed that fundamental frequencies of single and double-walled carbon nanotubes having the same outside diameter were within 10%, where multi-walled carbon nanotubes showing lower values. The noncoaxial vibration of double-walled nanotubes was observed to occur at the third resonant frequency.

Vibrations of both zigzag and armchair single-walled carbon nanotubes were investigated using finite element method in reference [48] where the authors considered three cases: (10, 0), (15, 0) and (20, 0) for the zigzag type and also three cases: (10, 10), (15, 15) and (20, 20) for the armchair nanotubes. Three different lengths of 15, 20 and 25 nm were considered for each nanotube and also reported the detailed investigation on the dependence of the frequencies on various parameters such as diameter, chirality, etc. Lu et al. [49] proposed a modified form of the molecular mechanics that according to them can be used to study stability and vibration of single-walled carbon nanotubes via continuum models. Vibrations of single and multi-walled carbon nanotubes were studied by others researchers using the frame finite element models in the molecular structural mechanics approach [50, 51]. Other interesting works reported in the literature are concerned with the vibrations of single-walled carbon nanotubes [52-54]. Lawer et al. [55] performed calculations for the radial breathing modes of 105 single-walled carbon nanotubes within the rolling geometry diameter range of 0.4 to 1.4 nm and compared frequencies with the available data from other analytical and experimental studies. By proposing an atomic-scale finite element method, Liu et al. [56] studied the vibration of a cantilevered armchair (5, 5) carbon nanotube with 400 atoms and presented the first three vibration modes, of which the first two are beam bending modes and the third being the breathing mode. They found this method to be as accurate as and more efficient than the molecular mechanics simulation technique.

Batra and Gupta [57, 58] used an equivalent continuum structure model, in which the single-walled carbon nanotube was taken to be a hollow cylinder with equal mean radius and length, to find thickness of the equivalent cylinder so that its free vibrational characteristics were the same as those of single-walled carbon nanotube. They studied axial, torsional, radial (breathing) and bending vibrations of several traction free-traction free single-walled carbon nanotubes of different helicities and diameters. In their studies, free vibration of thirty three armchair, zigzag and chiral single-walled carbon nanotubes of length/diameter ratio between 3 and 15 was examined and it was observed that these tubes exhibited Rayleigh and Love inextensional modes of vibration and the lowest natural mode of vibration occurred at a circumferential wave number greater than one.

An in-depth study of the vibrational properties of composite plates made of a purely isotropic elastic host matrix of three different types (epoxy, rubber, and concrete) with embedded single-walled carbon nanotubes was presented by Formica et al. [59]. They also assessed how the modal properties were influenced both globally and locally by carbon nanotube alignment and volume fraction. Using the finite element method, Harrar and Gibson [60] studied the effects of waviness and aspect ratio on the modal vibration response of carbon nanotubes, so that a better understanding of their mechanical properties could be established. The structural, elastic, and vibrational properties of single-walled carbon nanotubes with different radii and chiralities were obtained in the study [61] using pseudo-potential-density-functional theory. This theory allowed calculations on systems with a large number of atoms per cell. Since there are significant uncertainties in the material properties of carbon nanotubes, Scarpa and Adhikari [62] proposed a probabilistic approach to take into account of the uncertainties and derived in closed form the probability density function of the natural frequencies. They compared results with high-fidelity stochastic finite element simulations. Hüttel et al. [63] observed the transverse vibration of suspended carbon nanotubes actuated contact-free by the radio frequency electric field of a nearby antenna at millikelvin temperatures by measuring the single electron tunneling current. By adjusting the radio frequency power on the antenna, they observed that the nanotube resonator can easily be driven into the nonlinear regime. A gradual beam-to-string transition from multi-walled carbon nanotubes to single-walled carbon nanotubes with the crossover from bending rigidity dominant regime to extensional rigidity dominant regime was investigated experimentally by Wei et al. [64] and they found that the resonant frequency under tension and transition of vibration behavior from beam to string befitted well with the continuum beam theory.

2.4.2. Shell theories

The geometric and material properties of carbon nanotubes were studied and reported in the literature by a large number of researchers using experimental and numerical modeling techniques. One of the important objectives of such studies was to apply these properties to study the vibrations and buckling of nanotubes using continuum theory of

elasticity. As carbon nanotubes are tubular in geometry, temptation to use it as a cylindrical shell grew among some researchers. Wang and Ru [65] used Flügge's shell theory to calculate frequencies and associated modes of multi-walled carbon nanotubes of innermost radii of 0.50 and 0.65 nm, respectively, with emphasis on the effects of van der Waals force. Wang and co-workers [66] studied in detail the effects of pressure on the breathing modes based on a multiple-elastic shell model where each layer of the tube was considered to be coupled with adjacent layers through the van der Waals force. Simplified Donnell's shell theory was used to obtain explicit formulas for the radially dominated natural frequencies and mode shapes of double and triple-walled carbon nanotubes with various radii and number of tubes [67]. Effects of van der Waals interaction were found to be significant at higher natural modes of vibration. Donnell's shell theory was also used by Sun and Liu [68, 69] for the vibration of multi-walled carbon nanotubes subject to axial and pressure loadings. An investigation on the nonlinear vibration of double-walled carbon nanotubes using harmonic balance method was reported by Yan et al. [70]. The question on the appropriate use of shell theories to study the responses of single-walled carbon nanotube was raised by Penga and co-workers [71] who studied the order of error to approximate the modeling of single-walled carbon nanotubes as thin shells. They defined the order by the ratio of the atomic spacing to the radius of the carbon nanotube and used atomistic finite deformation shell theory where the modulus of elasticity and thickness were avoided.

A second-order strain gradient nonlocal shell model was established by Shi et al. [72] to study the mode transformation in single-walled carbon nanotubes. Their analyses showed that only a negative second-order nonlocal shell model was appropriate for the purpose, as nonlocal length was evidently related to the vibrational modes and radius-to-thickness ratio. Use of the nonlocal theory was reported very recently to study the vibration characteristics of single-walled carbon nanotubes with different boundary conditions subjected to initial strain [73]. A study by applying the finite element method on the vibration of multi-walled carbon nanotubes with emphasis on the effect of the mixed boundary conditions was reported and the results showed the vibration frequency to be most sensitive to the fixing of the outermost tubes [74]. The transverse vibrations of single and double-walled simply supported carbon nanotubes were investigated under

axial load by applying the Euler-Bernoulli and Timoshenko beam theories and the Donnell's shell theory and the authors modified classical models using the nonlocal theory for the accurate prediction of the vibrational characteristics [75].

Shell theories discussed here are very well established theories. These theories are able to model mechanical behaviors of carbon nanotubes. Shells are capable of modeling the cross sectional deformation of the tubes as well as their bending, torsional and extensional behaviors. However, these theories cannot be used to study the effects of atomic structure of the tube on its vibrational characteristics. The geometrical and mechanical parameters which are used in these studies are basically obtained from empirical or numerical studies. The correctness of the results is heavily dependent on the way these parameters are calculated.

2.4.3. Beam theories

Vibrations of single and multi-walled nanotubes have been studied by many researchers within the last ten years using different beam theories. For multi-walled carbon nanotubes, inner and outer tubes are generally modeled as individual elastic beams interacting by van der Waals forces. Yoon et al. [76] calculated frequencies and associated mode shapes of noncoaxial isolated multi-walled carbon nanotubes. They also studied individual multi-walled carbon nanotubes embedded in an elastic medium using multiple-elastic beam model [77]. Vibrations of double-walled carbon nanotubes were considered for different boundary conditions and various ways of incorporating van der Waals force into the analyses [78-83]. Elishakoff and Penaras [79] obtained fundamental frequencies under various boundary conditions and derived explicit expressions for the natural frequencies by applying the Bubnov-Galerkin and Petrov-Galerkin methods. Timoshenko beam theory was also applied in the free vibration analysis of multi-walled carbon nanotubes [83-87]. In these studies, the rotary inertia and shear deformation were seen to influence the natural frequencies and corresponding mode shapes. Effects of compressive load (or in-plane stress) on the vibration of double-walled carbon nanotube

were also examined by simple beam theory [88, 89] and by the Timoshenko beam theory [90].

Nonlinear free vibration of embedded multi-walled carbon nanotubes based on the continuum mechanics and a multiple-elastic beam model was investigated by Fu et al. [91] by using the incremental harmonic balance and iterative methods in their analysis. They discussed the effects of the surrounding elastic medium, van der Waals forces and aspect ratio on the amplitude-frequency response characteristics. By treating the van der Waals force as nonlinear, vibrations of multi-walled carbon nanotubes were studied by some researchers (Xu et al. [92], Mahdavi et al. [93, 94]). A double-walled carbon nanotube under harmonic excitation was modeled as two doubly clamped beams coupled through nonlinear continuous springs representing the van der Waals bonds [95]. Geometric nonlinearity was included due to mid-plane stretching in the Galerkin approach to discretize the integro-partial differential equation leading to two nonlinear coupled second-order ordinary differential governing equations. The geometrically nonlinear modeling of functionally graded Timoshenko beam reinforced by single-walled carbon nanotubes were studied by Ke et al. [96] and they discussed in their paper the effects of nanotube volume fraction, vibration amplitude, slenderness ratio, end supports and carbon nanotube distribution on the nonlinear free vibration characteristics.

As seen, different beam theories are used extensively to model the mechanical behaviors of carbon nanotubes. Beam theories are relatively simple, comparing to molecular dynamic techniques and shell theories, and closed form solutions are available in the literature for their static and modal analyses. However, cross sectional deformation of carbon nanotubes cannot be simulated by these theories. The accuracy of above simulations are based on the precision of geometrical and stiffness parameters used in the formulas. These parameters are obtained either from experimental works or numerical simulations.

2.4.4. Nonlocal theory of elasticity

Elastic high frequency waves show dispersive characteristics which are not considered in classical theory of elasticity and also ignore the long range intermolecular forces [97]. Therefore, Eringen [98] proposed a nonlocal theory of micro orphic continua extending his previous works to improve the classical continuum mechanics for granular and fibrous solids. According to this theory, the stress at an arbitrary point in the elastic body not only depends on the strain at that point, but it also on the strains at all other points in the body. Eringen studied two problems, viz. the screw dislocation and Rayleigh surface waves, by this theory and found results which are supported by atomic lattice dynamics and experiments. Based on this nonlocal theory, Wang and Wang [99] developed constitutive relations for application in the analysis of carbon nanotubes modeled as Euler-Bernoulli beams, Timoshenko beams or as cylindrical shells. Reddy and Pang [100] also presented equations of motion for Euler Bernoulli and Timoshenko beams using this theory and applied those to investigate static bending, vibration and buckling of beams with various boundary conditions. Pradhan and Murmu [101] employed both Winkler-type and Pasternak-type foundation models to simulate the interaction of the single-walled carbon nanotubes with the surrounding elastic medium, when they studied the vibration response by the method of differential quadrature. The geometrically nonlinear case of this problem was examined by Ke et al. [102]. Several other papers have also been published on carbon nanotubes modeled by different beam theories in conjunction with the nonlocal theory of elasticity [103-108].

2.5. Vibration of graphitic sheets

A graphene sheet is formed by carbon atoms arranged in the form of hexagonal cells in a two-dimensional array in which an atom is shared by three cells. A free standing graphene structure was reported for the first time in 2005 by Novoselov et al [109, 110]. Since then, researchers studied synthesis methods, mechanical characteristics and potential applications of graphene structures [111, 112]. In earlier sections, it is found that single and multi-walled carbon nanotubes have been studied and reported in the literature

by a large number of researchers using many different techniques. But, the literature available on the vibrations of graphene sheets is not quite that vast. In the following, a brief discussion on the published research on this topic is presented.

A continuum plate model was developed by Liew et al. [113] to study the vibrations of multi-layered graphene sheets embedded in elastic matrix. They carried out analytical simulations to examine the effects of van der Waals forces on the natural frequencies of double and triple-layered graphene sheets. The authors went on to investigate further the influence of the van der Waals forces on the frequencies and mode shapes of multi-layered graphene sheets [114]. Wang et al. [115] used the same idea for vibrational analysis of multi-layered graphene sheets. They increased the accuracy of van der Waals forces in their simulations. Vibration analysis of multi-layered graphene sheet embedded in an elastic continuum was also reported by Behfar and Naghdabadi [116] considering different values of the elastic moduli in two perpendicular in-plane directions.

Garcia-Sanchez [117] carried out measurements on nano-electro-mechanical systems based on multi-layered graphene sheets suspended over trenches in silicon oxide. The suspended graphene sheets were electro statically driven at resonance using applied radio frequency voltages and their eigen modes were identified and imaged spatially. They modeled the suspended sheets by the finite element method and the analysis showed that eigen modes were the result of nonuniform stress with remarkably large magnitudes (up to 1.5 GPa). Many different molecular dynamic simulations are used in the literature to find mechanical properties [118-120] and vibrational characteristics of graphitic sheets [121, 122]. Vibrations with fundamental resonant frequencies in the megahertz range of the nano-electro-mechanical systems, were fabricated from single and multi-layered graphene sheets by mechanically exfoliating thin sheets from graphite over trenches in silicon oxide, were actuated either optically or electrically and detected optically by interferometry [123]. Gillen et al. [124] investigated the lattice vibrations in graphene nano-ribbons with zigzag and armchair type edges, by the density functional theory. The boundary conditions induced by the nano-ribbon edges allowed for an interpretation of the phonons as fundamental modes and their respective overtones.

The lattice structure method discussed earlier is used to study the mechanical properties and vibrational behaviors of graphitic sheets. The natural frequencies and mode shapes of single-layered graphene sheets with different chirality and boundary conditions were reported by Sakhaee-Pour et al. [125]. Georgantzinis et al. [126] used this method to find overall mechanical characteristics of multi-layered graphene sheets. Avila et al. [127] studied the vibrational behavior of multi-layered graphene sheets using this method. The elastic buckling of single-layered cantilevered and bridged graphene sheets with zigzag and armchair chiralities was also studied and reported [128].

Classical and first order shear deformable thin plate theories were reformulated by Pradhan and Phadikar [129] using the nonlocal theory of elasticity and the Navier's approach to investigate the vibration of simply supported double-layered graphene sheets. Murmu and Pradhan used the nonlocal elasticity theory on the vibration of graphene sheets embedded in elastic medium [130] and in-plane vibration condition [131]. In these studies, nonlocal effects were found to be quite significant. Nonlinear vibration of a simply supported, rectangular, single-layered graphene sheet in thermal environments was presented by Shen et al. [132] with von Karman nonlinearity and nonlocal elasticity theory. Jomehzadeh and Saidi [133] and Arash and Wang [134] are also used nonlocal elasticity to simulate graphitic sheets. A finite element model based on nonlocal elasticity is also presented by Ansari et al. [135]. It was observed that nonlocal plate model could predict remarkably accurate nonlinear dynamic behavior of graphene sheet, if the small scale parameters and materials properties were selected properly. Nonlinear vibration of single-layered graphene sheets used as electro-mechanical resonators was studied by Sadeghi and Naghdabadi [122] by a hybrid atomistic-structural element based on an empirical inter-atomic potential function. Vibrational properties of graphene nano-ribbons with armchair and zigzag-type edges by means of first-principles calculations was reported in [136] on the basis of density-functional theory.

2.6. Concluding remarks

The structural components are becoming smaller and smaller in macro-to-micro-to-nano scales. Graphitic sheets and nanotubes are used as replacements of the fibers in composites due to enhanced properties. Additionally, the applications of nano-size structures are growing at a very rapid rate and the need of new methods to analyze and design with them is also growing. These reasons have caused explosion in the research carried out in nanotechnology throughout this world and the interest to grow further will remain very high.

Researchers have proposed methods to produce carbon nano-structures. Improvements are being made continuously on controlling the size and atomic structures so that their mechanical properties can be enhanced. To understand the properties further, many experimental techniques such as atomic force microscopy, high resolution electron microscopy, and scanning electron microscopy have also been used. In this paper, attempts are made to bring out the essentials that are required to understand the properties of carbon nanostructures by engineers with structural mechanics background so that analyzing such materials becomes simple and straight forward. A brief survey of the subject matter from vibrational aspect is presented including some basic characterization of the carbon nanotubes and graphitic sheets.

Different molecular dynamic methods have been suggested by researchers to simulate the static, vibration and buckling behavior of carbon nanotubes and graphitic sheets. These techniques, beside their exceptional accuracy, are just able to model very short-duration phenomena and also, they cannot be used for systems with more than several hundred particles. The relatively new structural mechanical approach reviewed in this paper is much more efficient than molecular dynamics while having very good accuracy. From this type of analyses, it is found that carbon nanotubes and graphene sheets behave like shell and plate structures respectively.

Although some researchers have used shell and plate theories in their analyses, this approach has serious limitations with regards to defining the thickness, Young's modulus and other mechanical properties of the structure. Therefore, treating carbon nanotubes and

graphitic sheets as an elastic shell continuum may not be fully justified as there is no consensus on how the shell thickness and/or other properties can be used in this method. Simplified models based on classical and shear deformable beam theories have also been used by many for modeling the mechanical behavior of carbon nanotubes. Owing to the simplicity of beam theories, this analytical technique has relatively less computational and mathematical rigor. However, beam theories, same as shell theories, cannot model the atomic structure of carbon nano structures. Moreover, beam models are unable to simulate cross sectional deformation of carbon nanotubes. Nonlocal elasticity theories are also used along with shell and beam theories in the literature for modeling carbon nanotubes. Nano-plates with nonlocal elastic properties are used for modeling graphitic sheets. While nonlocal elasticity provides more accurate results, scientists could not present a systematic way for finding nonlocal moduli.

Research should continue in the direction on how to establish very clear and concise links connecting the chemistry and engineering applications of nano-structures. Numerical methods to compute properties of composites embedded with nano-fibers and structural analysis in general and vibration studies in particular are expected to make a huge difference in the outlooks of the scientists and engineers. New simple, straightforward and accurate methods are expected to be developed in near future to help researchers get a better understanding about mechanical behavior of carbon based nano-structures.

References

- [1] Kroto, H. W., Heath, J. R., O'Brien, S. C., Curl, R. F., and Smalley, R. E., 1985, "C₆₀: Buckminsterfullerene," *Nature*, 318(6042), pp. 162-163.
- [2] Kratschmer, W., Lamb, L. D., Fostiropoulos, K., and Huffman, D. R., 1990, "Solid C₆₀: A new form of carbon," *Nature*, 347(6291), pp. 354-358.
- [3] Iijima, S., 1991, "Helical microtubules of graphitic carbon," *Nature*, 354(6348), pp. 56-58.
- [4] Iijima, S., and Ichihashi, T., 1993, "Single-shell carbon nanotubes of 1-nm diameter," *Nature*, 363(6430), pp. 603-605.

- [5] Treacy, M. M. J., Ebbesen, T. W., and Gibson, J. M., 1996, "Exceptionally high Young's modulus observed for individual carbon nanotubes," *Nature*, 381(6584), pp. 678-680.
- [6] Salvétat, J. P., Bonard, J. M., Thomson, N. B., Kulik, A. J., Forró, L., Benoit, W., and Zuppiroli, L., 1999, "Mechanical properties of carbon nanotubes," *Applied Physics A: Materials Science and Processing*, 69(3), pp. 255-260.
- [7] Dresselhaus, M. S., Dresselhaus, G., and Eklund, P. C., 1995, *Science of fullerenes and carbon nanotubes*, Academic Press, New York.
- [8] Harris, P. J. F., 1999, *Carbon nanotubes and related structures: new materials for the twenty-first century*, Cambridge University Press, Cambridge.
- [9] Dresselhaus, M. S., Dresselhaus, G., and Avouris, P., 2001, "Carbon nanotubes: Synthesis, structure, properties and applications," Springer-Verlag Berlin Heidelberg.
- [10] Reich, S., Thomsen, C., and Maultzsch, J., 2004, *Carbon nanotubes: Basic Concepts and physical properties*, Wiley-VCH Verlag GmbH & Co. KGaA, Weinheim.
- [11] Iijima, S., 2002, "Carbon nanotubes: Past, present, and future," *Physica B: Condensed Matter*, 323(1-4), pp. 1-5.
- [12] Thostenson, E. T., Ren, Z., and Chou, T. W., 2001, "Advances in the science and technology of carbon nanotubes and their composites: A review," *Composites Science and Technology*, 61(13), pp. 1899-1912.
- [13] Harris, P. J. F., 2004, "Carbon nanotube composites," *International Materials Reviews*, 49(1), pp. 31-43.
- [14] Qian, D., Wagner, G. J., Liu, W. K., Yu, M. F., and Ruoff, R. S., 2002, "Mechanics of carbon nanotubes," *Applied Mechanics Reviews*, 55(6), pp. 495-532.
- [15] Chen, X., and Huang, Y., 2008, "Nanomechanics modeling and simulation of carbon nanotubes," *Journal of Engineering Mechanics*, 134(3), pp. 211-216.
- [16] Gibson, R. F., Ayorinde, E. O., and Wen, Y. F., 2007, "Vibrations of carbon nanotubes and their composites: A review," *Composites Science and Technology*, 67(1), pp. 1-28.
- [17] Chou, T. W., Gao, L., Thostenson, E. T., Zhang, Z., and Byun, J. H., 2010, "An assessment of the science and technology of carbon nanotube-based fibers and composites," *Composites Science and Technology*, 70(1), pp. 1-19.
- [18] Brown, T. E., LeMay, H. E., and Bursten, B. E., 2005, Prentice Hall.

- [19] Lennard-Jones, J. E., 1924, "The determination of molecular fields: from the variation of the viscosity of a gas with temperature," *Proceedings of the Royal Society of London. Series A, Containing Papers of a Mathematical and Physical Character*, 106.
- [20] Battezzati, L., Pisani, C., and Ricca, F., 1975, "Equilibrium conformation and surface motion of hydrocarbon molecules physisorbed on graphite," *Journal of the Chemical Society, Faraday Transactions 2: Molecular and Chemical Physics*, 71, pp. 1629-1639.
- [21] Marx, D., and Hutter, J., 2009, *Molecular Dynamics*, Cambridge University Press, Cambridge.
- [22] Tersoff, J., 1988, "New empirical approach for the structure and energy of covalent systems," *Physical Review B*, 37(12), pp. 6991-7000.
- [23] Robertson, D. H., Brenner, D. W., and Mintmire, J. W., 1992, "Energetics of nanoscale graphitic tubules," *Physical Review B*, 45(21), pp. 12592-12595.
- [24] Iijima, S., Brabec, C., Maiti, A., and Bernholc, J., 1996, "Structural flexibility of carbon nanotubes," *Journal of Chemical Physics*, 104(5), pp. 2089-2092.
- [25] Lu, J. P., 1997, "Elastic properties of carbon nanotubes and nanoropes," *Physical Review Letters*, 79(7), pp. 1297-1300.
- [26] Cornwell, C. F., and Wille, L. T., 1997, "Elastic properties of single-walled carbon nanotubes in compression," *Solid State Communications*, 101(8), pp. 555-558.
- [27] Yao, N., and Lordi, V., 1998, "Young's modulus of single-walled carbon nanotubes," *Journal of Applied Physics*, 84(4), pp. 1939-1943.
- [28] Xin, Z., Jianjun, Z., and Zhong-can, O. Y., 2000, "Strain energy and Young's modulus of single-wall carbon nanotubes calculated from electronic energy-band theory," *Physical Review B - Condensed Matter and Materials Physics*, 62(20), pp. 13692-13696.
- [29] Zhou, L. G., and Shi, S. Q., 2002, "Molecular dynamic simulations on tensile mechanical properties of single-walled carbon nanotubes with and without hydrogen storage," *Computational Materials Science*, 23(1-4), pp. 166-174.
- [30] Zhang, P., Huang, Y., Geubelle, P. H., Klein, P. A., and Hwang, K. C., 2002, "The elastic modulus of single-wall carbon nanotubes: A continuum analysis incorporating interatomic potentials," *International Journal of Solids and Structures*, 39(13-14), pp. 3893-3906.
- [31] Thostenson, E. T., and Chou, T. W., 2003, "On the elastic properties of carbon nanotube-based composites: Modelling and characterization," *Journal of Physics D: Applied Physics*, 36(5), pp. 573-582.

- [32] Odegard, G. M., Gates, T. S., Nicholson, L. M., and Wise, K. E., 2002, "Equivalent-continuum modeling of nano-structured materials," *Composites Science and Technology*, 62(14), pp. 1869-1880.
- [33] Gates, T. S., Odegard, G. M., Frankland, S. J. V., and Clancy, T. C., 2005, "Computational materials: Multi-scale modeling and simulation of nanostructured materials," *Composites Science and Technology*, 65(15-16 SPEC. ISS.), pp. 2416-2434.
- [34] Hu, N., Fukunaga, H., Lu, C., Kameyama, M., and Yan, B., 2005, "Prediction of elastic properties of carbon nanotube reinforced composites," *Proceedings of the Royal Society A: Mathematical, Physical and Engineering Sciences*, 461(2058), pp. 1685-1710.
- [35] Song, Y. S., and Youn, J. R., 2006, "Modeling of effective elastic properties for polymer based carbon nanotube composites," *Polymer*, 47(5), pp. 1741-1748.
- [36] Wang, X. Y., and Wang, X., 2004, "Numerical simulation for bending modulus of carbon nanotubes and some explanations for experiment," *Composites Part B: Engineering*, 35(2), pp. 79-86.
- [37] Lau, K. T., Chipara, M., Ling, H. Y., and Hui, D., 2004, "On the effective elastic moduli of carbon nanotubes for nanocomposite structures," *Composites Part B: Engineering*, 35(2), pp. 95-101.
- [38] Scarpa, F., and Adhikari, S., 2008, "A mechanical equivalence for Poisson's ratio and thickness of C-C bonds in single wall carbon nanotubes," *Journal of Physics D: Applied Physics*, 41(8).
- [39] Zhang, Z. Q., Liu, B., Chen, Y. L., Jiang, H., Hwang, K. C., and Huang, Y., 2008, "Mechanical properties of functionalized carbon nanotubes," *Nanotechnology*, 19(39).
- [40] Giannopoulos, G. I., Kakavas, P. A., and Anifantis, N. K., 2008, "Evaluation of the effective mechanical properties of single walled carbon nanotubes using a spring based finite element approach," *Computational Materials Science*, 41(4), pp. 561-569.
- [41] Chang, T., Geng, J., and Guo, X., 2006, "Prediction of chirality- and size-dependent elastic properties of single-walled carbon nanotubes via a molecular mechanics model," *Proceedings of the Royal Society A: Mathematical, Physical and Engineering Sciences*, 462(2072), pp. 2523-2540.
- [42] Kirtania, S., and Chakraborty, D., 2007, "Finite element based characterization of carbon nanotubes," *Journal of Reinforced Plastics and Composites*, 26(15), pp. 1557-1570.
- [43] Li, C., and Chou, T. W., 2003, "A structural mechanics approach for the analysis of carbon nanotubes," *International Journal of Solids and Structures*, 40(10), pp. 2487-2499.
- [44] Coates, R. C., Coutie, M. G., and Kong, F. K., 1972, *Structural Analysis*, John Wiley and sons Inc., New York.

- [45] Li, C., and Chou, T. W., 2003, "Elastic moduli of multi-walled carbon nanotubes and the effect of van der Waals forces," *Composites Science and Technology*, 63(11), pp. 1517-1524.
- [46] Li, C., and Chou, T. W., 2003, "Single-walled carbon nanotubes as ultrahigh frequency nanomechanical resonators," *Physical Review B - Condensed Matter and Materials Physics*, 68(7), pp. 734051-734053.
- [47] Li, C., and Chou, T. W., 2004, "Vibrational behaviors of multiwalled-carbon-nanotube-based nanomechanical resonators," *Applied Physics Letters*, 84(1), pp. 121-123.
- [48] Mir, M., Hosseini, A., and Majzoubi, G. H., 2008, "A numerical study of vibrational properties of single-walled carbon nanotubes," *Computational Materials Science*, 43(3), pp. 540-548.
- [49] Lü, J. N., Chen, H. B., Lü, P., and Zhang, P. Q., 2007, "Research of natural frequency of single-walled carbon nanotube," *Chinese Journal of Chemical Physics*, 20(5), pp. 525-530+i.
- [50] Fan, C. W., Liu, Y. Y., and Hwu, C., 2009, "Finite element simulation for estimating the mechanical properties of multi-walled carbon nanotubes," *Applied Physics A: Materials Science and Processing*, 95(3), pp. 819-831.
- [51] Sakhaee-Pour, A., Ahmadian, M. T., and Vafai, A., 2009, "Vibrational analysis of single-walled carbon nanotubes using beam element," *Thin-Walled Structures*, 47(6-7), pp. 646-652.
- [52] Shi, M. X., Li, Q. M., Liu, B., Feng, X. Q., and Huang, Y., 2009, "Atomic-scale finite element analysis of vibration mode transformation in carbon nanorings and single-walled carbon nanotubes," *International Journal of Solids and Structures*, 46(25-26), pp. 4342-4360.
- [53] Kang, J. W., Kwon, O. K., Lee, J. H., Choi, Y. G., and Hwang, H. J., 2009, "Frequency change by inter-walled length difference of double-wall carbon nanotube resonator," *Solid State Communications*, 149(37-38), pp. 1574-1577.
- [54] Georgantzinos, S. K., Giannopoulos, G. I., and Anifantis, N. K., 2009, "An efficient numerical model for vibration analysis of single-walled carbon nanotubes," *Computational Mechanics*, 43(6), pp. 731-741.
- [55] Lawler, H. M., Areshkin, D., Mintmire, J. W., and White, C. T., 2005, "Radial-breathing mode frequencies for single-walled carbon nanotubes of arbitrary chirality: First-principles calculations," *Physical Review B - Condensed Matter and Materials Physics*, 72(23), pp. 1-4.
- [56] Liu, B., Huang, Y., Jiang, H., Qu, S., and Hwang, K. C., 2004, "The atomic-scale finite element method," *Computer Methods in Applied Mechanics and Engineering*, 193(17-20), pp. 1849-1864.

- [57] Batra, R. C., and Gupta, S. S., 2008, "Wall thickness and radial breathing modes of single-walled carbon nanotubes," *Journal of Applied Mechanics, Transactions ASME*, 75(6), pp. 0610101-0610106.
- [58] Gupta, S. S., Bosco, F. G., and Batra, R. C., 2010, "Wall thickness and elastic moduli of single-walled carbon nanotubes from frequencies of axial, torsional and inextensional modes of vibration," *Computational Materials Science*, 47(4), pp. 1049-1059.
- [59] Formica, G., Lacarbonara, W., and Alessi, R., 2010, "Vibrations of carbon nanotube-reinforced composites," *Journal of Sound and Vibration*, 329(10), pp. 1875-1889.
- [60] Harrar, M. S., and Gibson, R. F., 2009, "Numerical simulation of modal vibration response of wavy carbon nanotubes," *Journal of Composite Materials*, 43(5), pp. 501-515.
- [61] Sánchez-Portal, D., Artacho, E., Soler, J. M., Rubio, A., and Ordejón, P., 1999, "Ab initio structural, elastic, and vibrational properties of carbon nanotubes," *Physical Review B - Condensed Matter and Materials Physics*, 59(19), pp. 12678-12688.
- [62] Scarpa, F., and Adhikari, S., 2008, "Uncertainty modeling of carbon nanotube terahertz oscillators," *Journal of Non-Crystalline Solids*, 354(35-39), pp. 4151-4156.
- [63] Hüttel, A. K., Steele, G. A., Witkamp, B., Poot, M., Kouwenhoven, L. P., and Van Der Zant, H. S. J., 2009, "Carbon nanotubes as ultrahigh quality factor mechanical resonators," *Nano Letters*, 9(7), pp. 2547-2552.
- [64] Wei, X., Chen, Q., Xu, S., Peng, L., and Zuo, J., 2009, "Beam to string transition of vibrating carbon nanotubes under axial tension," *Advanced Functional Materials*, 19(11), pp. 1753-1758.
- [65] Wang, C. Y., Ru, C. Q., and Mioduchowski, A., 2005, "Free vibration of multiwall carbon nanotubes," *Journal of Applied Physics*, 97(11), pp. 1-11.
- [66] Wang, C. Y., Ru, C. Q., and Mioduchowski, A., 2005, "Pressure effect on radial breathing modes of multiwall carbon nanotubes," *Journal of Applied Physics*, 97(2), pp. 024310-024311-024310-024310.
- [67] He, X. Q., Eisenberger, M., and Liew, K. M., 2006, "The effect of van der Waals interaction modeling on the vibration characteristics of multiwalled carbon nanotubes," *Journal of Applied Physics*, 100(12).
- [68] Sun, C., and Liu, K., 2007, "Vibration of multi-walled carbon nanotubes with initial axial loading," *Solid State Communications*, 143(4-5), pp. 202-207.
- [69] Sun, C. Q., and Liu, K. X., 2009, "Vibration of multi-walled carbon nanotubes with initial axial force and radial pressure," *Journal of Physics D: Applied Physics*, 42(17).

- [70] Yan, Y., Zhang, L. X., and Wang, W. Q., 2008, "Dynamical mode transitions of simply supported double-walled carbon nanotubes based on an elastic shell model," *Journal of Applied Physics*, 103(11).
- [71] Peng, J., Wu, J., Hwang, K. C., Song, J., and Huang, Y., 2008, "Can a single-wall carbon nanotube be modeled as a thin shell?," *Journal of the Mechanics and Physics of Solids*, 56(6), pp. 2213-2224.
- [72] Shi, M. X., Li, Q. M., and Huang, Y., 2009, "A nonlocal shell model for mode transformation in single-walled carbon nanotubes," *Journal of Physics Condensed Matter*, 21(45).
- [73] Arash, B., and Ansari, R., 2010, "Evaluation of nonlocal parameter in the vibrations of single-walled carbon nanotubes with initial strain," *Physica E: Low-Dimensional Systems and Nanostructures*, 42(8), pp. 2058-2064.
- [74] Chowdhury, R., Wang, C. Y., and Adhikari, S., 2010, "Low frequency vibration of multiwall carbon nanotubes with heterogeneous boundaries," *Journal of Physics D: Applied Physics*, 43(8).
- [75] Ghorbanpourarani, A., Mohammadimehr, M., Arefmanesh, A., and Ghasemi, A., 2010, "Transverse vibration of short carbon nanotubes using cylindrical shell and beam models," *Proceedings of the Institution of Mechanical Engineers, Part C: Journal of Mechanical Engineering Science*, 224(3), pp. 745-756.
- [76] Yoon, J., Ru, C. Q., and Mioduchowski, A., 2002, "Noncoaxial resonance of an isolated multiwall carbon nanotube," *Physical Review B - Condensed Matter and Materials Physics*, 66(23), pp. 2334021-2334024.
- [77] Yoon, J., Ru, C. Q., and Mioduchowski, A., 2003, "Vibration of an embedded multiwall carbon nanotube," *Composites Science and Technology*, 63(11), pp. 1533-1542.
- [78] Xu, K. Y., Aifantis, E. C., and Yan, Y. H., 2008, "Vibrations of double-walled carbon nanotubes with different boundary conditions between inner and outer tubes," *Journal of Applied Mechanics, Transactions ASME*, 75(2), pp. 0210131-0210139.
- [79] Elishakoff, I., and Pentaras, D., 2009, "Fundamental natural frequencies of double-walled carbon nanotubes," *Journal of Sound and Vibration*, 322(4-5), pp. 652-664.
- [80] Dalir, H., Amin, S. S., and Farshidianfar, A., 2009, "Effects of a small length scale on vibrations of an embedded double-walled carbon nanotube," *Mechanics of Composite Materials*, pp. 1-10.
- [81] Amin, S. S., Dalir, H., and Farshidianfar, A., 2009, "Carbon nanotube-reinforced composites: Frequency analysis theories based on the matrix stiffness," *Computational Mechanics*, 43(4), pp. 515-524.

- [82] Shayan-Amin, S., Dalir, H., and Farshidianfar, A., 2009, "Molecular dynamics simulation of double-walled carbon nanotube vibrations: Comparison with continuum elastic theories," *Journal of Mechanics*, 25(4), pp. 337-343.
- [83] Natsuki, T., Lei, X. W., Ni, Q. Q., and Endo, M., 2010, "Free vibration characteristics of double-walled carbon nanotubes embedded in an elastic medium," *Physics Letters, Section A: General, Atomic and Solid State Physics*, 374(26), pp. 2670-2674.
- [84] Yoon, J., Ru, C. Q., and Mioduchowski, A., 2005, "Terahertz vibration of short carbon nanotubes modeled as Timoshenko beams," *Journal of Applied Mechanics, Transactions ASME*, 72(1), pp. 10-17.
- [85] Wang, C. M., Tan, V. B. C., and Zhang, Y. Y., 2006, "Timoshenko beam model for vibration analysis of multi-walled carbon nanotubes," *Journal of Sound and Vibration*, 294(4), pp. 1060-1072.
- [86] Aydogdu, M., 2008, "Effects of shear deformation on vibration of doublewalled carbon nanotubes embedded in an elastic medium," *Archive of Applied Mechanics*, 78(9), pp. 711-723.
- [87] Aydogdu, M., 2008, "Vibration of multi-walled carbon nanotubes by generalized shear deformation theory," *International Journal of Mechanical Sciences*, 50(4), pp. 837-844.
- [88] Zhang, Y., Liu, G., and Han, X., 2005, "Transverse vibrations of double-walled carbon nanotubes under compressive axial load," *Physics Letters, Section A: General, Atomic and Solid State Physics*, 340(1-4), pp. 258-266.
- [89] Wang, X., and Cai, H., 2006, "Effects of initial stress on non-coaxial resonance of multi-wall carbon nanotubes," *Acta Materialia*, 54(8), pp. 2067-2074.
- [90] Aydođdu, M., and Ece, M. C., 2007, "Vibration and buckling of in-plane loaded double-walled carbon nano-tubes," *Turkish Journal of Engineering and Environmental Sciences*, 31(5), pp. 305-310.
- [91] Fu, Y. M., Hong, J. W., and Wang, X. Q., 2006, "Analysis of nonlinear vibration for embedded carbon nanotubes," *Journal of Sound and Vibration*, 296(4-5), pp. 746-756.
- [92] Xu, K. Y., Guo, X. N., and Ru, C. Q., 2006, "Vibration of a double-walled carbon nanotube aroused by nonlinear intertube van der Waals forces," *Journal of Applied Physics*, 99(6).
- [93] Mahdavi, M. H., Jiang, L. Y., and Sun, X., 2009, "Nonlinear vibration of a single-walled carbon nanotube embedded in a polymer matrix aroused by interfacial van der Waals forces," *Journal of Applied Physics*, 106(11).

- [94] Mahdavi, M. H., Jiang, L. Y., and Sun, X., 2011, "Nonlinear vibration of a double-walled carbon nanotube embedded in a polymer matrix," *Physica E: Low-Dimensional Systems and Nanostructures*.
- [95] Hawwa, M. A., and Al-Qahtani, H. M., 2010, "Nonlinear oscillations of a double-walled carbon nanotube," *Computational Materials Science*, 48(1), pp. 140-143.
- [96] Ke, L. L., Yang, J., and Kitipornchai, S., 2010, "Nonlinear free vibration of functionally graded carbon nanotube-reinforced composite beams," *Composite Structures*, 92(3), pp. 676-683.
- [97] Eringen, A. C., 1972, "Nonlocal polar elastic continua," *International Journal of Engineering Science*, 10(1), pp. 1-16.
- [98] Eringen, A. C., 1983, "On differential equations of nonlocal elasticity and solutions of screw dislocation and surface waves," *Journal of Applied Physics*, 54(9), pp. 4703-4710.
- [99] Wang, Q., and Wang, C. M., 2007, "The constitutive relation and small scale parameter of nonlocal continuum mechanics for modelling carbon nanotubes," *Nanotechnology*, 18(7).
- [100] Reddy, J. N., and Pang, S. D., 2008, "Nonlocal continuum theories of beams for the analysis of carbon nanotubes," *Journal of Applied Physics*, 103(2).
- [101] Pradhan, S. C., and Murmu, T., 2009, "Small-scale effect on vibration analysis of single-walled carbon nanotubes embedded in an elastic medium using nonlocal elasticity theory," *Journal of Applied Physics*, 105(12).
- [102] Ke, L. L., Xiang, Y., Yang, J., and Kitipornchai, S., 2009, "Nonlinear free vibration of embedded double-walled carbon nanotubes based on nonlocal Timoshenko beam theory," *Computational Materials Science*, 47(2), pp. 409-417.
- [103] Shakouri, A., Lin, R. M., and Ng, T. Y., 2009, "Free flexural vibration studies of double-walled carbon nanotubes with different boundary conditions and modeled as nonlocal Euler beams via the Galerkin method," *Journal of Applied Physics*, 106(9).
- [104] Karaoglu, P., and Aydogdu, M., 2010, "On the forced vibration of carbon nanotubes via a non-local Euler-Bernoulli beam model," *Proceedings of the Institution of Mechanical Engineers, Part C: Journal of Mechanical Engineering Science*, 224(2), pp. 497-503.
- [105] Yang, J., Ke, L. L., and Kitipornchai, S., 2010, "Nonlinear free vibration of single-walled carbon nanotubes using nonlocal Timoshenko beam theory," *Physica E: Low-Dimensional Systems and Nanostructures*, 42(5), pp. 1727-1735.
- [106] Ansari, R., and Ramezannezhad, H., 2011, "Nonlocal Timoshenko beam model for the large-amplitude vibrations of embedded multiwalled carbon nanotubes including

thermal effects," *Physica E: Low-Dimensional Systems and Nanostructures*, 43(6), pp. 1171-1178.

[107] Mehdipour, I., Soltani, P., Ganji, D. D., and Farshidianfar, A., 2011, "Nonlinear vibration and bending instability of a single-walled carbon nanotube using nonlocal elastic beam theory," *International Journal of Nanoscience*, 10(3), pp. 447-453.

[108] Lei, X. w., Natsuki, T., Shi, J. x., and Ni, Q. q., 2011, "Surface effects on the vibrational frequency of double-walled carbon nanotubes using the nonlocal Timoshenko beam model," *Composites Part B: Engineering*.

[109] Novoselov, K. S., Jiang, D., Schedin, F., Booth, T. J., Khotkevich, V. V., Morozov, S. V., and Geim, A. K., 2005, "Two-dimensional atomic crystals," *Proceedings of the National Academy of Sciences of the United States of America*, 102(30), pp. 10451-10453.

[110] Geim, A. K., and Novoselov, K. S., 2007, "The rise of graphene," *Nature Materials*, 6(3), pp. 183-191.

[111] Wu, Y. H., Yu, T., and Shen, Z. X., 2010, "Two-dimensional carbon nanostructures: Fundamental properties, synthesis, characterization, and potential applications," *Journal of Applied Physics*, 108(7).

[112] Stankovich, S., Dikin, D. A., Dommett, G. H. B., Kohlhaas, K. M., Zimney, E. J., Stach, E. A., Piner, R. D., Nguyen, S. T., and Ruoff, R. S., 2006, "Graphene-based composite materials," *Nature*, 442(7100), pp. 282-286.

[113] Liew, K. M., He, X. Q., and Kitipornchai, S., 2006, "Predicting nanovibration of multi-layered graphene sheets embedded in an elastic matrix," *Acta Materialia*, 54(16), pp. 4229-4236.

[114] He, X. Q., Kitipornchai, S., and Liew, K. M., 2005, "Resonance analysis of multi-layered graphene sheets used as nanoscale resonators," *Nanotechnology*, 16(10), pp. 2086-2091.

[115] Wang, J., He, X., Kitipornchai, S., and Zhang, H., 2011, "Geometrical nonlinear free vibration of multi-layered graphene sheets," *Journal of Physics D: Applied Physics*, 44(13).

[116] Behfar, K., and Naghdabadi, R., 2005, "Nanoscale vibrational analysis of a multi-layered graphene sheet embedded in an elastic medium," *Composites Science and Technology*, 65(7-8), pp. 1159-1164.

[117] Garcia-Sanchez, D., Van Der Zande, A. M., San Paulo, A., Lassagne, B., McEuen, P. L., and Bachtold, A., 2008, "Imaging mechanical vibrations in suspended graphene sheets," *Nano Letters*, 8(5), pp. 1399-1403.

- [118] Scarpa, F., Adhikari, S., and Srikantha Phani, A., 2009, "Effective elastic mechanical properties of single layer graphene sheets," *Nanotechnology*, 20(6).
- [119] Jiang, J. W., Wang, J. S., and Li, B., 2009, "Young's modulus of graphene: A molecular dynamics study," *Physical Review B - Condensed Matter and Materials Physics*, 80(11).
- [120] Karnet, Y. N., Nikitin, S. M., Nikitina, E. A., and Yanovskii, Y. G., 2010, "Computer simulation of mechanical properties of carbon nanostructures," *Mechanics of Solids*, 45(4), pp. 595-609.
- [121] Neek-Amal, M., and Peeters, F. M., 2010, "Linear reduction of stiffness and vibration frequencies in defected circular monolayer graphene," *Physical Review B - Condensed Matter and Materials Physics*, 81(23).
- [122] Sadeghi, M., and Naghdabadi, R., 2010, "Nonlinear vibrational analysis of single-layer graphene sheets," *Nanotechnology*, 21(10).
- [123] Bunch, J. S., Van Der Zande, A. M., Verbridge, S. S., Frank, I. W., Tanenbaum, D. M., Parpia, J. M., Craighead, H. G., and McEuen, P. L., 2007, "Electromechanical resonators from graphene sheets," *Science*, 315(5811), pp. 490-493.
- [124] Gillen, R., Mohr, M., Maultzsch, J., and Thomsen, C., 2009, "Lattice vibrations in graphene nanoribbons from density functional theory," *Physica Status Solidi (B) Basic Research*, 246(11-12), pp. 2577-2580.
- [125] Sakhaee-Pour, A., Ahmadian, M. T., and Naghdabadi, R., 2008, "Vibrational analysis of single-layered graphene sheets," *Nanotechnology*, 19(8).
- [126] Georgantzinou, S. K., Giannopoulos, G. I., and Anifantis, N. K., 2010, "Numerical investigation of elastic mechanical properties of graphene structures," *Materials and Design*, 31(10), pp. 4646-4654.
- [127] Ávila, A. F., Eduardo, A. C., and Neto, A. S., 2011, "Vibrational analysis of graphene based nanostructures," *Computers and Structures*, 89(11-12), pp. 878-892.
- [128] Sakhaee-Pour, A., 2009, "Elastic buckling of single-layered graphene sheet," *Computational Materials Science*, 45(2), pp. 266-270.
- [129] Pradhan, S. C., and Phadikar, J. K., 2009, "Nonlocal elasticity theory for vibration of nanoplates," *Journal of Sound and Vibration*, 325(1-2), pp. 206-223.
- [130] Murmu, T., and Pradhan, S. C., 2009, "Vibration analysis of nano-single-layered graphene sheets embedded in elastic medium based on nonlocal elasticity theory," *Journal of Applied Physics*, 105(6).

- [131] Murmu, T., and Pradhan, S. C., 2009, "Small-scale effect on the free in-plane vibration of nanoplates by nonlocal continuum model," *Physica E: Low-Dimensional Systems and Nanostructures*, 41(8), pp. 1628-1633.
- [132] Shen, L., Shen, H. S., and Zhang, C. L., 2010, "Nonlocal plate model for nonlinear vibration of single layer graphene sheets in thermal environments," *Computational Materials Science*, 48(3), pp. 680-685.
- [133] Jomehzadeh, E., and Saidi, A. R., 2011, "A study on large amplitude vibration of multilayered graphene sheets," *Computational Materials Science*, 50(3), pp. 1043-1051.
- [134] Arash, B., and Wang, Q., 2011, "Vibration of single- and double-layered graphene sheets," *Journal of Nanotechnology in Engineering and Medicine*, 2(1).
- [135] Ansari, R., Rajabiehfarid, R., and Arash, B., 2010, "Nonlocal finite element model for vibrations of embedded multi-layered graphene sheets," *Computational Materials Science*, 49(4), pp. 831-838.
- [136] Gillen, R., Mohr, M., Thomsen, C., and Maultzsch, J., 2009, "Vibrational properties of graphene nanoribbons by first-principles calculations," *Physical Review B - Condensed Matter and Materials Physics*, 80(15).

CHAPTER 3

On The Vibrations of Single-Walled Carbon Nanotubes[†]

3.1. Introduction

Iijima [1] reported a new type of finite needle-like carbon structures which were produced in the soot by an arc-discharge evaporation technique and possessed amazing physical properties. Later in 1993, he reported the formation of single-shell carbon tubules of 1 nanometer diameter in the soot-like deposits formed in carbon-arc chamber [2]. Several synthetic methods were developed afterwards for preparing carbon nanotubes in the form of nanoscale whiskers that were seen to be light weight and stiff as graphite along the graphene layers. A carbon nanotube can be characterized by a fullerene, a cage-like structure of carbon atoms and composed of many hexagonal and/or pentagonal cells, and is similar in structure to stacked graphene of linked hexagonal cells. Therefore, in simple and idealistic terms, carbon nanotubes are hollow cylindrical tubules composed of concentric graphitic shells with diameters on the scale of nanometers and found to exist in both single and multi-walled forms. Because of this nanometric scale along with strength and exceptionally high Young's modulus, such carbon fibers have natural edge over conventional carbon fibers in strengthening the current and future composite materials [3-6]. To design with such materials, one requires a thorough understanding of the

[†] A version of this chapter is published in the Journal of Sounds and Vibration as: Arghavan, S., and Singh, A. V., 2011, "On the vibrations of single-walled carbon nanotubes," Journal of Sounds and Vibration, 330(13), pp. 3102-3122.

morphologies, length, thickness, number of concentric shells, stiffness, strength, toughness in addition to knowing the vibrational characteristics.

Simulation of the behaviors of carbon nanotubes was started by molecular dynamic techniques using realistic many-body inter-atomic potential functions [7-9]. Classical molecular dynamics techniques used predefined potential functions (force fields), either based on empirical data or structural calculations of the total potential energy of a system [10]. Typically, using some inter-atomic potential functions, total energy of a system of particles can be calculated. Most notably Lennard-Jones 6-12 potential function and the exponential Morse potential are the two that are used in this method [11]. When the total potential energy and force fields of a system are obtained, the realistic calculations of the behavior and subsequently, the properties of a system of atoms and molecules can be carried.

Other atomistic modeling techniques such as tight binding molecular dynamics [12], density functional theory [13], Morse potential function model [14] and modified Morse potential function model [15] were also reported later on. Difficulties of molecular dynamic simulations, besides their huge computational requirement, limit atomistic modeling of systems with only a small number of molecules or atoms and the studies are usually confined to relatively short-lived phenomena from picoseconds to nanoseconds [16, 17]. Such difficulties and shortfalls motivated many researchers to find macroscopic mechanical structures to describe the behaviors of carbon nanotubes. Consequently, Yakobson [18-21] published his work on describing remarkable similarities between molecular dynamic simulation of carbon nanotubes and macroscopic shell model. He et al. [22] simulated the vibrational characteristics of multi-walled carbon nanotubes using an elastic shell model and studied in detail the effects of van der Waals forces on the longitudinal, torsional and radial natural frequencies.

On the other hand, it was shown that mechanical and electrical properties of carbon nanotubes were strongly dependent on the helicity and atomic structure of the tubes [23] and the shell model was unable to simulate these phenomena. Yuan and Liew [24] showed how the chiral angle affected the elastic properties of boron-nitride nanotubes. Moreover, shell theory in carbon nanotube simulation required some additional

information about the structure such as the Young's Modulus of elasticity of the tube which must be acquired from other sources such as experimental analyses. As a result, this method cannot be used independently and the reliance on it can be heavily dependent on the accuracy of Young's modulus determination. However, despite this shortcoming, shell theory remained as the main simulation technique for some researchers in modeling carbon nanotubes during the recent years. Ru [25] presented an article on modeling single-walled carbon nanotubes using an anisotropic shell model which covered the shortfalls from the shell theory in accommodating the chiral-dependent characteristics of carbon nanotubes.

Beam theory also has been used by many researchers in modeling the behavior of carbon nanotubes. This theory, as in the case of the shell theory, cannot model the chirality of carbon nanotubes and also is incapable of finding the Young's modulus of elasticity by itself. In 2002, Yoon et al. [26] have shown that resonant frequencies of an N-walled tube can be obtained by modifying the Euler-Bernoulli equation to include van der Waals interaction forces. Later on, they developed a double Timoshenko beam model to characterize the motions of the inner and outer tubes in a double-walled carbon nanotube [27]. This method, because of the inherent characteristics of beams, cannot simulate deformations in the cross section of the tube. As a result, this method is unable produce a large number of accurate natural frequencies and mode shapes. Even though this theory cannot simulate either the atomic structure or the deformations in the cross section of the tube, it continued to attract researchers in recent years [28-30]. Application of the advanced elasticity theories such as nonlocal elasticity theory, have been suggested to provide more accurate results [31]. Hu et al. [32] used nonlocal Euler-Bernoulli and Timoshenko beam theories to study wave propagation in double-walled carbon nanotubes. Their study showed that nonlocal Timoshenko beam model was an accurate model versus molecular dynamic simulation in analyzing the flexural wave propagation in coaxial double-walled carbon nanotubes. In another study, they applied nonlocal shell theory to investigate the transverse waves in single and double-walled carbon nanotubes [33] and provided concluding notes on the advantage of nonlocal elasticity theory over local theory.

Li and Chou [16] have presented a method for modeling the behaviors of carbon nanotubes. Their method has significantly less computational rigor than the molecular dynamic techniques and is more accurate than the above mentioned other theories since they considered the chirality of carbon nanotubes along with the atomistic behavior of carbon atoms. Consequently, it seems to be an efficient and reliable method in modeling carbon nanotubes. Later on, they applied their method in the analysis of multi-walled carbon nanotubes with nonlinear van den Waals forces [34] and showed that their method was even capable of modeling multi-walled carbon nanotubes in an accurate and efficient way. They were able to find the natural frequencies and mode shapes of both single-walled [35] and multi-walled [36] carbon nanotubes. Recently some numerical results on the frequencies and mode shapes of single-walled carbon nanotubes have been reported by Mir et al. [37] and Sakhaee Pour et al. [38]. From the above, it is found that earlier researchers have only conducted free vibration analysis of single-walled carbon nanotubes and had some attempt on the multi-walled ones as well. But, not much has been reported in the literature on the different types of modes of vibration and also on the forced vibration analysis of single-walled carbon nanotubes [39].

The present study is concerned with the detailed free and forced vibration analyses of the single-walled carbon nanotubes using the geometric and material properties available in the literature. The carbon atoms in the simulation technique are assumed to be connected by very stiff three-dimensional frame elements forming hexagonal cells on the nanotube's surface and the mass is assumed to be concentrated in the carbon atoms [35]. The natural frequencies and mode shapes are obtained through the eigen-analysis of the lattice cylindrical shell structure. A large number of eigen-values and eigen-vectors are calculated. It is found that different types of modes of vibration with bending, twisting and stretching deformation patterns appear together. This huge amount of data is overwhelming and one is unable to distinguish between the different vibrational modes. To fully understand the interaction (or the lack of it) between these types of vibrational modes of single-walled carbon nanotubes, the transient response analysis under step loading of relatively short duration is performed by Newmark's direct integration method. The fast Fourier transformation of the transient response data is performed to examine the contributions of individual natural modes to the overall response. This exercise produces

peaks at the dominant natural frequencies which are checked against the natural frequencies obtained from the free vibration analysis. Two types of carbon nanotubes with zigzag and armchair chiralities are considered with two sets of boundary conditions, namely clamped-free and clamped-clamped cases. The zigzag case shows both the axial, bending, torsional and circumferential modes of vibration decoupled from each other, but the coupling of these three types of vibrational modes is evident in the armchair case.

3.2. Modeling procedure

Researchers have described single walled carbon nanotube as a graphene sheet rolled into a tube with hexagonal cells around the circumference. Here, the carbon atoms are arranged in a two-dimensional hexagonal array wherein each atom is shared by three hexagons. The pattern of carbon atoms in a single-walled carbon nanotube is chiral meaning that the hexagons are arranged helically around the circumference without the seam. The chiral angles of 0° and 30° represent the two special cases of chirality known as “zigzag” and “armchair” respectively [40]. The atoms have covalent bonds between each other to keep them connected. These covalent bonds are taken as the connecting elements between the carbon atoms characterized by their lengths and angles in a three-dimensional space and form hexagons on the wall of the tube. Therefore, in this modeling approach the carbon atoms are considered to be connected by space frame elements with extensional, bending and torsional stiffness properties. The frame elements are assumed to be identical throughout the model and circular in cross section. The atomic mass is assumed to be concentrated at the nucleus which is taken as a node in this modeling approach [35]. The geometric and elastic properties of such elements have been obtained experimentally using graphite sheets by other researchers. Values pertaining to extensional, bending and torsional stiffness are available in the literature and given as $938 \text{ kcal. mol}^{-1} \cdot \text{\AA}^{-2}$, $126 \text{ kcal. mol}^{-1} \cdot \text{rad}^{-2}$ and $40 \text{ kcal. mol}^{-1} \cdot \text{rad}^{-2}$ respectively [41, 42]. These are then converted into equivalent mechanical units appropriate for the analysis of space frame structures and presented in Table 2.1 (Chapter 2) in which $1 \text{ \AA} = 10^{-10} \text{ m}$. The

carbon nanotube is now considered as a lattice cylindrical shell structure with stiffness coming from the three-dimensional frame elements.

Standard finite element method [43] has been used in this type of analysis by others and also in the present study. Stiffness matrix for each element are calculated in element coordinate system using the properties from Table 2.1 and then transformed into the global coordinates to build an assembled global stiffness matrix. The global mass matrix is built with the mass of each atom lumped at the nodal points. The stiffness matrix in element coordinates is the same for all elements of single-walled carbon nanotubes since material properties and length of all covalent bonds are the same. Finally, equation of motion can be written as:

$$\mathbf{M} \ddot{\mathbf{x}}(t) + \mathbf{K} \mathbf{x}(t) = \mathbf{F}(t) \quad (3.1)$$

where \mathbf{M} , \mathbf{K} and \mathbf{F} are mass matrix, stiffness matrix and force vector respectively, all assembled in global coordinate systems. Vector $\mathbf{x}(t)$ is composed of the six degree of freedoms, namely three translational and three rotational at each node in the model and the over-dot represents the differentiation with respect to time. Looking at the values of the properties of the frame element, it is found that there is a significant mismatch between the order of coefficients of mass and stiffness matrices in Eq. (3.1). To avoid such numerical imbalance and subsequently the computational difficulties, the equation of motion is further nondimensionalized and expressed as follows.

$$\tilde{\mathbf{M}} \ddot{\tilde{\mathbf{x}}}(\tilde{t}) + \tilde{\mathbf{K}} \tilde{\mathbf{x}}(\tilde{t}) = (1/EL^2) \mathbf{F}(\tilde{t}) \quad (3.2)$$

where $\tilde{\mathbf{M}} = (1/m_c) \mathbf{M}$, $\tilde{\mathbf{K}} = (1/EL) \mathbf{K}$, $\tilde{\mathbf{x}} = (1/L) \mathbf{x}$ and $\tilde{t} = t\sqrt{EL/m_c}$.

To obtain natural frequencies of the structure, free vibration analysis should be carried out. To do so, the force vector $\mathbf{F}(\tilde{t})$ which represents external forces acting on the structure is dropped from the equation of motion. Considering the motion to be harmonic motion, one can easily deduce that $\ddot{\tilde{\mathbf{x}}} = -\Omega^2 \tilde{\mathbf{x}}$ and write:

$$|\tilde{\mathbf{K}} - \Omega^2 \tilde{\mathbf{M}}| = 0 \quad (3.3)$$

Here, $\Omega = \frac{1}{2\pi} \omega \sqrt{m_c / EL}$ represents the dimensionless frequency parameter and ω is the natural frequency in radian per second. The natural frequencies and corresponding mode shapes of the structure are obtained simultaneously in this study using the matrix iteration method [44]. For the forced vibration studies, Newmark's direct integration method is used to solve Eq. (3.2) without undergoing the free vibration analysis.

3.3. Results and discussion

A computer code has been developed in-house in C++ environment with all the finite element's essentials including the plotting of results. The computation side of this project requires extra attention for creating the geometry of a carbon nanotube with (m, n) chirality. Hence, special program has been written to generate the mesh of the carbon nanotubes automatically for the zigzag and armchair chiralities. Both free and transient vibration analyses are performed to study their vibrational characteristics and reported in this paper on zigzag and armchair layouts of the hexagonal cells. For each case, the free vibration analysis is carried first to obtain the eigen-values and corresponding eigen-vectors. Literally, this analysis is performed for a few dozens of natural modes in order to capture all possible modes of vibrations, such as beam like bending, bending along the surface of the tube in both axial and circumferential directions, torsional, and extensional. Since these appear together in one set of analysis, it is extremely difficult to detect their types exactly from the visual inspection. Hence, the Newmark's direct integration technique [43] is used for the transient response calculations of the nanotubes subject to step loading of short duration. The selection of this step load becomes crucial in the sense that it has to be applied in a very specific way to trigger one particular type of vibrational mode, e.g. in order to excite the longitudinal modes, all unrestrained nodes are subject to the same magnitude of load along the axis of the carbon nanotube. Through the fast Fourier transform of the response-time histories at selected nodes, contributions of the individual natural modes of vibration of the single-walled carbon nanotube are revealed as detailed below.

In the initial step, the free vibration analysis is performed to validate the accuracy of the model and the computer code by comparing results with what have been reported by Li and Chou [35] and Sakhaee-Pour et al. [38]. Fig. 3.1 and Fig. 3.2 show the comparison of the fundamental natural frequency versus the aspect ratio (length/diameter) of the clamped-free and clamped-clamped boundary conditions respectively from the present and the previously published results [35]. Here the frequency is plotted on the logarithmic scale along the ordinate and found within one percent of each other for both zigzag and armchair chiralities. Natural frequencies are further compared with the results from ref. [38]. For this, an (8, 0) zigzag carbon nanotube with the length of 5.826 nm is considered for clamped-free and clamped-clamped boundary conditions and the results are presented in Table 3.1. The frequencies are seen to be in good agreement within 3 percent. Similarly, analysis is carried out on a 5.66 nm long (6, 6) armchair carbon nanotube and the values of the frequencies are presented in Table 3.2. It is seen that the results from the two studies in this case are also in close agreement, within 5 percent, until the eighth modes for the clamped-free conditions. But the difference is greater than ten percent for

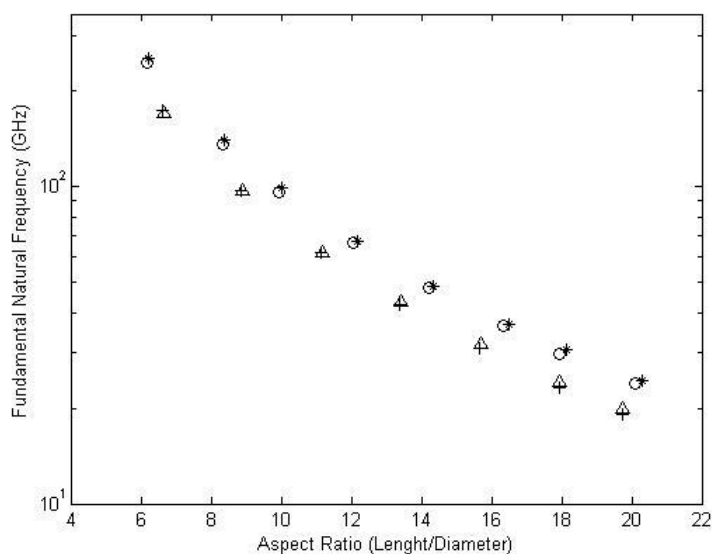


Fig. 3.1 Fundamental natural frequencies (GHz) of clamped-free carbon nanotubes with different aspect ratios, o:(5, 0) Reference [35], *:(5, 0) Present, Δ:(4, 4) Reference [35], +:(4, 4) Present

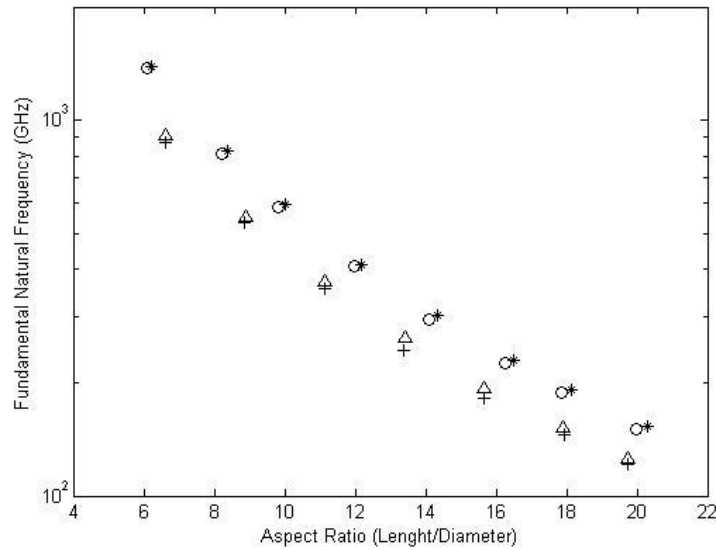


Fig. 3.2 Fundamental natural frequencies (GHz) of clamped-clamped carbon nanotubes with different aspect ratios, o:(5, 0) Reference [35], *:(5, 0) Present, Δ:(4, 4) Reference [35], +:(4, 4) Present

the ninth and tenth modes. In the case of clamped-clamped condition, the frequencies from the two studies remain within five percent until the fifth mode, but the difference increases beyond the fifth mode, when the frequencies from the earlier study [38] increases by a large margin after 1.32 THz for both cases. It seems that some eigenvalues have been missed by the previous researchers, when the frequencies are greater than 1.30 THz.

3.3.1. Case i: clamped-free zigzag single-walled carbon nanotube

In order to understand the in-depth vibrational behavior of carbon nanotubes, a (6, 0) cantilevered zigzag carbon nanotube with the length of 5.2 nm and aspect ratio (length/diameter) of 11 is considered and the results are discussed. The tube consists of 300 carbon atoms which make the mass of the whole tube equal to 5.983×10^{-24} Kg. Before starting vibrational analysis, a static analysis is performed on the tube to evaluate its Young's modulus of elasticity of the whole tube and it is found to be 0.978 TPa and

also consistent with published data [17]. Next, the first eight-values of nondimensional natural frequency Ω from the eigenvalue analysis of the tube are obtained as 0.000351 (0.0694 THz), 0.000351 (0.0694 THz), 0.002086 (0.4124 THz), 0.002086 (0.4124 THz), 0.003561 (0.7039 THz), 0.005073 (1.0028 THz), 0.005435 (1.0744 THz) and 0.005435 (1.0744 THz) respectively and their mode shapes are shown in Fig. 3.3 by solid lines, while the dotted lines show the undeformed geometry. The frequencies in GHz in the parenthesis are obtained by substituting the values of the single-walled carbon nanotube's properties from Table 2.1 into the expression of Ω . From the mode shapes, it is seen that there are three pairs of bending modes. Each pair has the same frequency, but with different phase angle, and shows repeated roots of the characteristic eigen-equation. Modes 5 and 6 do not show bending along the axis of the tube. Here, mode 5 with $\Omega = 0.003561$ appears to be torsional, while the sixth with $\Omega = 0.005073$ is definitely the extensional. In all of these modes, the cross sections do not deform significantly from the nearly circular perimeter. The bending, extensional and torsional modes are seen to be uncoupled, meaning that torsional modes show only twisting of the tube. Frequencies higher than the above eight modes have also been calculated and are reported sporadically

Table 3.1 Frequencies in THz of a zigzag single-walled carbon nanotube (8, 0) with diameter = 0.626 nm and length = 5.826 nm

Mode No.	Clamped-Free		Clamped-Clamped	
	Present	Ref. [38]	Present	Ref. [38]
1	0.0746	0.072	0.4323	0.427
2	0.0746	0.072	0.4323	0.427
3	0.4316	0.421	1.0582	1.050
4	0.4316	0.421	1.0582	1.050
5	0.6296	0.628	1.2661	1.270
6	0.9049	0.882	1.8194	1.780
7	1.0917	1.070	1.8391	1.830
8	1.0917	1.070	1.8391	1.830
9	1.8868	1.870	2.5284	2.540
10	1.9031	1.870	2.6993	2.690

Table 3.2 Frequencies in THz of a armchair single-walled carbon nanotube (6, 6) with diameter = 0.814 nm and length = 5.66 nm

Mode No.	Clamped-Free		Clamped-Clamped	
	Present	Ref. [38]	Present	Ref. [38]
1	0.1039	0.104	0.5374	0.557
2	0.1042	0.104	0.5401	0.557
3	0.5565	0.562	1.2155	1.280
4	0.5592	0.562	1.2486	1.280
5	0.6255	0.650	1.2671	1.320
6	0.9371	0.947	1.7866	1.910
7	1.3180	1.340	1.7872	2.130
8	1.3358	1.340	1.8526	2.130
9	1.7522	1.950	1.9367	2.150
10	1.7542	2.080	1.9360	2.150

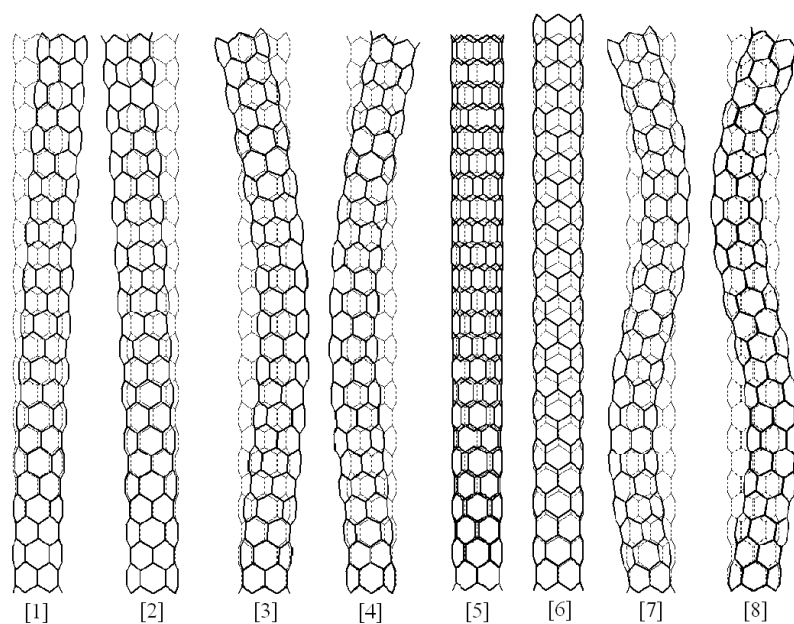


Fig. 3.3 First eight mode shapes of the (6, 0) zigzag single-walled carbon nanotube, clamped-free boundary condition

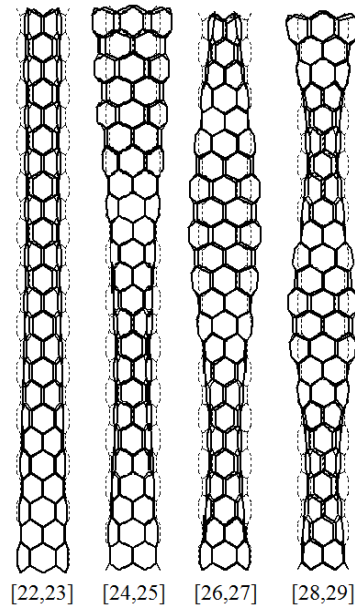


Fig. 3.4 First four mode shapes of the (6, 0) zigzag single-walled carbon nanotube with cross sectional distortion, clamped-free boundary condition

in this paper as per the needs of the discussions.

As the natural frequencies increase, the sinusoidal wave forms along the axial and circumferential directions develop and become visible in the mode shapes. This is consistent with the vibrational response behaviors of thin isotropic shells of revolution. To illustrate this phenomenon, 22nd to 29th mode shapes are presented in Fig. 3.4 with four pairs of frequencies as 0.027077 (5.3525 THz), 0.027395 (5.4154 THz), 0.02803 (5.5409 THz) and 0.029047 (5.7419 THz) respectively. The wave patterns along the axis of the carbon nanotube are clearly visible. The cross section in each of these eight modes becomes oval in accommodating the axial wave forms. For instance, the major axis of the deformed cross section is horizontal and the minor is perpendicular to it, i.e. the plane of the paper. For example, in case of the widest section of 26th and 27th modes and the axes reverse on the narrowest section in these modes. This oval behavior corresponds to the case with one sinusoidal wave in the circumferential direction. Given in Fig. 3.5 are three different forms of cross sectional variation, viz. (a) the breathing type mode in which the cross section oscillates in and out of the original shape with zero circumferential wave number, (b) beam bending type mode of the shell structure with one circumferential

wave, and (c) the type with two circumferential waves. Higher circumferential wave numbers do occur as modes of vibration get higher and the overall beam-like bending diminishes with it. It is worth mentioning that the breathing modes are found to be at very high frequencies. The nanotube considered in this study can literally have hundreds of meaningful waves formed with such combinations of wave-forms.

To further examine how modes of vibration contribute to the transient response, a step load is applied equally to all nodes in the axial direction for $\tilde{t} = 600$. Initially the response near the free end of the tube where it is expected to be the largest is considered. The fast Fourier transformation plot of it exhibits contribution only from the first axial mode. Then the transient response is recorded at a node in the proximity of the clamped end and is shown in Fig. 3.6 along with its fast Fourier transformation. The oscillation occurs for the first 600 time-units at a constant mean value and then continues at zero mean after the load is no longer applied. Five peaks are identified at $\Omega = 0.005112$,

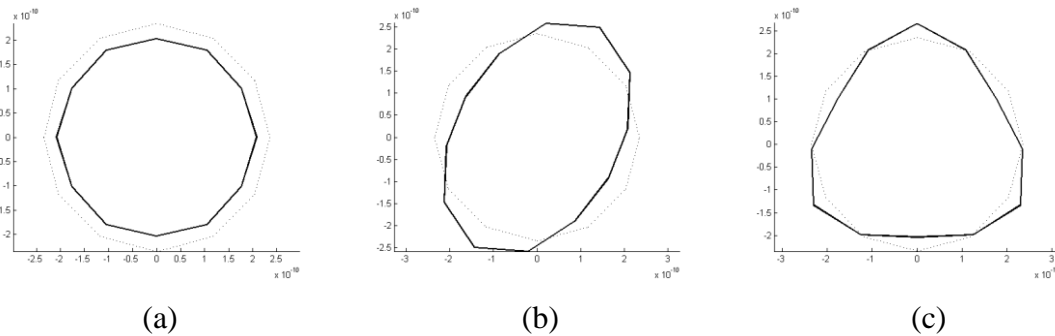


Fig. 3.5 Cross sectional deformation as circumferential wave-forms

0.01523, 0.02534, 0.03542 and 0.04543 respectively, which correspond very closely to the 6th, 14th, 19th, 38th and 50th natural frequencies obtained through eigen-analysis as 0.005073 (1.0028 THz), 0.01519 (3.0027 THz), 0.02529 (4.9992 THz), 0.03526 (6.9701 THz) and 0.04509 (8.9133 THz) respectively and their natural modes shapes are shown in Fig. 3.7. This exercise confirms that the transient response due to an axial load applied to the nanotube has contributions only from the axial/longitudinal natural modes of vibration.

Similarly, the above step load is applied to all nodes of the tube but in the horizontal plane perpendicular to the axis of the nanotube. Again, the response of a pre-selected node and its fast Fourier transformation are presented in Fig. 3.8. Three peaks are seen in this case at the nondimensional frequencies of 0.0003531, 0.002086 and 0.005434, which correspond to the six bending modes of the clamped-free tube as shown in Fig. 3.3. Evidently, other high order bending modes do contribute here, but their shares are negligibly small. To check this, fast Fourier transformation is re-plotted without the first three bending modes, but is not included here to further lengthen the paper. This exercise shows nine peaks at 0.009757, 0.0147, 0.01997, 0.02538, 0.03077, 0.03605, 0.04115, 0.04604 and 0.05054, which actually correspond to nine pairs of bending modes. All together contributions from twelve pairs of vibrational mode are observed to significant degrees. Amongst these peaks, the 5th and 6th modes are shown in Fig. 3.3 belonging to the longitudinal and torsional categories are not found.

To excite the torsional modes, equal tangential step loads are applied to all nodes of the tube to produce a counter clockwise torque about the axis of the tube. Fig. 3.9 shows the displacement versus time plot of a node near the lower end. Four peaks stand out clearly at 0.003615, 0.01069, 0.01774 and 0.02475 respectively in the fast Fourier transformation plot. Moreover, five other small peaks have been seen at 0.03167, 0.03844, 0.04511, 0.05163 and 0.05796, but the fast Fourier transformation plot is not included in this paper. From the free vibration analysis, the first four torsional modes occur at the 5th, 11th, 15th and 18th natural modes with corresponding frequencies of 0.003561 (0.7039 THz), 0.010671 (2.1094 THz), 0.017740 (3.5068 THz) and 0.024744 (4.8913 THz) respectively and their mode shapes are shown in Fig. 3.10. The torsional modes are seen to have relatively lower natural frequencies in comparison with extensional modes, but higher than the bending modes. The above transient response analyses also confirm what has been observed that the bending, longitudinal and torsional modes are decoupled.

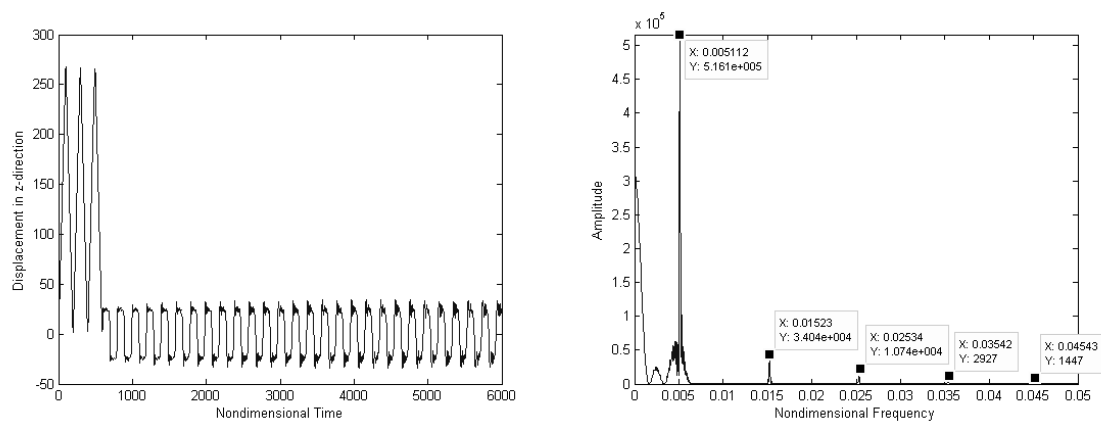


Fig. 3.6 Time history and fast Fourier transformation plot of the (6, 0) zigzag single-walled carbon nanotube, clamped-free boundary condition, load and response are in axial direction

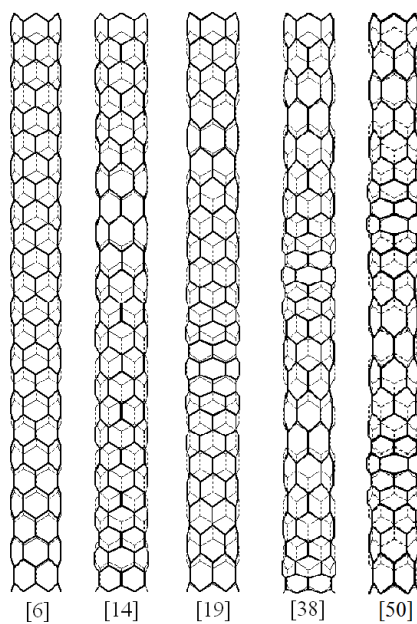


Fig. 3.7 First five extensional mode shapes of the (6, 0) zigzag single-walled carbon nanotube, clamped-free boundary condition

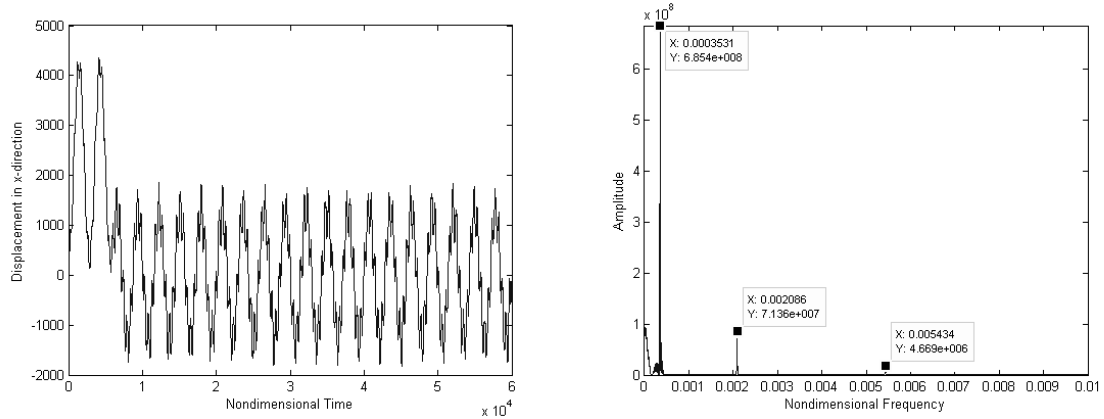


Fig. 3.8 Time history and fast Fourier transformation plot of the (6, 0) zigzag single-walled carbon nanotube, clamped-free boundary condition, load and response are in horizontal plane

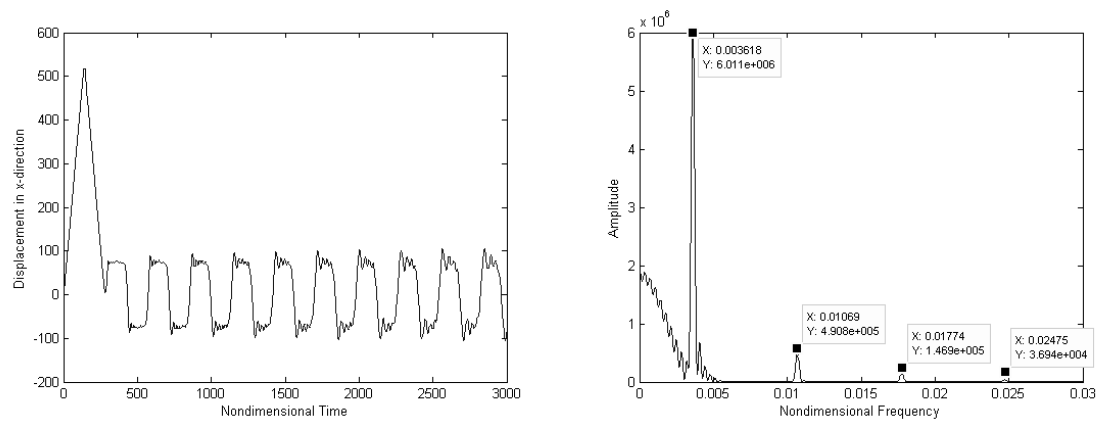


Fig. 3.9 Time history and fast Fourier transformation plot of the (6, 0) zigzag single-walled carbon nanotube, clamped-free boundary condition, torsional load is applied, response is obtained in horizontal plane

3.3.2. Case ii: clamped-clamped zigzag single-walled carbon nanotube

In this case, a nanotube with both ends clamped is investigated using the same geometric properties as above for the zigzag chirality. Again, the first eight nondimensional natural frequencies are found to be: 0.002112 (0.4175 THz), 0.002112 (0.4175 THz), 0.005347

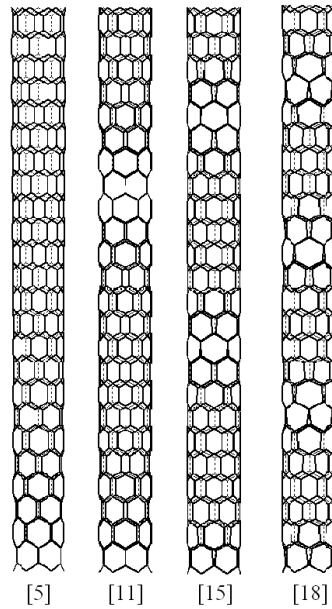


Fig. 3.10 First four torsional mode shapes of the (6, 0) zigzag single-walled carbon nanotube, clamped-free boundary condition

(1.0570 THz), 0.005347 (1.0570 THz), 0.007166 (1.4166 THz), 0.009559 (1.8896 THz), 0.009559 (1.8896 THz) and 0.010208 (2.0179 THz) respectively. The frequency values obviously are much higher for this case than the above clamped-free carbon nanotube. Their mode shapes are shown in Fig. 3.11 in which modes 1-4 and 6-7 are seen to be bending type while the 5th and 8th mode shapes are non-bending type. The cross sections in bending modes which appear in pairs remain nearly circular, i.e. without deformation. It is difficult to judge whether mode 5 (or 8) is either axial or torsional as there is no change in length due to the fixed ends. In this case, significant cross sectional deformation starts at the 18th mode rather than the 22nd in case i. The sinusoidal waves are both circumferential and axial and wave lengths decrease as the natural frequencies increase. Fig. 3.12 shows such mode shapes with deformation in the cross section occurring at nondimensional frequencies of 0.027172 (5.3713 THz), 0.028403 (5.6146 THz), 0.028691 (5.6715 THz) and 0.030242 (5.9781 THz) respectively. Symmetry and asymmetry about the mid-length of the carbon nanotube are clearly noticed.

To identify the axial modes amongst the natural modes of vibration, equal axial step loads are applied at all nodes except the ones at the fixed ends and the time-history of the

response of one of the nodes located near the lower end is shown in Fig. 3.13 along with its fast Fourier transformation plot. Four distinct peaks at nondimensional frequencies of 0.01023, 0.03057, 0.05072 and 0.06965 are detected. Extremely close to these four modes are the 8th, 29th, 51st and 81st natural modes at 0.010208 (2.0179 THz), 0.03055 (6.0390 THz), 0.05072 (10.026 THz) and 0.069662 (13.771 THz) respectively. Fig. 3.14 shows seven extensional mode shapes of the clamped-clamped tube including the four just mentioned. They appear to be symmetric and asymmetric about the middle point of the axis. Since the load is applied to all nodes in one direction, only asymmetric modes 8th, 29th, 51st and 81st out of the seven axial modes are participating in the transient response. Fig. 3.15 shows the transient response due to the load applied horizontally to all nodes and its fast Fourier transformation plot indicates two clear peaks at $\Omega = 0.002117$ and 0.009556 respectively, which correspond to the pairs of 1st and 2nd and 6th and 7th bending modes respectively. Also, additional peaks are found at frequencies 0.01952, 0.03025 and 0.0408, but they are too small to be visible with the first and sixth bending modes. Here, due to the symmetric loading condition, only the symmetric modes about the mid-point on the axis of the tube are seen to be active. Evidently, the asymmetric modes, such as the third and fourth do not participate. The torsional modes of vibration are excited by applying step load causing twisting action. By obtaining the time history and its fast Fourier transformation as shown in Fig. 3.16, the peaks are identified at frequencies $\Omega = 0.007194$, 0.02139 and 0.0353 . From the eigenvalue analysis, the torsional modes are seen to occur at $\Omega = 0.007166$ (1.4166 THz), 0.014306 (2.8280 THz), 0.021396 (4.2295 THz), 0.028403 (5.6146 THz) and 0.035308 (6.9796 THz). Due to the symmetric loading, only symmetric torsional modes about the mid-length, namely 5th, 15th and 35th as shown in Fig. 3.17 are participating in the transient response.

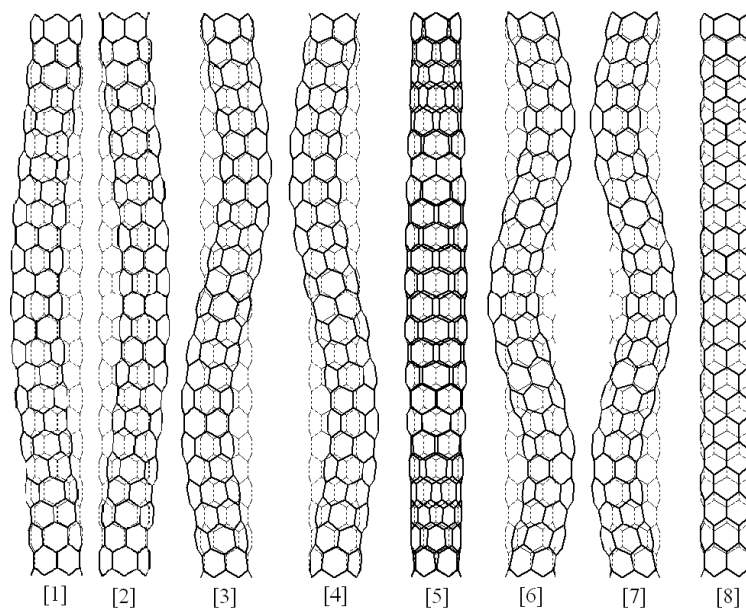


Fig. 3.11 First eight mode shapes of the (6, 0) zigzag single-walled carbon nanotube, clamped-clamped boundary conditions

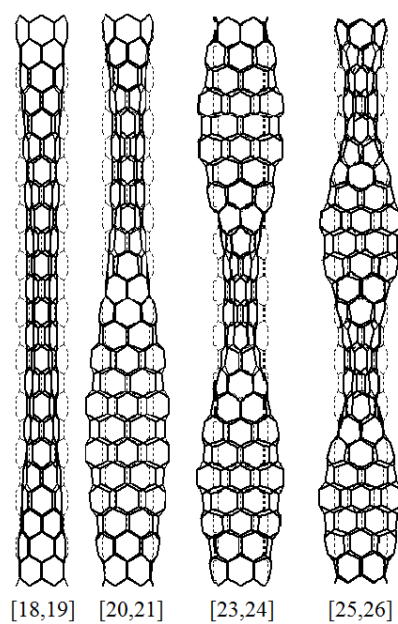


Fig. 3.12 First four mode shapes of the (6, 0) zigzag single-walled carbon nanotube with cross sectional distortion, clamped-clamped boundary condition

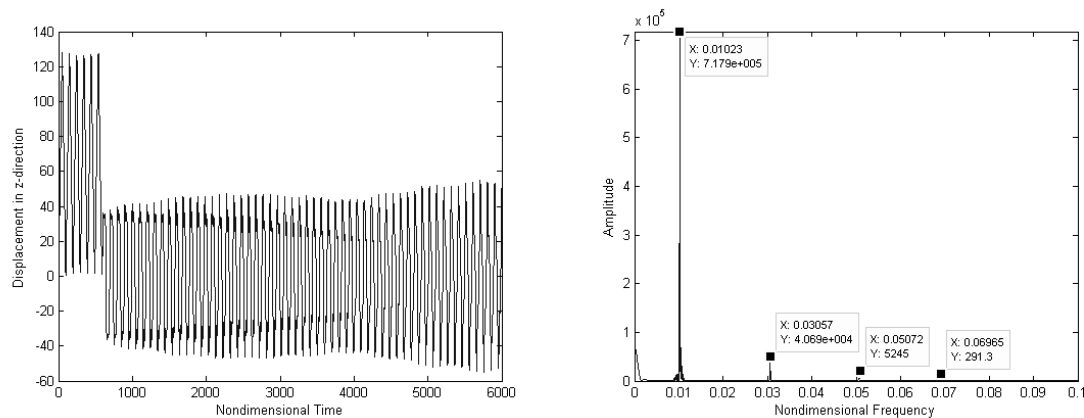


Fig. 3.13 Fast Fourier transformation plot of the (6, 0) zigzag single-walled carbon nanotube, clamped-clamped boundary conditions, load and response are in axial direction

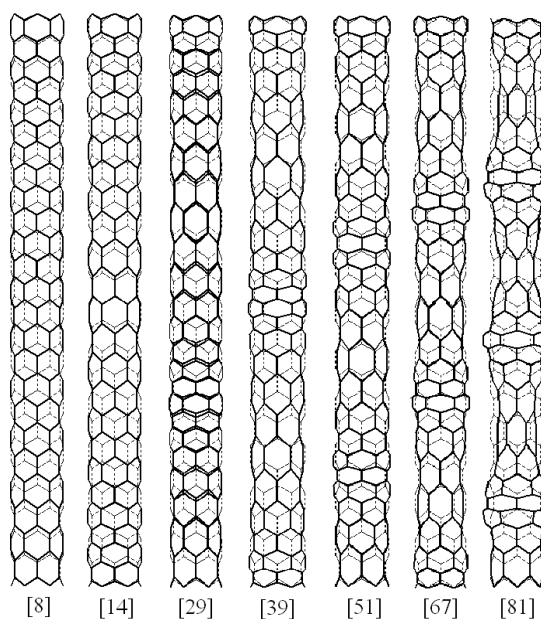


Fig. 3.14 First seven extensional mode shapes of the (6, 0) zigzag single-walled carbon nanotube, clamped-clamped boundary condition

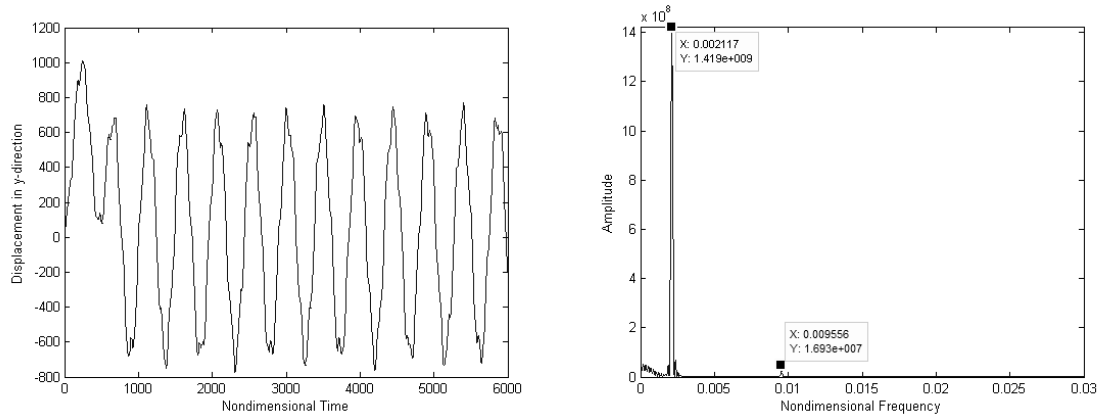


Fig. 3.15 Time history and fast Fourier transformation plot of the (6, 0) zigzag single-walled carbon nanotube, clamped-clamped boundary condition, load and response are in horizontal plane

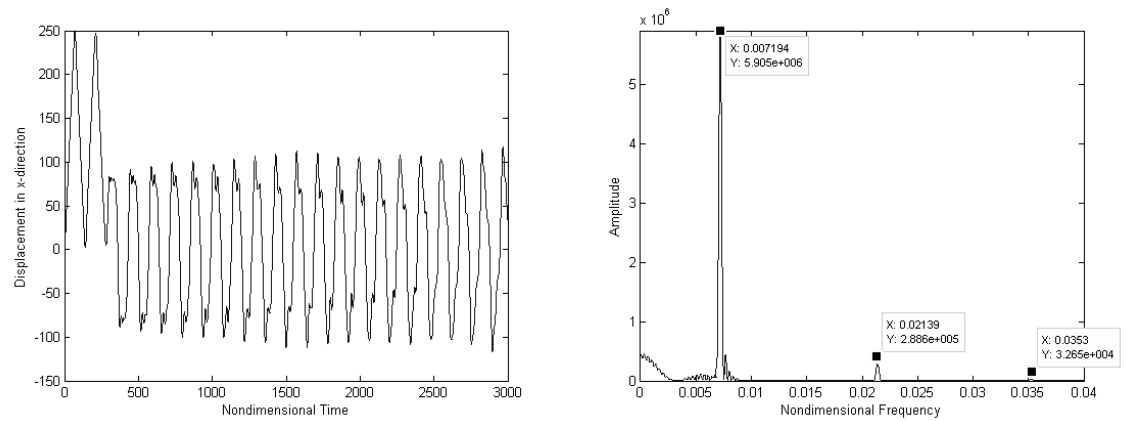


Fig. 3.16 Time history and fast Fourier transformation plot of the (6, 0) zigzag single-walled carbon nanotube, clamped-clamped boundary condition, torsional load is applied, response is obtained in horizontal plane

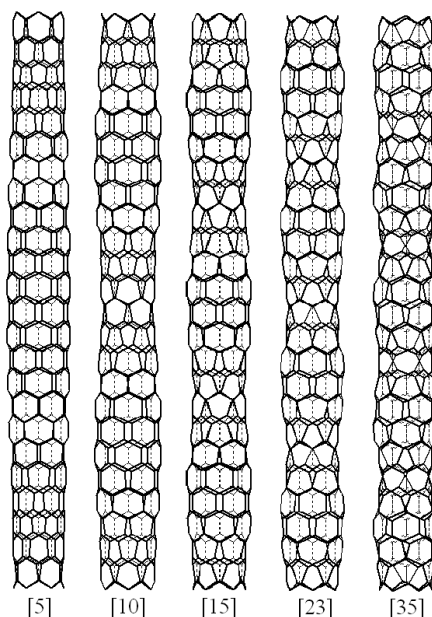


Fig. 3.17 First five torsional mode shapes of the (6, 0) zigzag single-walled carbon nanotube, clamped-clamped boundary condition

3.3.3. Case iii: clamped-free armchair single-walled carbon nanotube

Now, the study is sifted to a (4, 4) armchair clamped-free carbon nanotube with the length of 5.4 nm and aspect ratio (Length/Diameter) of 10.2. With these dimensions, the single-walled carbon nanotube is equivalent to the zigzag case studied above. Static analysis shows that the Young's modulus of elasticity is 1.054 TPa while 388 carbon atoms exist in the structure and total mass of the tube is 7.738×10^{-24} Kg. Young's modulus of elasticity is about 8% higher than the zigzag tube while 30% increase is seen in the mass of the tube. The eigen-analysis of this case yields the first eight frequencies as 0.000371 (0.07334 THz), 0.000371 (0.07334 THz), 0.002141 (0.4232 THz), 0.002144 (0.4238 THz), 0.00306472 (0.6058 THz), 0.004781 (0.9451 THz), 0.005413 (1.0700 THz) and 0.005435 (1.0744 THz) respectively and their mode shapes are presented in Fig. 3.18. The mode shapes and natural frequencies show very close resemblance in both zigzag and armchair carbon nanotubes including the sequence and range of natural frequencies.

In this case, cross section deforms more easily than the zigzag case. In many longitudinal and torsional modes, cross section will not remain circular and hence, some irregular circumferential waves can be seen. Fig. 3.19 shows severe cross sectional deformity at modes 20 and 26. As seen, cross sectional deformation is not as symmetric as in the case of the clamped-free zigzag carbon nanotube. Also, one can hardly find clear axial and circumferential waves in this set of natural modes which occur in the frequency range of 0.01847 (3.6511 THz) to 0.02107 (4.1650 THz). This range is significantly less than the zigzag case.

The transient response analysis is performed in the same manner as in the above two cases by applying a step load to all nodes and plotting the response time histories at pre-selected nodes. All three types of loading; namely axial, bending and torsional are considered separately. The fast Fourier transformation plot of axial response as shown in Fig. 3.20 reveals only two peaks at natural frequencies of 0.004781 (0.9451 THz) and 0.014515 (2.8693 THz) corresponding to 6th and 14th modes respectively. The fast Fourier transformation spectrum is re-plotted beyond these frequency values and peaks at 0.024133 (4.7705 THz) and 0.033584 (6.6387 THz) for 32nd and 45th modes are found. Fig. 3.21 shows the mode shapes at these four frequencies. Here, some wave-like patterns showing flexibility in the cross section are seen along the axis of the tube which is in contrast to the axial modes of case i. The values of these four axial modes for the armchair case are slightly lower than the corresponding four axial frequencies of the zigzag case. From the basic layout of the carbon atoms, it can be said that the zigzag carbon nanotubes have some elements parallel to the axis of the tube while armchair case doesn't. As a result, longitudinal and bending stiffnesses of zigzag carbon nanotubes are expected to be higher than that of the armchair carbon nanotubes. The analysis with horizontally applied step load shows that the bending modes at frequencies 0.0003715, 0.002141, 0.005435 and 0.009614. Similarly, the active torsional modes are found to be the 5th, 9th, 15th and 27th at frequencies 0.003065 (0.6059 THz), 0.009187 (1.8161 THz), 0.01553 (3.0699 THz) and 0.02176 (4.3014 THz) and the corresponding mode shapes are shown in Fig. 3.22.

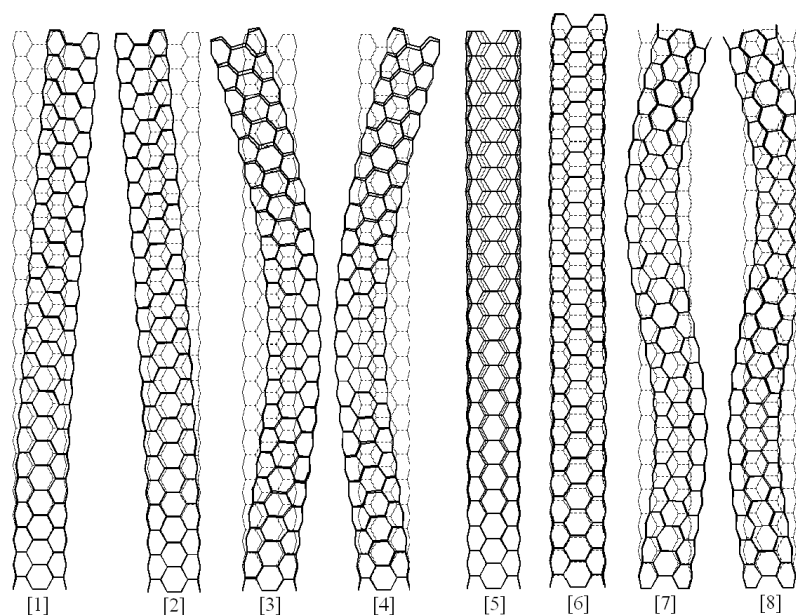


Fig. 3.18 First eight mode shapes of the (4, 4) armchair single-walled carbon nanotube, clamped-free boundary conditions

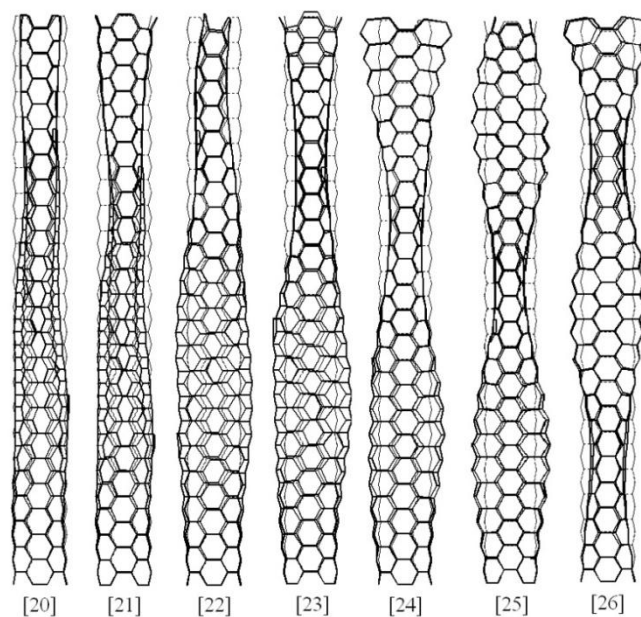


Fig. 3.19 First eight mode shapes of the (4, 4) armchair single-walled carbon nanotube with cross sectional distortion, clamped-free boundary condition

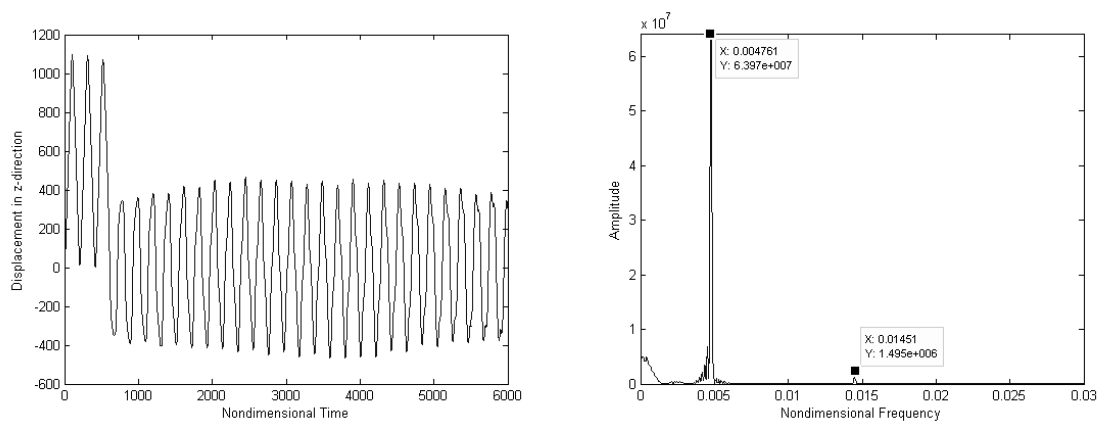


Fig. 3.20 Time history and fast Fourier transformation plot of the (4, 4) armchair single-walled carbon nanotube, clamped-free boundary condition, load and response are in axial direction

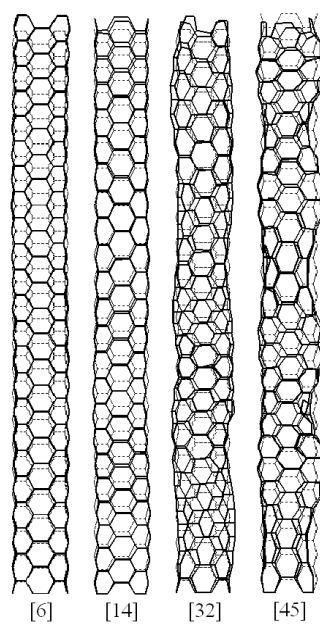


Fig. 3.21 First four extensional mode shapes of the (4, 4) armchair single-walled carbon nanotube, clamped-free boundary condition

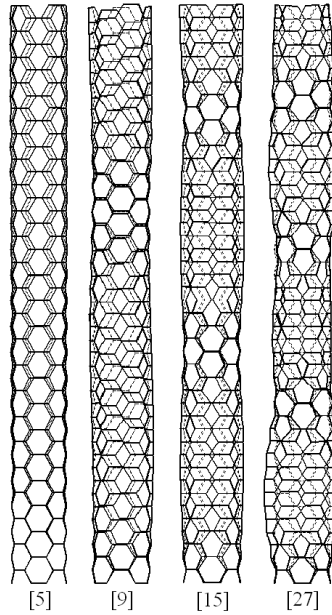


Fig. 3.22 First four torsional mode shapes of the (4, 4) armchair single-walled carbon nanotube, clamped-free boundary condition

3.3.4. Case iv: clamped-clamped armchair single-walled carbon nanotube

The first eight calculated natural frequencies of the clamped-clamped conditions of the armchair single-walled carbon nanotube having the same properties as given in case iii are: 0.002092 (0.4135 THz), 0.002095 (0.4141 THz), 0.005141 (1.0163 THz), 0.005175 (1.0230 THz), 0.006134 (1.2126 THz), 0.008994 (1.7779 THz), 0.009137 (1.8062 THz) and 0.009488 (1.8756 THz) respectively. The corresponding mode shapes are presented in Fig. 3.23, wherein the mode shapes are seen to follow essentially the same trend as in case ii but at relatively lower frequencies. Moreover, it seems that clamped-clamped boundary condition forces the tube to show more regular pattern when it comes to deformation in the cross section. Fig. 3.24 shows five pairs of modes with cross sectional distortion occurring at 0.01952 (3.8587 THz), 0.02001 (3.9556 THz), 0.02086 (4.1235 THz), 0.02232 (4.4121 THz) and 0.02437 (4.8174 THz) respectively. Here, the wave-like patterns along the axis of the tube are reasonably regular as compared to case iii. But once again, these modes get excited at lower frequencies than its counterpart the zigzag case

which maintains regularity in the wave form patterns. The symmetry and asymmetry about the mid-axis of the carbon nanotube are clearly noted. Again following the fast Fourier transformation analysis, the first four of the longitudinal mode shapes occurring at 0.009488 (1.8756 THz), 0.01912 (3.7796 THz), 0.02891 (5.7148 THz) and 0.03829 (7.5690 THz) are identified.

These four frequencies correspond to the 8th, 15th, 33rd, and 46th modes respectively of the clamped-clamped carbon nanotube (Fig. 3.25). Here also symmetry (modes 15th and 46th) and asymmetry about the mid-axis is observed. With regards to the bending and torsional modes, the following is observed. From the transient response analysis, the peaks are found at the Ω values of 0.006104, 0.01872 and 0.03128. Similarly, the torsional modes are found to occur at the frequencies of 0.006134 (1.2126 THz), 0.01240 (2.4512 THz), 0.01872 (3.7005 THz), 0.02510 (4.9617 THz) and 0.03129 (6.1853 THz) the mode shapes corresponding to which are shown in Fig. 3.26. Both symmetric and asymmetric behaviors along the axis of the carbon nanotube are observed. Also, since the applied twisting load is symmetric, only symmetric modes get excited.

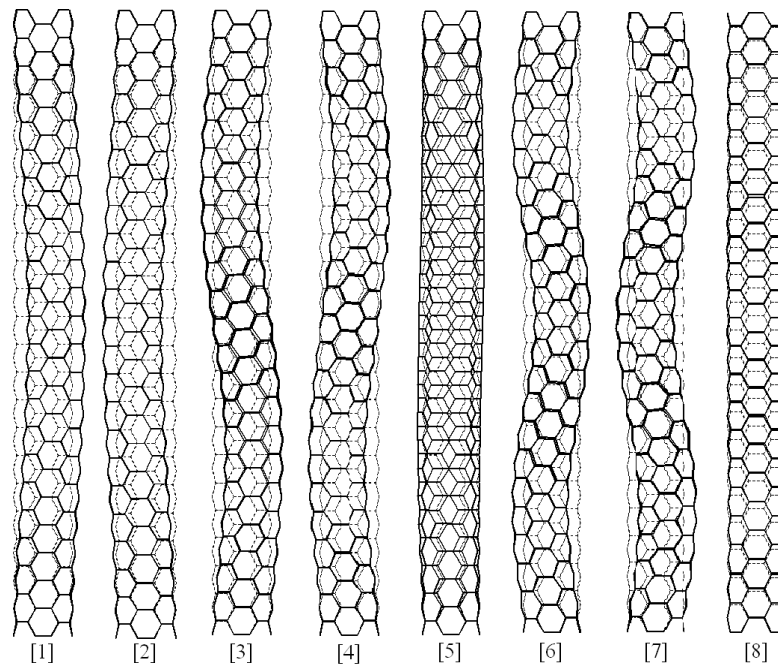


Fig. 3.23 First eight mode shapes of the (4, 4) armchair single-walled carbon nanotube, clamped-clamped boundary condition

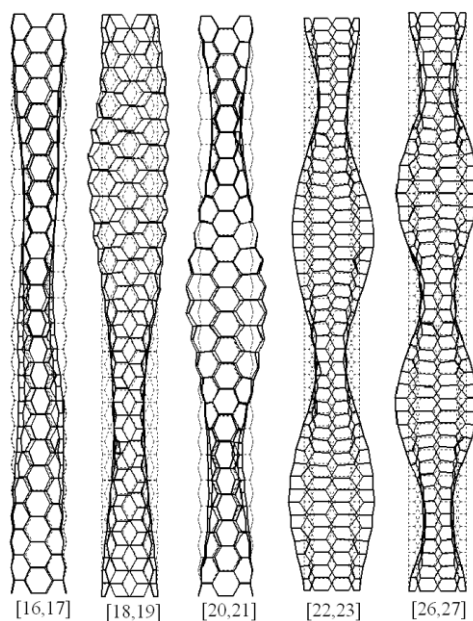


Fig. 3.24 First five mode shapes of the (4, 4) armchair single-walled carbon nanotube with cross sectional distortion, clamped-clamped boundary condition

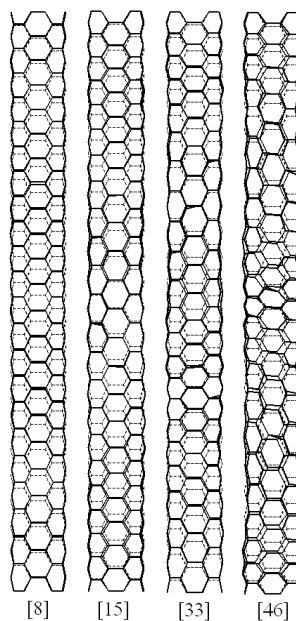


Fig. 3.25 First four extensional mode shapes of the (4, 4) armchair single-walled carbon nanotube, clamped-clamped boundary condition

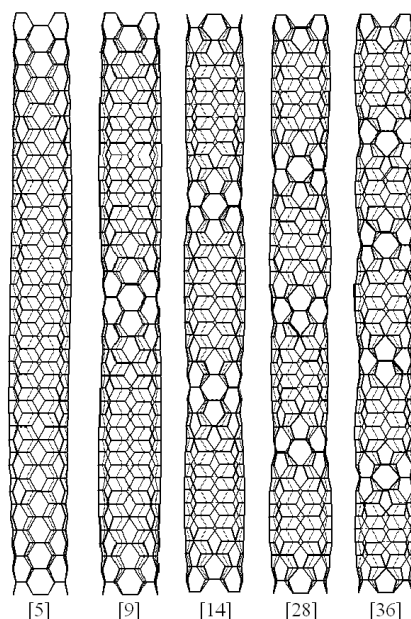


Fig. 3.26 First five torsional mode shapes of the (4, 4) armchair single-walled carbon nanotube, clamped-clamped boundary condition

From the above numerical results, it is found that single-walled carbon nanotubes of both zigzag and armchair types show very similar characteristics at the lower modes of vibration. However, their vibrational behavior diverge both quantitatively and qualitatively at very high frequency level even though the Young's moduli of the two tubes are very close to each other. To examine this behavior very closely, Fig. 3.27 is included here. It shows the first 30 natural frequencies for clamped-clamped and clamped-free boundary conditions. The frequency of the armchair single-walled carbon nanotube is seen to be much lower in this figure than that of the zigzag case. It is justifiable due to the fact that the number of carbon atoms is 30 percent higher in the armchair case and also the influence of this increased mass becomes considerably significant at higher modes of vibration.

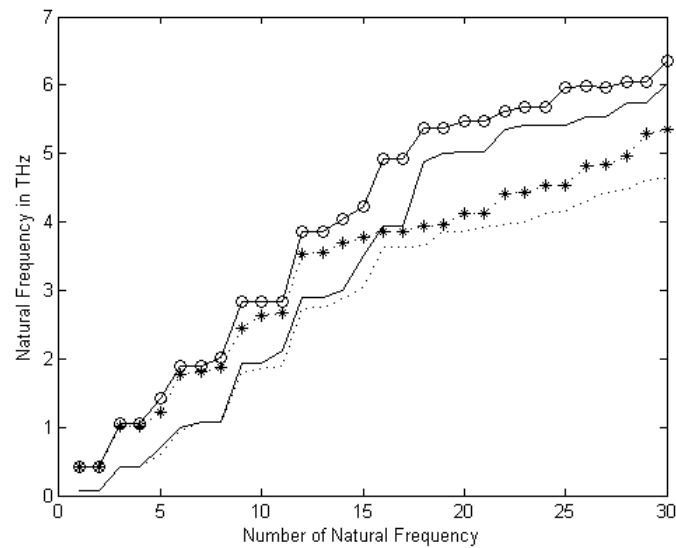


Fig. 3.27 First 30 natural frequencies of single-walled carbon nanotubes with different atomic structures and boundary conditions, ...: Armchair single-walled carbon nanotube with clamped-free boundary condition, ___: Zigzag single-walled carbon nanotube with clamped-free boundary condition, *: Armchair single-walled carbon nanotube with clamped-clamped bound, o: Zigzag single-walled carbon nanotube with clamped-clamped boundary condition

3.4. Concluding remarks

A detailed numerical investigation of the free and forced vibration analyses of single-walled carbon nanotubes has been presented. Two different layouts, viz. zigzag and armchair respectively, of the atomic structure are analyzed considering clamped-free and clamped-clamped boundary conditions. When a large number of frequencies and mode shapes are calculated by eigen-analysis, the frequencies and mode shapes are found to be from categories like bending, axial, and torsional and they all come in one pack. From their mode shapes, it is observed that carbon nanotubes behave along the same line as that of vibrating cylindrical shells and it is extremely difficult to categorize them just from visual inspection. Through the transient response analysis by the Newmark's direct integration method it becomes possible to identify the above three categories of the

modes of vibration. Both zigzag and armchair cases are found to have natural frequencies in the same numerical vicinity for the first few bending, torsional, and axial modes of vibration. Both zigzag and armchair cases exhibit very similar frequency distribution. The bending modes of vibration appear in pairs; whereas the axial and torsional mode shapes are sporadic.

The armchair chirality exhibits relatively lower natural frequencies than the counterpart zigzag case despite its slightly higher Young's modulus. Zigzag tube shows regularly formed symmetric axial and circumferential waves more along the line of continuous cylindrical shells and no coupling between longitudinal, bending, and torsional modes. On the contrary, the bending and axial modes seem to be coupled and the cross sectional deformities are quite severe, particularly if the ends are not constrained. The beam-like bending modes are found in the initial modes of vibration and seem to weaken at higher modes at which the axis of the carbon nanotube appears to be undeformed. The torsional and axial modes are found between the bending modes. In this situation, the tube deforms by bending along the surface forming waves in both the longitudinal and circumferential directions and also, for obvious reasons, the wave lengths are shorter as the frequency increases.

Acknowledgement

This research has been made possible by: (i) funding from the Natural Sciences and Engineering Research Council of Canada (NSERC) and (ii) support from the Shared Hierarchical Academic Research Computing Network (SHARCNET: <http://www.sharcnet.ca>) facilities.

References

[1] Iijima, S., 1991, "Helical microtubules of graphitic carbon," *Nature*, 354(6348), pp. 56-58.

- [2] Iijima, S., and Ichihashi, T., 1993, "Single-shell carbon nanotubes of 1-nm diameter," *Nature*, 363(6430), pp. 603-605.
- [3] Qian, D., Dickey, E. C., Andrews, R., and Rantell, T., 2000, "Load transfer and deformation mechanisms in carbon nanotube-polystyrene composites," *Applied Physics Letters*, 76(20), pp. 2868-2870.
- [4] Andrews, R., Jacques, D., Rao, A. M., Rantell, T., Derbyshire, F., Chen, Y., Chen, J., and Haddon, R. C., 1999, "Nanotube composite carbon fibers," *Applied Physics Letters*, 75(9), pp. 1329-1331.
- [5] Treacy, M. M. J., Ebbesen, T. W., and Gibson, J. M., 1996, "Exceptionally high Young's modulus observed for individual carbon nanotubes," *Nature*, 381(6584), pp. 678-680.
- [6] Salvétat, J. P., Bonard, J. M., Thomson, N. B., Kulik, A. J., Forró, L., Benoit, W., and Zuppiroli, L., 1999, "Mechanical properties of carbon nanotubes," *Applied Physics A: Materials Science and Processing*, 69(3), pp. 255-260.
- [7] Iijima, S., Brabec, C., Maiti, A., and Bernholc, J., 1996, "Structural flexibility of carbon nanotubes," *Journal of Chemical Physics*, 104(5), pp. 2089-2092.
- [8] Cornwell, C. F., and Wille, L. T., 1997, "Elastic properties of single-walled carbon nanotubes in compression," *Solid State Communications*, 101(8), pp. 555-558.
- [9] Yao, N., and Lordi, V., 1998, "Young's modulus of single-walled carbon nanotubes," *Journal of Applied Physics*, 84(4), pp. 1939-1943.
- [10] Marx, D., and Hutter, J., 2009, *Molecular Dynamics*, Cambridge University Press, Cambridge.
- [11] Tersoff, J., 1988, "New empirical approach for the structure and energy of covalent systems," *Physical Review B*, 37(12), pp. 6991-7000.
- [12] Hernández, E., Goze, C., Bernier, P., and Rubio, A., 1998, "Elastic properties of C and BxCyNz composite nanotubes," *Physical Review Letters*, 80(20), pp. 4502-4505.
- [13] Sánchez-Portal, D., Artacho, E., Soler, J. M., Rubio, A., and Ordejón, P., 1999, "Ab initio structural, elastic, and vibrational properties of carbon nanotubes," *Physical Review B - Condensed Matter and Materials Physics*, 59(19), pp. 12678-12688.
- [14] Belytschko, T., Xiao, S. P., Schatz, G. C., and Ruoff, R. S., 2002, "Atomistic simulations of nanotube fracture," *Physical Review B - Condensed Matter and Materials Physics*, 65(23), pp. 2354301-2354308.
- [15] Xiao, J. R., Gama, B. A., and Gillespie Jr, J. W., 2005, "An analytical molecular structural mechanics model for the mechanical properties of carbon nanotubes," *International Journal of Solids and Structures*, 42(11-12), pp. 3075-3092.

- [16] Li, C., and Chou, T. W., 2003, "A structural mechanics approach for the analysis of carbon nanotubes," *International Journal of Solids and Structures*, 40(10), pp. 2487-2499.
- [17] Qian, D., Wagner, G. J., Liu, W. K., Yu, M. F., and Ruoff, R. S., 2002, "Mechanics of carbon nanotubes," *Applied Mechanics Reviews*, 55(6), pp. 495-532.
- [18] Yakobson, B. I., and Smalley, R. E., 1997, "Fullerene nanotubes: C1,000,000 and beyond," *American Scientist*, 85(4), pp. 324-337.
- [19] Bernholc, J., Brabec, C., Buongiorno Nardelli, M., Maiti, A., Roland, C., and Yakobson, B. I., 1998, "Theory of growth and mechanical properties of nanotubes," *Applied Physics A: Materials Science and Processing*, 67(1), pp. 39-46.
- [20] Yakobson, B. I., Brabec, C. J., and Bernholc, J., 1996, "Structural mechanics of carbon nanotubes: From continuum elasticity to atomistic fracture," *Journal of Computer-Aided Materials Design*, 3(1-3), pp. 173-182.
- [21] Yakobson, B. I., Brabec, C. J., and Bernholc, J., 1996, "Nanomechanics of Carbon Tubes: Instabilities beyond Linear Response," *Physical Review Letters*, 76(14), p. 2511.
- [22] He, X. Q., Eisenberger, M., and Liew, K. M., 2006, "The effect of van der Waals interaction modeling on the vibration characteristics of multiwalled carbon nanotubes," *Journal of Applied Physics*, 100(12).
- [23] Lu, J. P., 1997, "Elastic properties of carbon nanotubes and nanoropes," *Physical Review Letters*, 79(7), pp. 1297-1300.
- [24] Yuan, J., and Liew, K. M., 2010, "The effects of grafted carboxyl groups on the elastic properties of single-walled boron nitride nanotubes," *Journal of Computational and Theoretical Nanoscience*, 7(10), pp. 1878-1884.
- [25] Ru, C. Q., 2009, "Chirality-dependent mechanical behavior of carbon nanotubes based on an anisotropic elastic shell model," *Mathematics and Mechanics of Solids*, 14(1-2), pp. 88-101.
- [26] Yoon, J., Ru, C. Q., and Mioduchowski, A., 2002, "Noncoaxial resonance of an isolated multiwall carbon nanotube," *Physical Review B - Condensed Matter and Materials Physics*, 66(23), pp. 2334021-2334024.
- [27] Yoon, J., Ru, C. Q., and Mioduchowski, A., 2004, "Timoshenko-beam effects on transverse wave propagation in carbon nanotubes," *Composites Part B: Engineering*, 35(2), pp. 87-93.
- [28] Aydogdu, M., 2008, "Vibration of multi-walled carbon nanotubes by generalized shear deformation theory," *International Journal of Mechanical Sciences*, 50(4), pp. 837-844.

- [29] Elishakoff, I., and Pentaras, D., 2009, "Fundamental natural frequencies of double-walled carbon nanotubes," *Journal of Sound and Vibration*, 322(4-5), pp. 652-664.
- [30] Xu, K. Y., Guo, X. N., and Ru, C. Q., 2006, "Vibration of a double-walled carbon nanotube aroused by nonlinear intertube van der Waals forces," *Journal of Applied Physics*, 99(6).
- [31] Reddy, J. N., and Pang, S. D., 2008, "Nonlocal continuum theories of beams for the analysis of carbon nanotubes," *Journal of Applied Physics*, 103(2).
- [32] Hu, Y. G., Liew, K. M., and Wang, Q., 2009, "Nonlocal elastic beam models for flexural wave propagation in double-walled carbon nanotubes," *Journal of Applied Physics*, 106(4).
- [33] Hu, Y. G., Liew, K. M., Wang, Q., He, X. Q., and Yakobson, B. I., 2008, "Nonlocal shell model for elastic wave propagation in single- and double-walled carbon nanotubes," *Journal of the Mechanics and Physics of Solids*, 56(12), pp. 3475-3485.
- [34] Li, C., and Chou, T. W., 2003, "Elastic moduli of multi-walled carbon nanotubes and the effect of van der Waals forces," *Composites Science and Technology*, 63(11), pp. 1517-1524.
- [35] Li, C., and Chou, T. W., 2003, "Single-walled carbon nanotubes as ultrahigh frequency nanomechanical resonators," *Physical Review B - Condensed Matter and Materials Physics*, 68(7), pp. 734051-734053.
- [36] Li, C., and Chou, T. W., 2004, "Vibrational behaviors of multiwalled-carbon-nanotube-based nanomechanical resonators," *Applied Physics Letters*, 84(1), pp. 121-123.
- [37] Mir, M., Hosseini, A., and Majzoobi, G. H., 2008, "A numerical study of vibrational properties of single-walled carbon nanotubes," *Computational Materials Science*, 43(3), pp. 540-548.
- [38] Sakhae-Pour, A., Ahmadian, M. T., and Vafai, A., 2009, "Vibrational analysis of single-walled carbon nanotubes using beam element," *Thin-Walled Structures*, 47(6-7), pp. 646-652.
- [39] Singh, A. V., and Arghavan, S., 2010, "Vibrations of carbon nanoscale structures: a critical review," *Computational Technology Reviews*, 1, pp. 281-314.
- [40] Reich, S., Thomsen, C., and Maultzsch, J., 2004, *Carbon nanotubes: Basic Concepts and physical properties*, Wiley-VCH Verlag GmbH & Co. KGaA, Weinheim.
- [41] Cornell, W. D., Cieplak, P., Bayly, C. I., Gould, I. R., Merz Jr, K. M., Ferguson, D. M., Spellmeyer, D. C., Fox, T., Caldwell, J. W., and Kollman, P. A., 1995, "A second generation force field for the simulation of proteins, nucleic acids, and organic molecules," *Journal of the American Chemical Society*, 117(19), pp. 5179-5197.

[42] Jorgensen, W. L., and Severance, D. L., 1990, "Aromatic-aromatic interactions: Free energy profiles for the benzene dimer in water, chloroform, and liquid benzene," *Journal of the American Chemical Society*, 112(12), pp. 4768-4774.

[43] Bathe, K. J., and Wilson, E. L., 1976, *Numerical methods in finite element analysis*, Prentice Hall Inc., New Jersey.

[44] Thomsom, W. T., 1972, *Theory of vibration with applications*, Prentice-Hall Inc, New Jersey.

CHAPTER 4

Mechanical Properties and Vibrational Characteristics of Graphenes[‡]

4.1. Introduction

Until very recently, it was a general perception that single-layered graphene sheets cannot exist in free-standing form. After years of ground breaking research, Novoselov and colleagues [1] demonstrated the existence of a two-dimensional free-standing carbon structure. This flat layer of carbon atoms tightly packed into a two-dimensional array of honeycomb-like cells was termed as graphene and could be prepared by cleavage from multi-layered graphitic material. Although graphene has a very short history, it has shown great potential for many future applications on the basis of its exceptional mechanical, electrical and thermal properties [2]. It can be wrapped up into fullerenes, rolled into nanotubes and stacked up to produce three-dimensional graphite [3]. Graphene-based materials have been quickly recognized as a new generation of nano-composites [4]. Though there is a vast amount of literature available on the evaluation of the mechanical properties and also on the vibrational analyses of carbon nanotubes, only a handful of articles can be found on the modeling and structural response behaviors of graphitic sheets [5].

[‡] A version of this chapter is published in the Journal of Applied Physics as: Arghavan, S., and Singh, A. V., 2011, "Atomic lattice structure and continuum plate theories for the vibrational characteristics of graphenes," Journal of Applied Physics, 110(8).

Different simulation methods have been introduced by researchers for modeling the mechanical and vibrational behaviors of single-layered graphene sheets [5]. Method of molecular dynamics has been used by researchers to simulate mechanical properties and vibrational behaviors of graphitic sheets for a wide range of applications [6-13]. This method is quite capable of predicting the accurate behaviors of nano-structures and typically needs very high-performance computational facilities. Because of such high end computational requirement, the method has severe drawback which limits its applications to small systems, usually in hundreds of atoms only. To mitigate such computational difficulties, researchers have resorted to continuum models based on the theories of plates and shells. Molecular dynamics and shell theory were used simultaneously to find effective Young's modulus and the thickness of single-layered graphene sheets [14-17]. The continuum models are relatively easy to understand, very well established in the sense that closed form/numerical solutions are readily available in the literature, and undoubtedly fast. The fact that a graphene sheet is seen to have gaps between atoms if examined at the nano-scale, has led to the use of the nonlocal elasticity theory for supposedly accurate predictions of the vibrational characteristics of nano-plates by researchers [18-24]. However, they were unable to report systematically on how to obtain nonlocal modulus of elasticity. Furthermore, they presented results with arbitrarily assumed nonlocal elastic moduli and provided no clear justification.

As mentioned above, a graphene sheet appears like a lattice of honeycomb cells wherein the carbon atoms, which possess mass at their nuclei, are held in place by covalent bonds. Similarly, a carbon nanotube is a cylindrical fullerene structure made of hexagonal cells. This phenomenon provides researchers the unique opportunity for the structural analyses of carbon nanotubes and graphene sheets [25-30]. Lattice structure modeling method, as it can be called, has been applied to the free and forced vibrations of single-walled carbon nanotubes and single-layered graphene sheets under different boundary conditions. This has the accuracy of molecular dynamic simulation along with the convenience and speed of the finite element method. Researchers have considered both the molecular dynamic and structural modeling methods to obtain the equivalent elastic moduli of single-layered graphene sheets and carbon nanotubes by in-plane and axial loading analyses respectively. The Young's modulus found in this manner is

approximately 1 TPa and used in their static and vibration analyses using continuum plate and shell theories. Such simulations are expected to yield sufficiently accurate results for the extensional modes of vibration of single-layered graphene sheets and single-walled carbon nanotubes. There is ample evidence in the literature that researchers used 1 TPa as the Young's modulus in the flexural response analyses of single-layered graphene sheets and carbon nanotubes. Although there is a significant amount of vibration results available in the literature, the comparisons between atomistic and continuous methods are few and far between.

In this paper, the extensional and flexural static and vibration analyses of single-layered graphene sheets by the lattice structure method and classical continuum plate theory are performed and reported. Static analyses are performed on the lattice structure model of the graphene sheet and displacements are then used to obtain the equivalent elastic moduli in bending and extension cases. Young's moduli along with other mechanical and geometrical properties are used later in calculating the natural frequencies of in-plane and out-of-plane vibrational modes of the rectangular single-layered graphene sheets by the classical continuum plate theory. Vibration results are also obtained by the lattice structure method and successfully compared with the results from continuous plate theory for both in-plane and out-of-plane modes. These two methods are presented and discussed in the following sections along with results pertaining to frequencies and associated mode shapes.

4.2. Lattice structure method

Lattice structure method is used widely in the literature for modeling the mechanical behavior of single and multi-layered graphene sheets [12, 27, 30] as well as carbon nanotubes [25, 28, 29]. In this section, the method is described briefly with the help of a rectangular graphene sheet of length a and width b as shown in Fig. 4.1. This honeycomb-like grid is made of hexagonal cells. Each side of a hexagonal cell represents covalent bond between two carbon atoms. Covalent bond here provides the axial, bending and torsional structural strength to keep the atoms together and is modeled as a frame element

in the finite element method [31]. The cross section of the frame element is assumed to be circular and the sectional properties suitable to be used in the finite element analysis are kept to be the same as what has been used before by other researchers [25]. The mass is assumed to be concentrated at the nucleus of each carbon atom, which is also used as a node with six degrees of freedom, viz. three translational and three rotational components with reference to the Cartesian axes. Lumped mass matrices are generated and assembled to form the global mass matrix of the graphene structure. Similarly, procedure of creating the local stiffness matrices and assembling those to form the global stiffness matrix is systematically followed. Reference for the details can be made of the readily available papers in the literature [25-30].

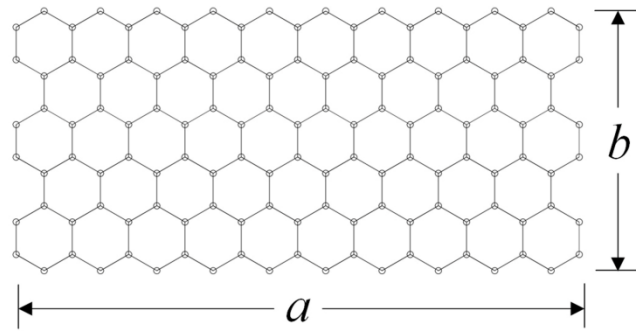


Fig. 4.1 Geometry of a graphene sheet lattice structure

Eqs. (4.1) and (4.2) express the governing equations for static and dynamic analyses respectively. Eq. (4.3) represents the characteristic equation that will be used to find the eigenvalues and corresponding eigenvectors of the graphene sheet.

$$\mathbf{K} \mathbf{x} = \mathbf{F} \quad (4.1)$$

$$\mathbf{M} \ddot{\mathbf{x}} + \mathbf{K} \mathbf{x} = \mathbf{F} \quad (4.2)$$

$$|\mathbf{K} - \omega^2 \mathbf{M}| = 0 \quad (4.3)$$

In the above equations, \mathbf{K} and \mathbf{M} represent the assembled stiffness and lumped mass matrices respectively; \mathbf{x} is the displacement vector composed of all global degrees of freedom; \mathbf{F} is the force vector built with applied forces and moments at the nodal points;

ω is the natural frequency; and the over-dot represents the differentiation with respect to time. It is to be noted here that numerical values of the material and geometric parameters in the above equations are at tera and nano levels respectively and are bound to cause numerical inequalities. To avoid such computational problems, the matrix equations are nondimensionalized. One can understand that matrix and vector size will increase considerably adding burden to the computing, if there is a slight increase in the length and width of the graphene sheets. Therefore, an equivalent continuum approach to deal with such nano-scale structure is proposed and discussed in the following section.

4.3. Equivalent continuum plate method

Classical theory of plates and shells has been used by many in the analyses of graphene sheets and carbon nanotubes to study their response behaviors under mechanical loading conditions. The most important cause for the scientists and engineers to take this route is the simplicity of the methods. Theories of plates and shells are very well researched and tested by structural engineers. Closed form solutions of standard and widely used rectangular plates are readily available for the prescribed values of the Young's modulus, Poisson's ratio and thickness. To take advantage of this knowledge of structural analysis, a simple and efficient method to obtain equivalent Young's modulus of a single-layered graphene sheet is described in this section using thickness $h = 3.4 \text{ \AA}$. For the in-plane condition, static analysis is performed on the lattice structure as shown in Fig. 4.1 Geometry of a graphene sheet lattice structure. For this, the graphene is fixed at one edge and subjected to an in-plane load P which is equally distributed to nodes on the opposite edge. The displacement u_0 at the loaded edge is found. Subsequently, the Young's modulus is obtained from $E_x = Pa / u_0 bh$.

Similarly, the lattice structure model of the rectangular graphene sheet is analyzed for the out-of-plane condition with two different cases of boundary conditions. In the first case, all edges are simply supported (SSSS), whereas in the second case the four edges are clamped (CCCC). The out-of-plane deflection v_0 under load P at the center is calculated and used to find the flexural rigidity of the equivalent isotropic plate from

$D = \eta P a^2 / \nu_0$ in which coefficient η is taken from the literature [32]. Using this flexural rigidity, the Young's modulus is obtained from $D = E_b h^3 / 12(1 - \nu^2)$ with $h = 3.4 \text{ \AA}$ and the Poisson's ratio $\nu = 0.16$. The natural frequency of the graphene is calculated using $f_{ij} = \lambda_{ij}^2 \sqrt{D / \rho h} / 2\pi a^2$ in Hz with mass density of $\rho = 2250 \text{ Kg m}^{-3}$ for the graphite. Indices i and j represent the numbers of half waves in a mode shape along the two in-plane axes respectively. The values of λ_{ij} are readily available in the literature for different aspect ratios and boundary conditions [33].

4.4. Results and discussion

The static analysis of rectangular single-layered graphene sheet is carried out by the lattice structure method to determine the equivalent Young's moduli appropriate for further use in the in-plane and out-of-plane conditions. Table 4.1 shows results concerning the equivalent elastic moduli and mass density of the graphene sheet for two values of length a , which are 20.18 nm and 30.03 nm respectively. As the overall size of the graphene sheet increases, the modulus of elasticity for the in-plane condition appears to be settling down between 1.03 and 1.04 TPa. This range is in very good match with results published earlier by others [10, 13]. Similarly, the Young's modulus converges to 0.112 TPa for the bending condition. Young's modulus for the in-plane conditions in the present study is found to be more than nine times the same for the bending conditions. Value of the flexural rigidity from the use of $\nu = 0.16$, $E_b = 0.112 \text{ TPa}$ and $h = 3.4 \text{ \AA}$, is $D = 3.765 \times 10^{-19} \text{ J}$ (2.35 eV). The last column of this table shows the equivalent mass density, which is obtained by simply counting the carbon atoms in a lattice structure model, multiplying the number by mass of a carbon atom (m_c) and then dividing by the volume ($a \times b \times h$). The values converge to 2250 Kg. m^{-3} which is actually the mass density for graphite.

Table 4.1 Equivalent Young's modulus and the mass density for different sizes of single-layered graphene sheets

a (nm)	b (nm)	Extensional		Flexural		ρ (Kg. m ⁻³)
		E_x (TPa)	E_y (TPa)	E_b (TPa) SSSS	E_b (TPa) CCCC	
20.18	20.32	1.0406	1.0339	0.1123	0.1114	2265.6
	27.99	1.0345	1.0362	0.1118	0.1115	2261.2
	33.96	1.0298	1.0369	0.1118	0.1118	2259.2
	40.78	1.0251	1.0373	0.1117	0.1116	2257.6
30.03	30.55	1.0399	1.0358	0.1120	0.1114	2255.8
	40.78	1.0352	1.0375	0.1116	0.1114	2253.1
	49.31	1.0311	1.0381	0.1117	0.1116	2251.8
	60.39	1.0262	1.0385	0.1116	0.1115	2250.6

As mentioned above, the lattice structure and continuum theories are expected to yield very close results for in-plane static and dynamic responses of graphene sheets, if the Young's modulus of approximately 1 TPa obtained by in-plane load/displacement condition is used. However, if the same value of 1 TPa is used in the bending of graphene sheets, the results will certainly be questionable. Still there are studies reported in the literature on the flexural vibration where $1.0 \text{ TPa} \leq E_x \leq 1.06 \text{ TPa}$ has been used in the classical plate [15, 16, 23] and nonlocal [20, 21] theories. Behfar and Naghdabadi [17] considered orthotropy in the graphene sheets and used Young's moduli of 1.588 TPa and 1.765 TPa for the flexural vibration by the classical plate theory. Scarpa et al [9] reported Young's modulus of single-layered graphene sheets in bending in the range of $1.8 \text{ TPa} \leq E_x \leq 4.06 \text{ TPa}$ by considering unrealistically low thickness $0.08 \text{ nm} \leq h \leq 0.12 \text{ nm}$. The use of such high values of the Young's modulus in the continuum plate theory is quite inappropriate and certainly provides erroneous results. There are also instances of using low values for the Young's modulus or the flexural rigidity. Arash and Wang [24] considered 1.78 eV in nonlocal elasticity theory; Gupta and Batra [13] 1.86 eV with 1 \AA

for the thickness; and Lu et al. [34] 1.4 eV in different molecular dynamic methods. Experimental investigations leading to different results for the Young's modulus of single-layered graphene sheets in flexure are also reported, e.g. Lee et al. [35] reported the Young's modulus of 1 TPa while Frank and Tanenbaum [36] reported 0.5 TPa. A recent experimental work on large size thick graphene papers suggested two different Young's moduli of elasticity for the in-plane and bending conditions [37]. Previous studies have used both much higher and lower value than 0.112 TPa for E_b and no one attempted to compare results with other published sources. From the above, it is certainly obvious that there is no consensus amongst the researchers on the value of the Young's modulus of the graphene in bending. In such situations, the use of $E_b = 0.112$ TPa with $h = 3.4 \text{ \AA}$ appears to be quite acceptable in order to obtain comparable results with the lattice structure method.

In the next step, the natural frequencies of single-layered graphene sheets are calculated using both the lattice structure and continuum classical plate methods. Both simply supported and clamped boundary conditions are considered. The thickness $h = 3.4 \text{ \AA}$ and mass density $\rho = 2250 \text{ Kg. m}^{-3}$ are used in the continuum plate model. Young's moduli of 1.035 TPa and 0.112 TPa are used respectively for the in-plane and out-of-plane conditions. Table 4.2 contains the first ten natural frequencies in THz for a plate with $a = 30.0 \text{ nm}$ and two values 30.6 nm and 60.4 nm respectively for b . These widths correspond to the aspect ratios of 1.02 and 2.01 respectively. As expected, the natural frequencies obtained from the lattice structure and continuum models agree very well and are within 1% of each other. For smaller plates natural frequencies from both theories match for the first few modes. At higher modes, the continuum plate theory yields considerably lower values than those from the lattice structure method. As the overall size of the graphene sheet increases, agreement in results improves significantly.

Natural frequencies for the first five odd modes (1, 3, 5, 7, and 9) are plotted against the aspect ratio b/a in Fig. 4.2 and Fig. 4.3 for the out-of-plane and in-plane conditions respectively. The calculations are performed on lattice structure model with $a = 30 \text{ nm}$ with all four clamped edges. The frequency decreases monotonically with the aspect ratio in both cases. The extensional modes, as expected, show frequencies that are much higher

than their counterparts in bending modes. Also, frequencies for the flexural and extensional modes are plotted against the length of square graphene sheets in Fig. 4.4 and

Table 4.2 Natural frequencies of single-layered graphene sheets (THz), $a = 30.0$ nm

Mode Number	Bending modes				Extensional modes	
	Frame method SSSS	Plate theory SSSS	Frame method CCCC	Plate theory CCCC	Frame method CCCC	Plane stress condition CCCC
$b = 30.6$ nm, $b/a = 1.02$						
1	0.0024	0.0024	0.0044	0.0044	0.4256	0.4156
2	0.0060	0.0059	0.0088	0.0088	0.4281	0.4185
3	0.0061	0.0061	0.0090	0.0090	0.5561	0.5260
4	0.0096	0.0096	0.0132	0.0131	0.6365	0.6172
5	0.0119	0.0118	0.0158	0.0158	0.7058	0.6925
6	0.0122	0.0122	0.0163	0.0162	0.7646	0.7274
7	0.0156	0.0155	0.0199	0.0199	0.7734	0.7352
8	0.0158	0.0157	0.0202	0.0201	0.7754	0.7709
9	0.0201	0.0201	0.0252	0.0252	0.8686	0.8464
10	0.0208	0.0207	0.0260	0.0260	0.8739	0.8507
$b = 60.4$ nm, $b/a = 2.01$						
1	0.0015	0.0015	0.0030	0.0030	0.3027	0.2903
2	0.0024	0.0024	0.0039	0.0039	0.3761	0.3717
3	0.0039	0.0039	0.0055	0.0055	0.4203	0.4064
4	0.0052	0.0052	0.0078	0.0078	0.4266	0.4162
5	0.0061	0.0061	0.0079	0.0079	0.4895	0.4674
6	0.0061	0.0061	0.0088	0.0088	0.5271	0.5018
7	0.0076	0.0076	0.0103	0.0103	0.5724	0.5537
8	0.0088	0.0088	0.0107	0.0107	0.5812	0.5612
9	0.0097	0.0097	0.0124	0.0124	0.6119	0.5896
10	0.0113	0.0113	0.0143	0.0142	0.6848	0.6525

Fig. 4.5 respectively. Here also, frequencies at all modes decrease with the size and the out-of-plane frequencies are approximately one tenth in value when compared to the in-plane modes. Fig. 4.6 and Fig. 4.7 exhibit the first six out-of-plane and first six in-plane mode shapes of a nearly square ($4.92 \text{ nm} \times 4.97 \text{ nm}$) single-layered graphene sheet, clamped at all four sides. The symmetry and anti-symmetry with reference to horizontal and vertical axes and also with the two diagonals are distinctly observed. These mode shapes reveal that there is an astounding similarity between the vibrational modes of the single-layered graphene sheet by lattice structure and the continuum plate methods.

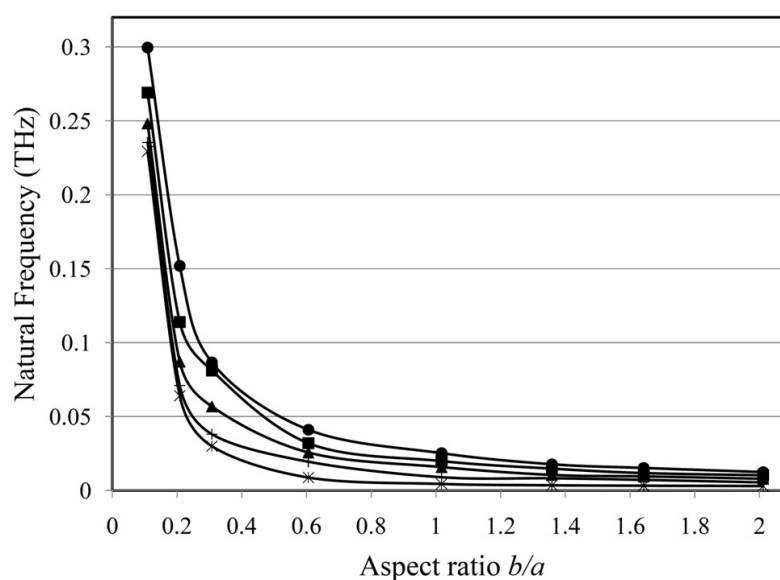


Fig. 4.2 Out-of-plane natural frequencies of rectangular single-layered graphene sheets of different aspect ratios, CCCC; *, Mode 1; +, Mode 3; ▲, Mode 5; ■, Mode 7; ●, Mode 9

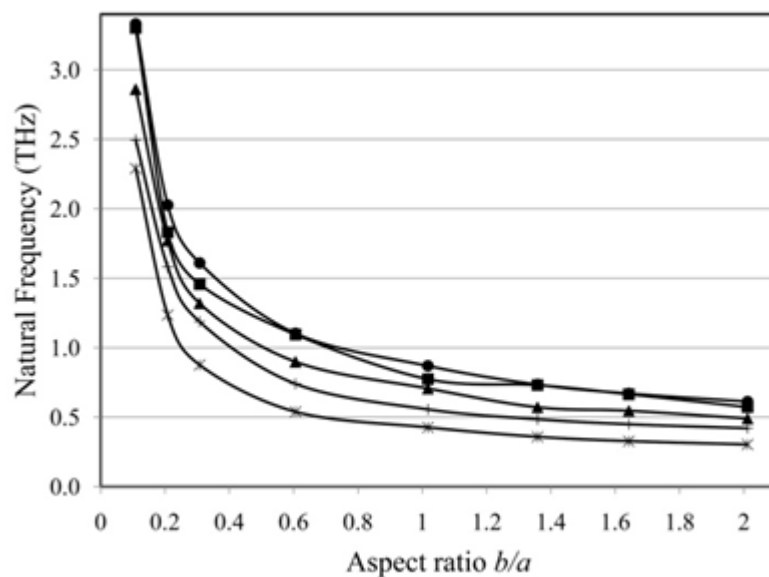


Fig. 4.3 In-plane natural frequencies of rectangular single-layered graphene sheets of different aspect ratios, CCCC; *, Mode 1; +, Mode 3; ▲, Mode 5; ■, Mode 7; ●, Mode 9

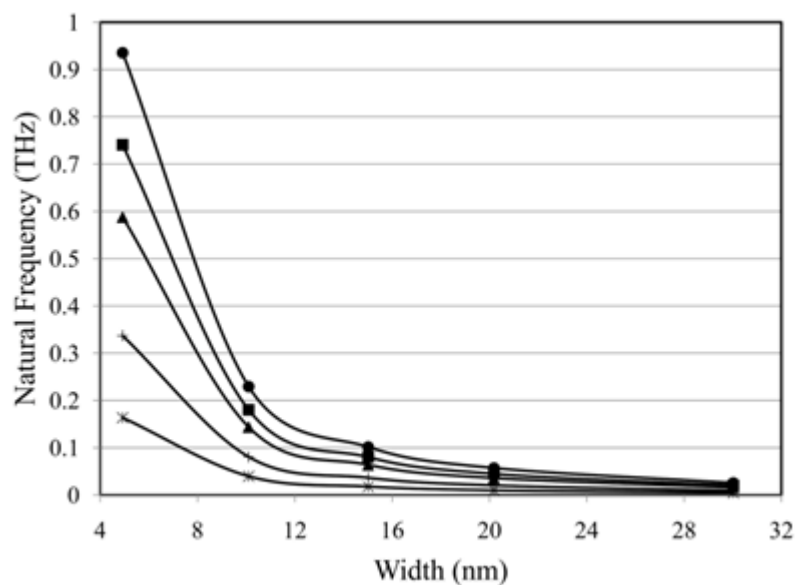


Fig. 4.4 Out-of-plane natural frequencies of square single-layered graphene sheets of different sizes, CCCC; *, Mode 1; +, Mode 3; ▲, Mode 5; ■, Mode 7; ●, Mode 9

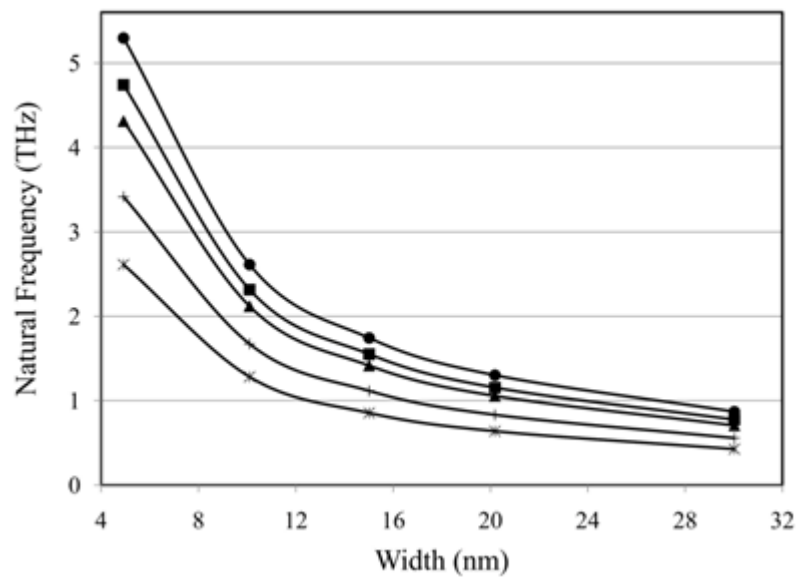


Fig. 4.5 In-plane natural frequencies of square single-layered graphene sheets of different sizes, CCCC; *, Mode 1; +, Mode 3; ▲, Mode 5; ■, Mode 7; ●, Mode 9

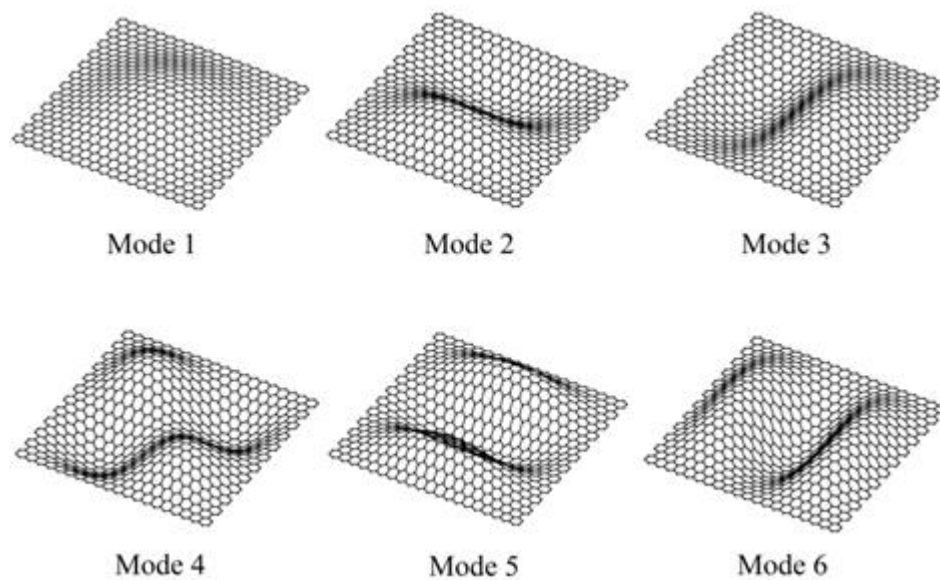


Fig. 4.6 First six out-of-plane mode shapes of a nearly square single-layered graphene sheet (4.92 nm×4.97 nm), CCCC

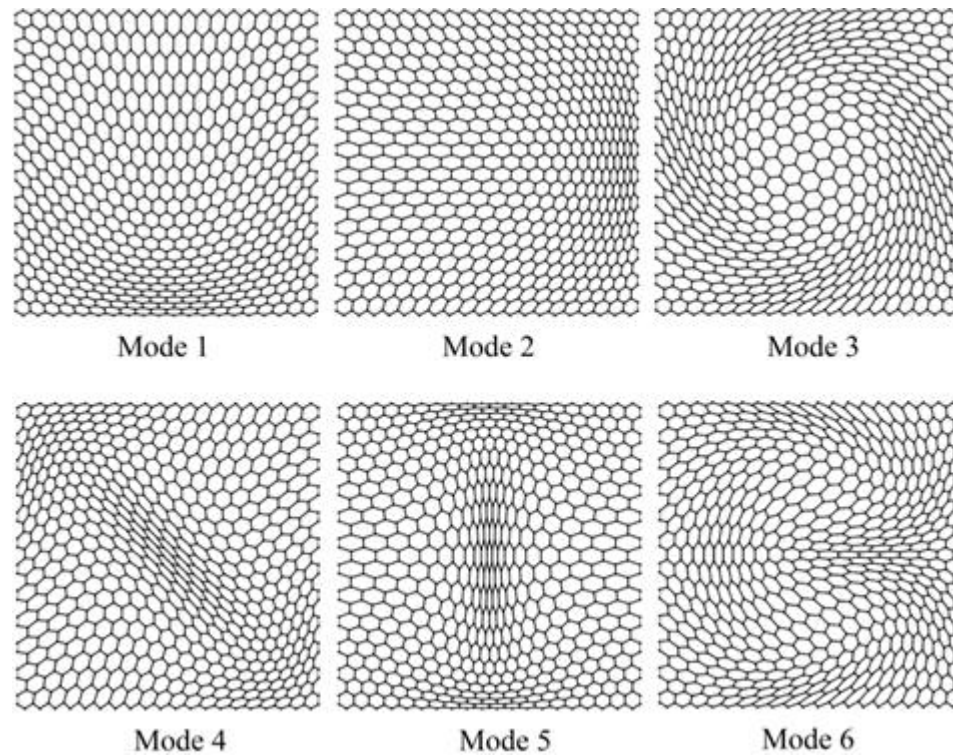


Fig. 4.7 First six in-plane mode shapes of a nearly square single-layered graphene sheet (4.92 nm×4.97 nm), CCCC

4.5. Concluding remarks

A graphene sheet is like a lattice formed with hexagonal cells in which the carbon atoms are held in place by covalent bond which in turn creates discontinuous distribution of matter. When the lattice model is analyzed under mechanical loads and constraints, it shows static and vibrational responses like a continuous plate. In this research, a direct relationship between the discrete lattice and continuous plate theories is established. To achieve it, the static analysis of rectangular single-layered graphene sheets is carried out by the lattice model to calculate the overall Young's moduli assuming thickness $h = 3.4 \text{ \AA}$ and the Poisson's ratio $\nu = 0.16$. The in-plane Young's modulus is found in the range of 1.03-1.04 TPa, which is close to what has been reported in the literature. The static bending analysis predicts a very low Young's modulus of 0.112 TPa. Free in-plane and out-of-plane vibrations of rectangular single-layered graphene sheets are also critically

investigated in this paper by the lattice structure and equivalent continuum plate methods. The in-plane and out-of-plane vibrations are found to be completely decoupled. The values of the natural frequencies calculated by two methods compare very well. As the size of graphene sheets increases, the agreement improves drastically for all modes of vibration. The bending frequencies are approximately one tenth in value of the in-plane modes. When the lattice structure models become too large to handle computationally, this study suggests that well established continuum plate theory can be used for reasonably accurate results using the appropriate values of Young's moduli.

References

- [1] Novoselov, K. S., Jiang, D., Schedin, F., Booth, T. J., Khotkevich, V. V., Morozov, S. V., and Geim, A. K., 2005, "Two-dimensional atomic crystals," *Proceedings of the National Academy of Sciences of the United States of America*, 102(30), pp. 10451-10453.
- [2] Wu, Y. H., Yu, T., and Shen, Z. X., 2010, "Two-dimensional carbon nanostructures: Fundamental properties, synthesis, characterization, and potential applications," *Journal of Applied Physics*, 108(7).
- [3] Geim, A. K., and Novoselov, K. S., 2007, "The rise of graphene," *Nature Materials*, 6(3), pp. 183-191.
- [4] Stankovich, S., Dikin, D. A., Dommett, G. H. B., Kohlhaas, K. M., Zimney, E. J., Stach, E. A., Piner, R. D., Nguyen, S. T., and Ruoff, R. S., 2006, "Graphene-based composite materials," *Nature*, 442(7100), pp. 282-286.
- [5] Singh, A. V., and Arghavan, S., 2010, "Vibrations of carbon nanoscale structures: a critical review," *Computational Technology Reviews*, 1, pp. 281-314.
- [6] Neek-Amal, M., and Peeters, F. M., 2010, "Linear reduction of stiffness and vibration frequencies in defected circular monolayer graphene," *Physical Review B - Condensed Matter and Materials Physics*, 81(23).
- [7] Sadeghi, M., and Naghdabadi, R., 2010, "Nonlinear vibrational analysis of single-layer graphene sheets," *Nanotechnology*, 21(10).
- [8] Van Lier, G., Van Alsenoy, C., Van Doren, V., and Geerlings, P., 2000, "Ab initio study of the elastic properties of single-walled carbon nanotubes and graphene," *Chemical Physics Letters*, 326(1-2), pp. 181-185.

- [9] Scarpa, F., Adhikari, S., and Srikantha Phani, A., 2009, "Effective elastic mechanical properties of single layer graphene sheets," *Nanotechnology*, 20(6).
- [10] Jiang, J. W., Wang, J. S., and Li, B., 2009, "Young's modulus of graphene: A molecular dynamics study," *Physical Review B - Condensed Matter and Materials Physics*, 80(11).
- [11] Karnet, Y. N., Nikitin, S. M., Nikitina, E. A., and Yanovskii, Y. G., 2010, "Computer simulation of mechanical properties of carbon nanostructures," *Mechanics of Solids*, 45(4), pp. 595-609.
- [12] Georgantzinos, S. K., Giannopoulos, G. I., and Anifantis, N. K., 2010, "Numerical investigation of elastic mechanical properties of graphene structures," *Materials and Design*, 31(10), pp. 4646-4654.
- [13] Gupta, S. S., and Batra, R. C., 2010, "Elastic properties and frequencies of free vibrations of single-layer graphene sheets," *Journal of Computational and Theoretical Nanoscience*, 7(10), pp. 2151-2164.
- [14] Hemmasizadeh, A., Mahzoon, M., Hadi, E., and Khandan, R., 2008, "A method for developing the equivalent continuum model of a single layer graphene sheet," *Thin Solid Films*, 516(21), pp. 7636-7640.
- [15] He, X. Q., Kitipornchai, S., and Liew, K. M., 2005, "Resonance analysis of multi-layered graphene sheets used as nanoscale resonators," *Nanotechnology*, 16(10), pp. 2086-2091.
- [16] Liew, K. M., He, X. Q., and Kitipornchai, S., 2006, "Predicting nanovibration of multi-layered graphene sheets embedded in an elastic matrix," *Acta Materialia*, 54(16), pp. 4229-4236.
- [17] Behfar, K., and Naghdabadi, R., 2005, "Nanoscale vibrational analysis of a multi-layered graphene sheet embedded in an elastic medium," *Composites Science and Technology*, 65(7-8), pp. 1159-1164.
- [18] Pradhan, S. C., and Phadikar, J. K., 2009, "Nonlocal elasticity theory for vibration of nanoplates," *Journal of Sound and Vibration*, 325(1-2), pp. 206-223.
- [19] Murmu, T., and Pradhan, S. C., 2009, "Vibration analysis of nanoplates under uniaxial prestressed conditions via nonlocal elasticity," *Journal of Applied Physics*, 106(10).
- [20] Murmu, T., and Pradhan, S. C., 2009, "Vibration analysis of nano-single-layered graphene sheets embedded in elastic medium based on nonlocal elasticity theory," *Journal of Applied Physics*, 105(6).

- [21] Murmu, T., and Pradhan, S. C., 2009, "Small-scale effect on the free in-plane vibration of nanoplates by nonlocal continuum model," *Physica E: Low-Dimensional Systems and Nanostructures*, 41(8), pp. 1628-1633.
- [22] Ansari, R., Rajabiehfard, R., and Arash, B., 2010, "Nonlocal finite element model for vibrations of embedded multi-layered graphene sheets," *Computational Materials Science*, 49(4), pp. 831-838.
- [23] Jomehzadeh, E., and Saidi, A. R., 2011, "A study on large amplitude vibration of multilayered graphene sheets," *Computational Materials Science*, 50(3), pp. 1043-1051.
- [24] Arash, B., and Wang, Q., 2011, "Vibration of single- and double-layered graphene sheets," *Journal of Nanotechnology in Engineering and Medicine*, 2(1).
- [25] Li, C., and Chou, T. W., 2003, "A structural mechanics approach for the analysis of carbon nanotubes," *International Journal of Solids and Structures*, 40(10), pp. 2487-2499.
- [26] Li, C., and Chou, T. W., 2003, "Single-walled carbon nanotubes as ultrahigh frequency nanomechanical resonators," *Physical Review B - Condensed Matter and Materials Physics*, 68(7), pp. 734051-734053.
- [27] Sakhaee-Pour, A., Ahmadian, M. T., and Naghdabadi, R., 2008, "Vibrational analysis of single-layered graphene sheets," *Nanotechnology*, 19(8).
- [28] Ávila, A. F., Eduardo, A. C., and Neto, A. S., 2011, "Vibrational analysis of graphene based nanostructures," *Computers and Structures*, 89(11-12), pp. 878-892.
- [29] Arghavan, S., and Singh, A. V., 2011, "On the vibrations of single-walled carbon nanotubes," *Journal of Sound and Vibration*, 330(13), pp. 3102-3122.
- [30] Tsai, J. L., and Tu, J. F., 2010, "Characterizing mechanical properties of graphite using molecular dynamics simulation," *Materials and Design*, 31(1), pp. 194-199.
- [31] Cornell, W. D., Cieplak, P., Bayly, C. I., Gould, I. R., Merz Jr, K. M., Ferguson, D. M., Spellmeyer, D. C., Fox, T., Caldwell, J. W., and Kollman, P. A., 1995, "A second generation force field for the simulation of proteins, nucleic acids, and organic molecules," *Journal of the American Chemical Society*, 117(19), pp. 5179-5197.
- [32] Timoshenko, S., and Woinowsky-Krieger, S., 1959, *Theory of plates and shells*, McGraw-Hill, New York.
- [33] Blevins, R. D., 1979, *Formulas for natural frequency and mode shapes*, Van Nostrand Reinhold, New York.
- [34] Lu, Q., Arroyo, M., and Huang, R., 2009, "Elastic bending modulus of monolayer graphene," *Journal of Physics D: Applied Physics*, 42(10).

- [35] Lee, C., Wei, X., Kysar, J. W., and Hone, J., 2008, "Measurement of the elastic properties and intrinsic strength of monolayer graphene," *Science*, 321(5887), pp. 385-388.
- [36] Frank, I. W., Tanenbaum, D. M., Van Der Zande, A. M., and McEuen, P. L., 2007, "Mechanical properties of suspended graphene sheets," *Journal of Vacuum Science and Technology B: Microelectronics and Nanometer Structures*, 25(6), pp. 2558-2561.
- [37] Ranjbartoreh, A. R., Wang, B., Shen, X., and Wang, G., 2011, "Advanced mechanical properties of graphene paper," *Journal of Applied Physics*, 109(1).

CHAPTER 5

Free Vibration of Single-Layered Graphene Sheets: Lattice Structure versus Continuum Plate Theories[§]

5.1. Introduction

Novoselov and his colleagues, after years of groundbreaking research, demonstrated the existence of a two-dimensional free-standing carbon structure in 2005 [1]. Before this time scientists did not consider any two-dimensional allotrope of carbon with a stable atomic structure. This flat layer of carbon atoms tightly packed into a honeycomb-like two-dimensional array was termed as graphene. A single-layered graphene sheet can be prepared by cleavage from the most strongly layered graphitic material and wrapped up into fullerenes, rolled into nanotubes and stacked up to produce three-dimensional graphite [2]. Even with such a short history, the graphene has shown great potential for many types of future applications in nano composites due to exceptional mechanical, electrical and thermal properties [3, 4]. In contrast to carbon nanotubes which caught significant amount of attention from researchers and have a vast amount of literature, just a few articles can be found on the modeling of the properties of graphitic sheets [5].

[§] A version of this chapter is published in the Journal of Nanotechnology in Engineering and Medicine as: Arghavan, S., and Singh, A. V., 2011, "Free vibration of single layer graphene sheets: lattice structure versus continuum plate theories," Journal of Nanotechnology in Engineering and Medicine, 2(3).

Different simulation techniques were introduced by researchers for modeling the mechanical and vibrational behaviors of single-layered graphene sheets. Molecular dynamics was used extensively in simulating the mechanical properties and vibrational behavior of graphitic sheets. Ab-initio calculations on single-walled carbon nanotubes and graphenes were performed by Van Lier et al. [6] to achieve a better insight into the Young's modulus and Poisson's ratio. Scarpa et al. [7] proposed truss type analytical models and cellular material mechanics theory to describe the in-plane linear elastic properties of single-layered graphene sheets in small strain uniaxial and pure shear loading. Jiang et al. [8] performed the thermal vibrations of graphene using molecular dynamic and calculated the Young's modulus. Karnet et al. [9] performed a computer simulation of the deformation and fracture mechanisms of carbon nanotubes and graphene under uniaxial tension. The elastic mechanical properties of graphene sheets, nano ribbons and graphite flakes were computed using spring based finite element models [10]. Molecular dynamic simulation technique and elasticity theory were used by Neek-Amal and Peeters [11] to examine the mechanical properties of single-layered graphene sheets with defects. A hybrid atomistic-structural element based was introduced by Sadeghi and Naghdabadi [12] to study both the infinitesimal and large amplitude vibrations of single-layered graphene sheets. Despite the accuracy and precision of molecular dynamic methods, there are some shortcomings that push researchers to find alternatives for mechanical analysis of graphene sheets. This method needs very high performance computational facilities, cannot be used for structures with more than a couple of hundreds particles and has its own complexities. Based on these, many researchers are encouraged to find other models for aforementioned simulations.

Continuum models based on the classical plate theories have emerged so fast as alternatives for molecular dynamic methods. These models are relatively easy to understand, very well established, undoubtedly fast and also, closed form solutions of different types of problems are available in the literature. Molecular dynamic and the continuum plate models were used simultaneously to develop the effective Young's modulus and the stiffness of a single-layered graphene sheet [13]. By coupled classical plate vibration equations, multi-layered graphene sheets which are used as resonators, embedded in elastic matrix and subjected to initial stress were studied by He and co-

workers [14-16]. Behfar and Naghdabadi [17, 18] used continuum orthotropic plate theory in the vibration analysis of multi-layered graphene sheets embedded in elastic medium. Beside all the advantages of the classical plate theory, no comparison study is found in the literature to verify the results, the accuracy of which essentially depends on the way the geometry and mechanical properties are obtained and used. Ample amount of vibration results, based on using approximately 1 TPa for the Young's modulus of elasticity even for the flexural modes are available in the literature. This value of the Young's modulus is found from the static stretching analysis of single-layered graphene sheets by the molecular dynamic method and yields significantly higher values of the flexural frequencies than the results from the molecular dynamic method. Gupta and Batra [19] determined basal plane stiffness and Poisson's ratio of single-layered graphene sheets using the molecular dynamic method. Different stiffness properties were obtained by using uniaxial tensile deformations and axial bending vibrations of single-layered graphene sheets. They justified the difference by manipulating the thickness of the plate for bending modes. Ranjbartoreh et al [20] reported the stiffness properties of fairly large size thick graphene papers using stretching and bending loading conditions in a set of experimental works. They suggested two different values of Young's modulus of elasticity for graphene papers.

A homogeneous material examined at the nano-scale can be seen to have gaps and the application of the continuum models in such case has been questioned. Therefore, nonlocal elasticity theory was suggested in the literature for the accurate predictions of the vibrational characteristics of single-layered graphene sheets by both the classical and the first order shear deformable plate theories [21-24]. Arash and Wang [25] studies vibration of single and double-layered graphene sheets and considered the effects of van der Waals forces on double-layered graphenes. Nonlocal elasticity theory, which has been used along with the plate theory by others [26, 27] as well, requires nonlocal modulus. It is dependent on the size, boundary condition and mode numbers. Hence, these studies couldn't be directly related to the vibration studies of graphitic sheets by other methods. Also, a systematic way to obtain the value of the nonlocal modulus for a graphitic sheet has not been reported in any of these studies.

This paper is concerned with the evaluation of the elastic properties of the single-layered graphene sheets by the lattice structure approach. Then the properties are applied to investigate the in-plane and out-of-plane free vibrations by the continuum plate theory. The lattice structure method includes the details of the atomic layout of graphene sheets and hence, is very accurate. First, the static analysis is carried out by the lattice structure method to obtain the equivalent elastic moduli of the single-layered graphene sheets in bending and extension assuming thickness $h = 3.4 \text{ \AA}$ and Poisson's ratio $\nu = 0.16$. The equivalent Young's moduli are found to be 1.04 TPa for the in-plane case and 0.11 TPa for the out-of-plane bending of the graphene sheets and then are used to calculate the natural frequencies of the skewed single-layered graphene sheets considering different aspect ratio by the classical plate theory. All four edges of the graphene sheet are subjected to (a) simply supported and (b) clamped conditions as separate cases. Frequencies and mode shapes of clamped circular plates are also studied here by both the direct lattice structure and classical plate methods. The results from the two methods are seen to compare extremely well with each other.

5.2. Methods of analysis

In this section, an overview of the methods by which vibration analyses of single-layered graphene sheets have been carried out is presented. Issues here mainly are concerned with the elastic and geometric properties of these nano-scale structures.

5.2.1. Lattice structure method of analysis

A graphene sheet as shown in Fig. 5.1 is treated in this study as a plane lattice structure made of honeycomb cells. Each side of a hexagonal cell represents the covalent bond between two carbon atoms it joins. The covalent bond provides structural strength to keep the atoms together and is modeled as a frame element with axial, bending and torsional stiffness [28]. The mass is assumed to be concentrated to the nuclei of the carbon atoms which are also considered as nodes in this method. Each node is assigned six degrees of

freedom, viz., three displacements and three rotation components about the Cartesian axes. The engineering properties used in this part are given as follows.

Length representing the covalent bond $L = 1.42 \text{ \AA}$, circular cross sectional area $A = 1.68794 \text{ \AA}^2$, moment of inertia $I = 0.22682 \text{ \AA}^4$, Young's modulus $E = 5.488 \times 10^{-8} \text{ N. \AA}^{-2}$, shear modulus $G = 8.711 \times 10^{-9} \text{ N. \AA}^{-2}$, and the mass of the carbon atom $m_c = 1.9943 \times 10^{-26} \text{ Kg}$.

Based on the data pertaining to the stiffness and geometric properties, the standard finite element model is created in this study for the static and vibration analyses [29-32]. Matrix equations are $\mathbf{K}\mathbf{x} = \mathbf{F}$ and $\mathbf{M}\ddot{\mathbf{x}} + \mathbf{K}\mathbf{x} = \mathbf{F}$ for the static and dynamic analyses respectively. \mathbf{K} , \mathbf{M} and \mathbf{F} represent assembled stiffness matrix, lumped mass matrix and load vector respectively. Here, \mathbf{x} represents the displacement vector composed of all the degrees of freedom and over-dot stands for the time derivative.

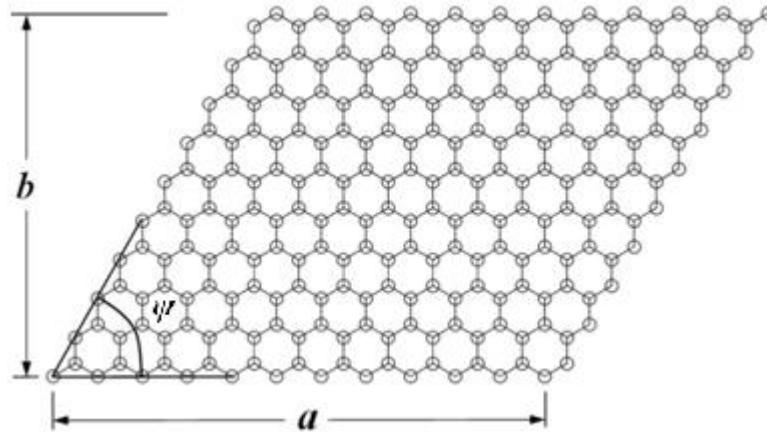


Fig. 5.1 Geometry of a graphene sheet

5.2.2. Equivalent continuum plate method

The classical plate theory is very well established and understood by researchers for the static and vibration analyses. Closed form solutions are readily available for rectangular

plates and finite element methods based on thin plate theory can be used very effectively for rectangular and other shaped plates. The analysis of thin plates requires the values of the Young's modulus, Poisson's ratio and the thickness of the plate. Hence, a simplified method to obtain the equivalent moduli of elasticity E of graphene sheets is introduced in this paper. In-plane static analysis is performed on a rectangular graphene with overall length a and width b . The value of the thickness h used is 3.4 \AA . The graphene fixed at one edge is subjected to an axial load P equally divided to nodes on the opposite edge of the lattice structure model and then analyzed for the static deflection u_0 at the loaded edge. From this value of u_0 and $h = 3.4 \text{ \AA}$, the value of E_x is obtained using $E_x = Pa / u_0bh$.

Similarly, for the out-of-plane condition, the rectangular graphene sheet with all edges either simply supported (SSSS) or clamped (CCCC), is subjected to a lateral point load at the center and the deflection v_0 under the load is calculated by the lattice structure model. The flexural rigidity of the equivalent isotropic plate is then calculated by $D = \eta Pa^2 / v_0$. The values of the coefficient η are given in the literature for different aspect ratios (b/a) and different boundary conditions [33]. The same study is carried out for a clamped circular graphene sheet with radius R , under uniformly distributed load q . In this case, deflection of the centre v_0 is calculated by the lattice structure model. The flexural rigidity of the circular continuum plate under the uniformly distributed load and clamped boundary conditions is given by $D = qR^4 / 64v_0$ [33]. From the found value of the flexural rigidity, the modulus of elasticity E is obtained with $h = 3.4 \text{ \AA}$ and the Poisson's ratio $\nu = 0.16$ using $E_b = 12 D (1 - \nu^2) / h^3$.

The natural frequency from the classical theory can be calculated using $f_{ij} = \lambda_{ij}^2 \sqrt{D / \rho h} / 2\pi a^2$ and $f_{ij} = \lambda_{ij}^2 \sqrt{D / \rho h} / 2\pi R^2$ in Hz for rectangular and circular plates respectively. For rectangular plates, indices i and j represent the numbers of half waves in a mode shape along horizontal and vertical axes, respectively. Similarly, they represent number of nodal diameters and number of nodal circles respectively for the circular plates. The values of λ_{ij} corresponding to these modes are readily available for different aspect ratios and boundary conditions [34]. The mass density $\rho = 2250 \text{ Kg. m}^{-3}$ for graphite can be used here. The equivalent Young's modulus found in this manner can also be used along with the thickness and Poisson's ratio, when the finite element method

is chosen for analysis. In this research, parabolic quadrilateral plane stress and plate bending finite elements are intended to be used as needed.

5.3. Results and discussion

In this study, first the static analyses on the rectangular and circular single-layered graphene sheets are carried out by the lattice structure method to determine the Young's modulus appropriate for the use in the continuum plate structure model as described above. The ranges of length a and width b are selected for rectangular plate in this computation are: $2.46 \text{ nm} \leq a \leq 30.03 \text{ nm}$ and $2.42 \text{ nm} \leq b \leq 60.39$ respectively. The equivalent Young's moduli E_x and E_y are calculated for rectangular single-layered graphene sheets by the method described above in section 5.2 for the in-plane loading conditions and the results are presented in Fig. 5.2 corresponding to four aspect ratios of 1, 1.34, 1.67, and 2 respectively. The values of E_x as presented in Fig. 5.2 are seen to be converging from above and settle between 1.025 and 1.040 TPa. But, those of E_y converge from below and settle in a narrow band of 1.035-1.040 TPa. This magnitude of the converged value of the Young's modulus in tension is in full agreement with the ones reported previously by other researchers.

The computation to find the Young's modulus in bending is then carried out again considering same four aspect ratios on rectangular graphene sheets as mentioned above. Two sets of boundary conditions, i.e. all four edges simply supported (SSSS) and all four edges clamped (CCCC) are considered. The Young's moduli for these cases are converging from above and settle down in a very narrow band of 0.111-0.112 TPa as seen in Fig. 5.3. Similarly, static analysis has been performed on clamped edge circular plate of radius 6, 8, 10, 12 and 14 nm, under the uniform lateral load. From the central deflections, the values of the Young's modulus for bending are found to be 0.1171, 0.116, 0.1146, 0.1143 and 0.1137 TPa respectively. As seen, the in-plane Young's modulus is seen to be about 10 times of the bending mode.

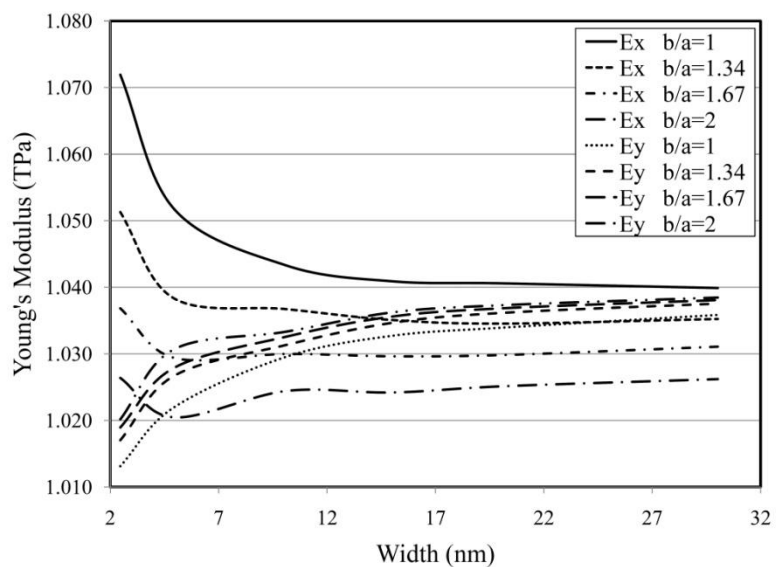


Fig. 5.2 In-plane Young's modulus of elasticity for different sizes of rectangular single-layered graphene sheets

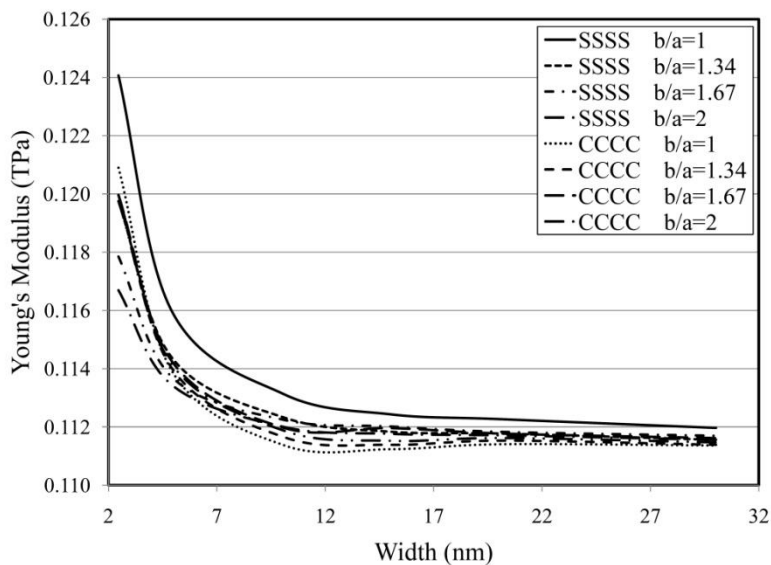


Fig. 5.3 Young's modulus of elasticity of bending modes for different sizes of rectangular single-layered graphene sheets

The out-of-plane Young's modulus reported here is not available in the literature and researchers, until very recently, have used $E_x = 1$ TPa with $h = 3.4$ Å for the bending of graphene sheets in the classical continuum plate theory. The use of $E_x = 1$ TPa in the case of bending is quite inappropriate and bound to yield erroneous results. Fig. 5.4 shows the equivalent mass density of the graphene sheet plotted against the width of the rectangular single-layered graphene sheets investigated above. The number of carbon atoms are counted for a given case with and then multiplied by m_c . The resulting mass is divided by the volume ($a \times b \times h$) with $h = 3.4$ Å to obtain the mass density which is plotted in Fig. 5.4 against the width for the above mentioned four cases of the specified aspect ratio. As the size of the sheet increases, effects of boundary nodes vanishes and mass density is seen to be converging from above to mass density of graphite (2250 Kg. m^{-3}).

In the next step, free vibrational analysis of single-layered graphene sheets is carried out using both lattice structure and continuum plate theories. The mass density used in the continuum model is that of the graphite $\rho = 2250 \text{ Kg. m}^{-3}$ and different values are used for Young's modulus of elasticity in in-plane and out-of-plane analyses. The natural frequencies of skewed single-layered graphene sheets with all edges clamped are

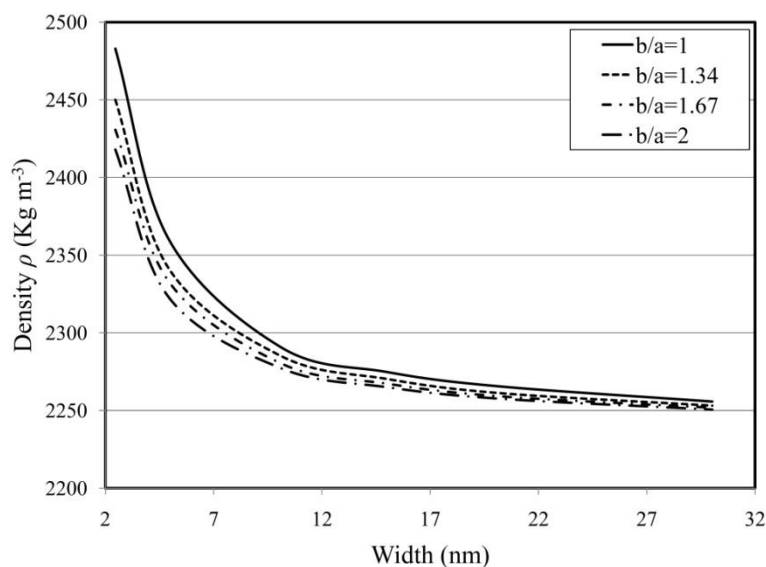


Fig. 5.4 Density of different sizes of rectangular single-layered graphene sheets based on number of carbon atoms

calculated for three values of skew angle viz. (a) 30° , (b) 60° and (c) 90° which is the rectangular plate. Both, the flexural (out-of-plane) and extensional (in-plane) modes of vibration are investigated with $a = 9.97, 14.89, 20.06, 25.11$ and 29.90 nm. These cover a very wide size-range from a flake to small graphene sheet. The aspect ratios considered are kept within the approximate range of $0.25 \leq b/a \leq 1.0$. As expected in the linear vibration case, the in-plane and out-of-plane modes of vibration are completely decoupled. Fig. 5.5, Fig. 5.6 and Fig. 5.7 show first, fifth and tenth in-plane natural frequencies of 30° , 60° and 90° skewed graphene sheets respectively, using both the lattice structure and continuum plate models. The frequencies decrease as the width of the single-layered graphene sheets increase for all cases. Similarly, Fig. 5.8, Fig. 5.9 and Fig. 5.10 show first, fifth and tenth out-of-plane natural frequencies of the plates for which the in-plane results are presented above in Fig. 5.5, Fig. 5.6 and Fig. 5.7. Extensional natural frequencies are generally higher than the flexural ones for a graphene sheet. As the size of the single-layered graphene sheet increases, natural frequencies decrease. The declension of frequencies versus size of the graphene is smoother for in-plane modes of vibration.

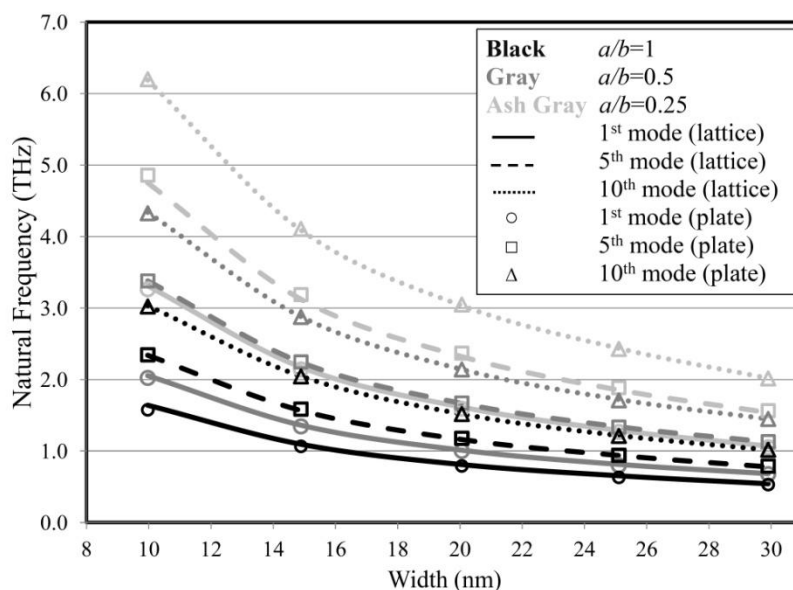


Fig. 5.5 In-plane natural frequencies of 30° skewed single-layered graphene sheets, all edges are clamped

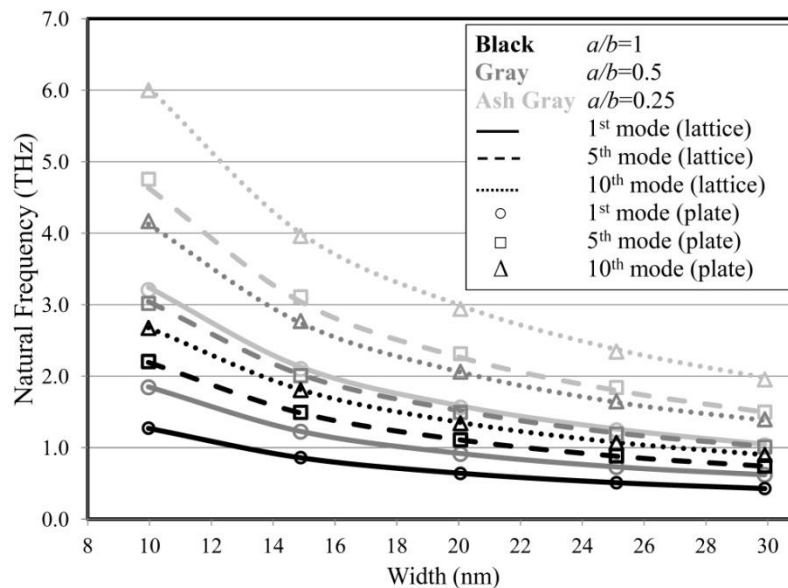


Fig. 5.6 In-plane natural frequencies of 60° skewed single-layered graphene sheets, all edges are clamped

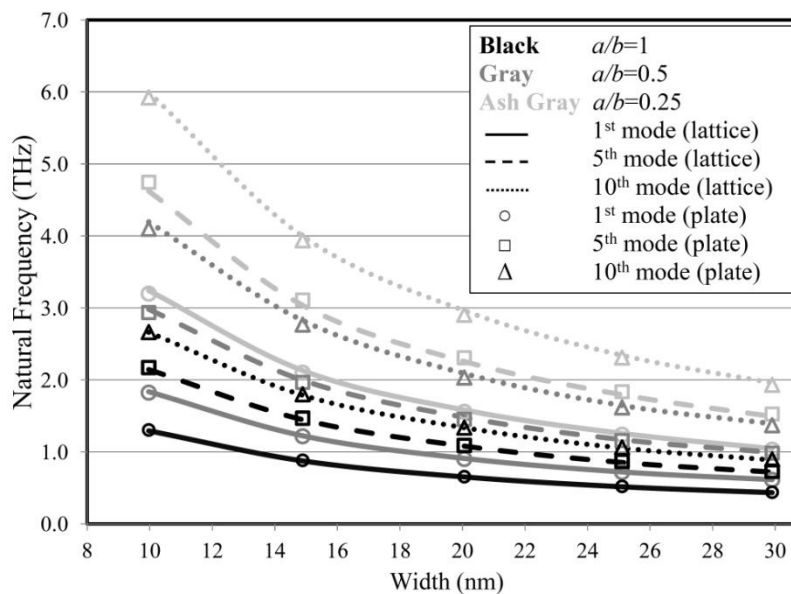


Fig. 5.7 In-plane natural frequencies of 90° skewed (rectangular) single-layered graphene sheets, all edges are clamped

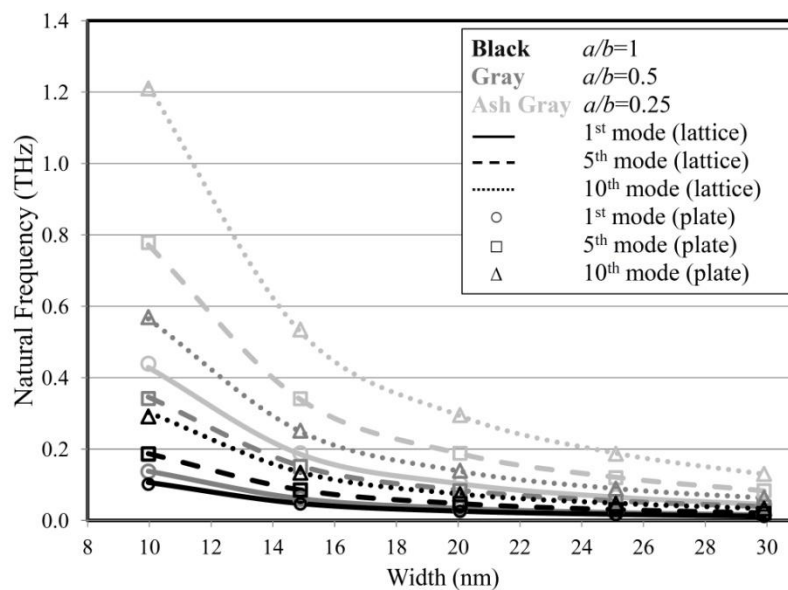


Fig. 5.8 Out-of-plane natural frequencies of 30° skewed single-layered graphene sheets, all edges are clamped

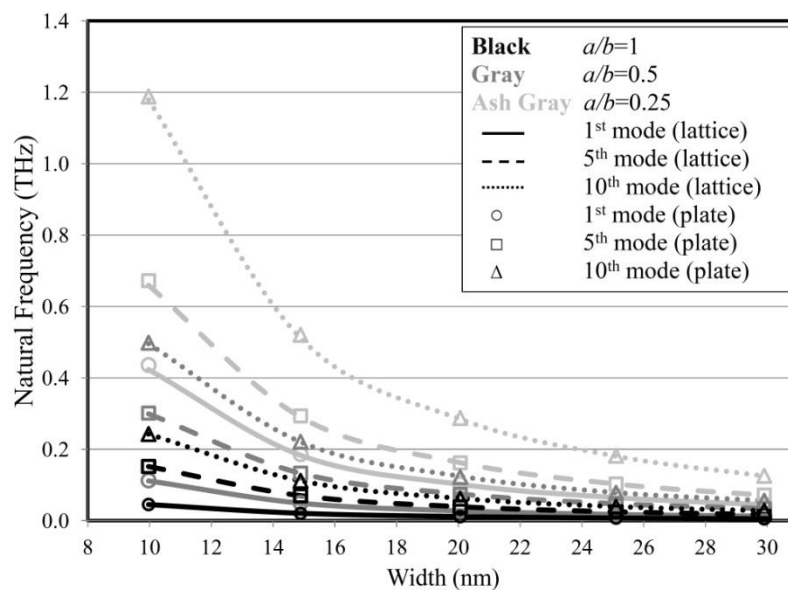


Fig. 5.9 Out-of-plane natural frequencies of 60° skewed single-layered graphene sheets, all edges are clamped

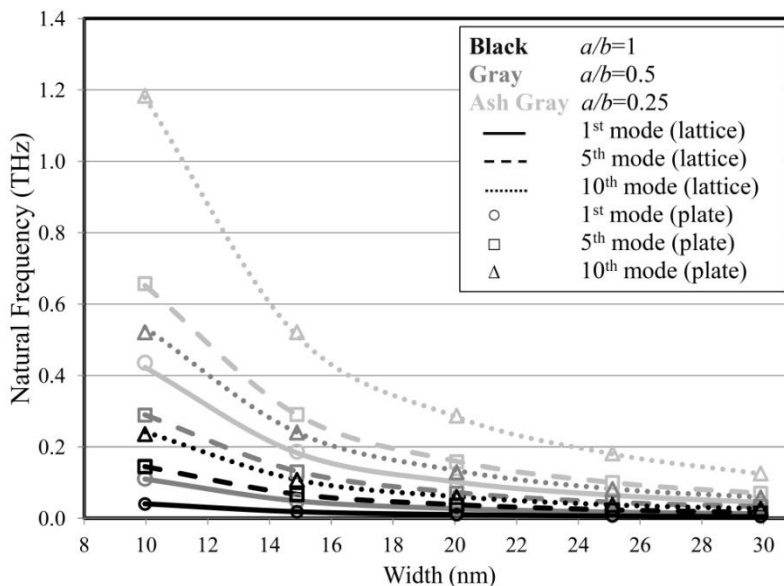


Fig. 5.10 Out-of-plane natural frequencies of 90° skewed (rectangular) single-layered graphene sheets, all edges are clamped

Frequencies decrease while skewed angle increases but the decline is essentially non-noticeable in these figures. This addresses the very small change (decrease) of the overall stiffness of the graphene sheets regarding the increase of the skew angle.

As noticed from the figures, results from the continuum plate theory match perfectly with those from lattice structure method for all angles, sizes, and vibrational modes of single-layered graphene sheets. The discrepancy in the results from the lattice structure and continuum models is found to be within 4% for small flakes and 1% for large size single-layered graphene sheets. As the aspect ratio and the size of the sheets increase, the agreement tends to improve. Circular graphene sheets of different radii are also considered in this study in order to show the close proximity and accuracy of the two methods. Fig. 5.11 and Fig. 5.12 show in-plane and out-of-plane natural frequencies of different sized fully clamped circular plate obtained by both theories. In-plane frequencies are higher than bending frequencies which decrease also in this case as the radius increases. Results from the continuum plate and lattice structure theories are very close to each other and fall within 1% difference of each other.

Results of the continuum plate theory, using values of 0.11 and 1.04 TPa for bending and stretching Young's moduli respectively, are very consistent with the lattice structure method which is based on accurate inter-atomic forces. Above examples show this consistency for different shapes and sizes of single-layered graphene sheets. This proves the accuracy of the continuum model for mechanical simulation of graphene structure. Based on these two values, membrane stiffness of the graphene $K = E_x h / (1 - \nu^2)$ is found to be 363 N. m^{-1} and bending stiffness $D = E_b h^3 / 12 (1 - \nu^2)$ is $3.7 \times 10^{-10} \text{ N. nm}$ which is equal to 2.3 eV.

Finally, first six in-plane and out-of-plane mode shapes of a circular graphene sheet are presented in Fig. 5.13 and Fig. 5.14 respectively to provide a clear understanding of the vibrational behavior of the graphenes. Radius of the sheet is 2 nm and the edge is clamped. Here, the symmetry and anti-symmetry modes are distinctly observed. First and second in-plane modes are repeated roots of the characteristic equation as well as fourth and fifth modes. Third in-plane mode shows a whirling about the center and can be seen as a torsional mode of vibration. First and sixth out-of-plane modes show an axisymmetric pattern. Second and third out-of-plane modes come in pairs as fourth and fifth ones. These mode shapes reveal that there is an astounding similarity between the vibrational modes of the single-layered graphene sheet by lattice structure and the continuum plate methods.

5.4. Concluding remarks

Understanding of the mechanical properties of graphene sheets is in a very early phase and a lot can be learned from the numerical modeling methods. Modeling of such nano-scale structures at atomic level is always desirable, but the computation can be quickly impeded even if the size increases from small to medium. In this paper, the single-layered graphene sheets are numerically studied in great detail by lattice structure method which includes the refined details of the structure and possess the accuracy of the molecular dynamics method. The results from the lattice structure method are then essentially

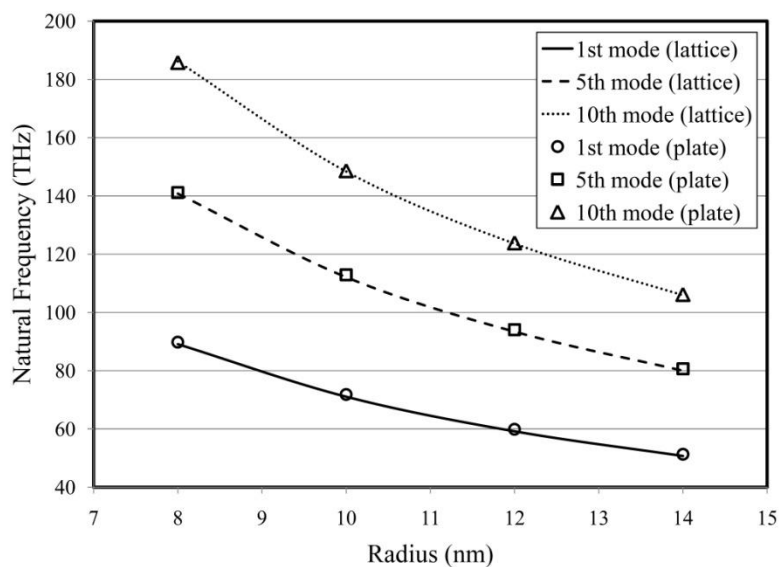


Fig. 5.11 In-plane natural frequencies of clamped edge circular single-layered graphene sheets

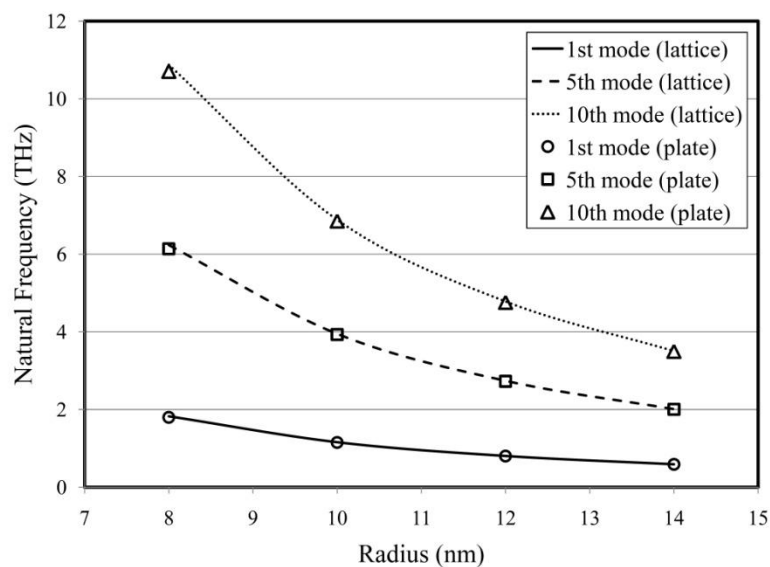


Fig. 5.12 Out-of-plane natural frequencies of clamped edge circular single-layered graphene sheets

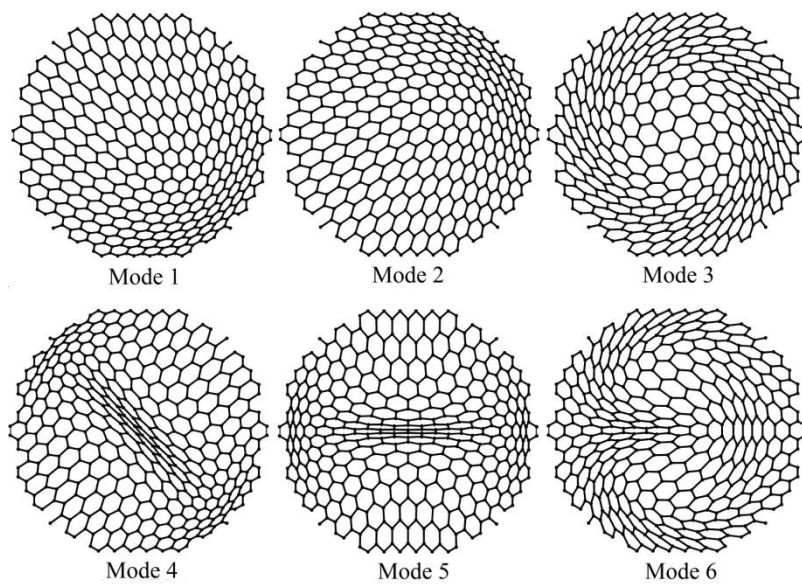


Fig. 5.13 First 6 in-plane mode shapes of a clamped edge circular single-layered graphene sheet

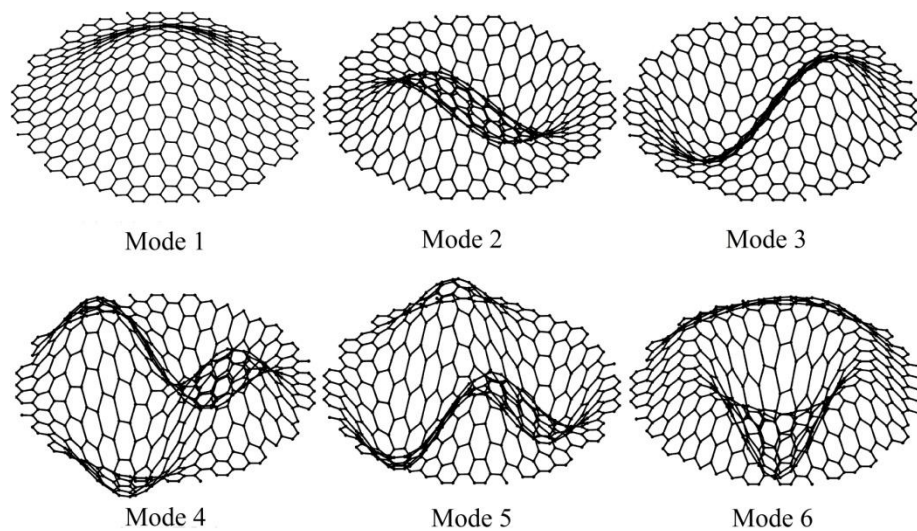


Fig. 5.14 First 6 out-of-plane mode shapes of a clamped edge circular single-layered graphene sheet

reproduced by the classical continuum plate theory which is well established and used by scientists and engineers.

By assuming thickness $h = 3.4 \text{ \AA}$ and the Poisson's ratio $\nu = 0.16$, the static analyses are performed by the lattice structure method to evaluate the equivalent Young's moduli for their use in the continuum model of the single-layered graphene sheet. Two different values of Young's modulus of elasticity of 1.04 TPa for in-plane condition and 0.11 TPa for the bending modes respectively are suggested from this study. Different examples with a variety of shapes and sizes are considered to show how the continuum plate model can be accurately applied in the analyses of single-layered graphene sheets. As the size of the single-layered graphene sheet increases, the agreement between the results from the two methods improves drastically at all modes of vibration. The bending frequencies are significantly lower in value than the in-plane frequencies for a given structure. Also, the flexural and extensional modes are completely decoupled in this linear elastic modeling approach used. Considering that when the graphene sheets become too large, it can be unbearable in the programming environment to hand their lattice structure models. The subtle and efficient numerical approach introduced here is expected to yield sufficiently accurate results for large size graphene sheets considered as a continuum plate. Also, the elastic properties suggested can be used in other numerical approaches within the continuum plate theory.

References

- [1] Novoselov, K. S., Jiang, D., Schedin, F., Booth, T. J., Khotkevich, V. V., Morozov, S. V., and Geim, A. K., 2005, "Two-dimensional atomic crystals," *Proceedings of the National Academy of Sciences of the United States of America*, 102(30), pp. 10451-10453.
- [2] Geim, A. K., and Novoselov, K. S., 2007, "The rise of graphene," *Nature Materials*, 6(3), pp. 183-191.
- [3] Stankovich, S., Dikin, D. A., Dommett, G. H. B., Kohlhaas, K. M., Zimney, E. J., Stach, E. A., Piner, R. D., Nguyen, S. T., and Ruoff, R. S., 2006, "Graphene-based composite materials," *Nature*, 442(7100), pp. 282-286.

- [4] Wu, Y. H., Yu, T., and Shen, Z. X., 2010, "Two-dimensional carbon nanostructures: Fundamental properties, synthesis, characterization, and potential applications," *Journal of Applied Physics*, 108(7).
- [5] Singh, A. V., and Arghavan, S., 2010, "Vibrations of carbon nanoscale structures: a critical review," *Computational Technology Reviews*, 1, pp. 281-314.
- [6] Van Lier, G., Van Alsenoy, C., Van Doren, V., and Geerlings, P., 2000, "Ab initio study of the elastic properties of single-walled carbon nanotubes and graphene," *Chemical Physics Letters*, 326(1-2), pp. 181-185.
- [7] Scarpa, F., Adhikari, S., and Srikantha Phani, A., 2009, "Effective elastic mechanical properties of single layer graphene sheets," *Nanotechnology*, 20(6).
- [8] Jiang, J. W., Wang, J. S., and Li, B., 2009, "Young's modulus of graphene: A molecular dynamics study," *Physical Review B - Condensed Matter and Materials Physics*, 80(11).
- [9] Karnet, Y. N., Nikitin, S. M., Nikitina, E. A., and Yanovskii, Y. G., 2010, "Computer simulation of mechanical properties of carbon nanostructures," *Mechanics of Solids*, 45(4), pp. 595-609.
- [10] Georgantzinos, S. K., Giannopoulos, G. I., and Anifantis, N. K., 2010, "Numerical investigation of elastic mechanical properties of graphene structures," *Materials and Design*, 31(10), pp. 4646-4654.
- [11] Neek-Amal, M., and Peeters, F. M., 2010, "Linear reduction of stiffness and vibration frequencies in defected circular monolayer graphene," *Physical Review B - Condensed Matter and Materials Physics*, 81(23).
- [12] Sadeghi, M., and Naghdabadi, R., 2010, "Nonlinear vibrational analysis of single-layer graphene sheets," *Nanotechnology*, 21(10).
- [13] Hemmasizadeh, A., Mahzoon, M., Hadi, E., and Khandan, R., 2008, "A method for developing the equivalent continuum model of a single layer graphene sheet," *Thin Solid Films*, 516(21), pp. 7636-7640.
- [14] Wang, L., and He, X., 2010, "Vibration of a multilayered graphene sheet with initial stress," *Journal of Nanotechnology in Engineering and Medicine*, 1(4).
- [15] He, X. Q., Kitipornchai, S., and Liew, K. M., 2005, "Resonance analysis of multi-layered graphene sheets used as nanoscale resonators," *Nanotechnology*, 16(10), pp. 2086-2091.
- [16] Liew, K. M., He, X. Q., and Kitipornchai, S., 2006, "Predicting nanovibration of multi-layered graphene sheets embedded in an elastic matrix," *Acta Materialia*, 54(16), pp. 4229-4236.

- [17] Behfar, K., Vafai, A., Naghdabadi, R., and Estekanchi, H. E., "Nanoscale vibrational analysis of an embedded multi-layered graphene sheet," pp. 569-572.
- [18] Behfar, K., and Naghdabadi, R., 2005, "Nanoscale vibrational analysis of a multi-layered graphene sheet embedded in an elastic medium," *Composites Science and Technology*, 65(7-8), pp. 1159-1164.
- [19] Gupta, S. S., and Batra, R. C., 2010, "Elastic properties and frequencies of free vibrations of single-layer graphene sheets," *Journal of Computational and Theoretical Nanoscience*, 7(10), pp. 2151-2164.
- [20] Ranjbartoreh, A. R., Wang, B., Shen, X., and Wang, G., 2011, "Advanced mechanical properties of graphene paper," *Journal of Applied Physics*, 109(1).
- [21] Murmu, T., and Pradhan, S. C., 2009, "Vibration analysis of nano-single-layered graphene sheets embedded in elastic medium based on nonlocal elasticity theory," *Journal of Applied Physics*, 105(6).
- [22] Murmu, T., and Pradhan, S. C., 2009, "Small-scale effect on the free in-plane vibration of nanoplates by nonlocal continuum model," *Physica E: Low-Dimensional Systems and Nanostructures*, 41(8), pp. 1628-1633.
- [23] Murmu, T., and Pradhan, S. C., 2009, "Vibration analysis of nanoplates under uniaxial prestressed conditions via nonlocal elasticity," *Journal of Applied Physics*, 106(10).
- [24] Pradhan, S. C., and Phadikar, J. K., 2009, "Nonlocal elasticity theory for vibration of nanoplates," *Journal of Sound and Vibration*, 325(1-2), pp. 206-223.
- [25] Arash, B., and Wang, Q., 2011, "Vibration of single- and double-layered graphene sheets," *Journal of Nanotechnology in Engineering and Medicine*, 2(1).
- [26] Ansari, R., Rajabiehfard, R., and Arash, B., 2010, "Nonlocal finite element model for vibrations of embedded multi-layered graphene sheets," *Computational Materials Science*, 49(4), pp. 831-838.
- [27] Jomehzadeh, E., and Saidi, A. R., 2011, "A study on large amplitude vibration of multilayered graphene sheets," *Computational Materials Science*, 50(3), pp. 1043-1051.
- [28] Cornell, W. D., Cieplak, P., Bayly, C. I., Gould, I. R., Merz Jr, K. M., Ferguson, D. M., Spellmeyer, D. C., Fox, T., Caldwell, J. W., and Kollman, P. A., 1995, "A second generation force field for the simulation of proteins, nucleic acids, and organic molecules," *Journal of the American Chemical Society*, 117(19), pp. 5179-5197.
- [29] Arghavan, S., and Singh, A. V., 2011, "On the vibrations of single-walled carbon nanotubes," *Journal of Sound and Vibration*, 330(13), pp. 3102-3122.

- [30] Li, C., and Chou, T. W., 2003, "A structural mechanics approach for the analysis of carbon nanotubes," *International Journal of Solids and Structures*, 40(10), pp. 2487-2499.
- [31] Li, C., and Chou, T. W., 2003, "Single-walled carbon nanotubes as ultrahigh frequency nanomechanical resonators," *Physical Review B - Condensed Matter and Materials Physics*, 68(7), pp. 734051-734053.
- [32] Sakhaee-Pour, A., Ahmadian, M. T., and Naghdabadi, R., 2008, "Vibrational analysis of single-layered graphene sheets," *Nanotechnology*, 19(8).
- [33] Timoshenko, S., and Woinowsky-Krieger, S., 1959, *Theory of plates and shells*, McGraw-Hill, New York.
- [34] Blevins, R. D., 1979, *Formulas for natural frequency and mode shapes*, Van Nostrand Reinhold, New York.

CHAPTER 6

Nonlinear Vibration of Multi-Layered Graphene Sheets ^{**}

6.1. Introduction

Graphite is the most stable allotrope of carbon and composed of sheets of chicken wire six-member carbon rings [1]. The stacked sheets, individually known as graphene, are held together by very weak van der Waals forces which allow them to slide on each other. Graphite has exceptional engineering properties which make it very desirable for numerous emerging applications. For example, it is an excellent electric conductor due to electron delocalization within layers and has highly anisotropic thermal and acoustic properties [2]. As more understanding and knowledge on the properties and mass production techniques are gained, new applications of graphitic plates in nano electromechanical devices such as sensors and actuators will be realized.

Researchers have performed and reported in the literature the vibrational analyses of multi-layered graphene sheets using different mathematical models. He and his research group [3, 4] modeled transverse vibration of multi-layered graphene sheets by the classical plate theory using the first order approximation of the van der Waals forces in the Taylor expansion. They considered van der Waals forces as pressure on each layer and presented the closed-form solutions for the natural frequencies of double and triple-

^{**} A version of this chapter is submitted to the Journal of Physics D: Applied Physics as: Arghavan, S., and Singh, A. V., 2012, "Nonlinear vibration of multi-layered graphene sheets," Journal of Physics D: Applied Physics.

layered graphene sheets. The vibration of embedded graphene sheets in elastic matrix was also studied using the classical plate theory by Liew et al. [5] and Behfar and Naghdabadi [6]. In their study involving the nonlinear free vibration of multi-layered graphene sheet by classical plate theory, Wang et al. [7] applied the third order approximation in the Taylor series to simulate van der Waals interactions in order to improve the accuracy. They reported a significant influence of the nonlinear terms and discussed the shortfalls of the earlier works [3, 4] based on the linear assumptions.

Along the continuum model line, nonlocal elasticity in classical and first order shear deformable plates has been used to study the transverse vibration of single-layered graphene sheets [8] and embedded single-layered graphene sheets in composite materials [9-11]. In these studies, Navier's solution is considered to solve the governing differential equations. Therefore, only simply-supported boundary condition is considered. Linear approximation of van der Waals forces which was reported by He et al. [3, 4] is used in above literatures to study the effects of these interactions. Nonlocal elasticity is used to study the vibrations of single-layered graphene sheets [12] and multi-layered graphene sheets [13, 14]. Since the generalized differential quadrature method is used in these studies, it was possible to analyze the clamped boundary conditions as well. This approach was also used by others [15-17] to study the graphene embedded composites. A finite element model is also introduced by Ansari et al. [18] for vibrations of embedded multi-layered graphene sheets subjected to various boundary conditions.

Above mentioned studies which considered continuous models to study vibrational behaviours of graphitic sheets have been dealt with by introducing different limitations in the formulations. No systematic way has appeared in above studies to find appropriate, globally accepted and uniform nonlocal parameters. The nonlocal parameters are defined in each case by matching the results with molecular dynamic approaches and often fail to relate such studies to other methods. Moreover, studies on equivalent mechanical properties of graphitic sheets often lack clear understanding of the mechanical characteristics of the sheets [19]. Additionally, highly nonlinear van der Waals interactions between layers are linearized in the same way as done by He et al. [3, 4]. The new studies show that effects of nonlinear terms cannot be neglected [7] and hence

continuous models do not reflect the true nature of atomic structures on the mechanical properties of the sheets.

Simulating mechanical and vibrational behaviours of nanoscale structures using atomic scale methods such as molecular dynamics and lattice structures attracted many attentions [20, 21]. These approaches use inter atomic force fields and stiffness properties which lead to significantly more accurate results comparing to the continuous fields. Realistic atomic structures can be produced by these methods and very precise inter atomic interactions are simulated independently. The lattice structure method presented by Li and Chou in 2003 [22] used by many scientists to model mechanical behaviour of nanoscale structures [23]. This method, which is based on finite element simulations and has very strong fundamental support [24], has been proven to give accurate results in modeling covalent bond between carbon atoms. Despite its relative simplicity comparing to molecular dynamic techniques, the method yields very accurate results in structural analyses of single-walled carbon nanotubes [25, 26] and graphene sheets [19, 27, 28].

Li and Chou have also modeled van der Waals interactions between adjacent tubes, using truss elements with nonlinear material properties and studied mechanical properties of multi-walled carbon nanotubes [29]. Van der Waals forces are converted to nonlinear stiffness properties and assembled in the global stiffness matrix along with the stiffness properties of the covalent bonds. Subsequently, coefficients of the stiffness matrix are functions of displacement components due to nonlinear material properties. Such nonlinearity increases the computational costs significantly as it includes inverting a fairly huge highly nonlinear stiffness matrix in each time step. Moreover, solving the modal problem and free vibration analysis of such nonlinear system is a big issue and requires complex numerical methods. To handle this problem, authors used the initial value of the stiffness for each truss element (based on the undeformed structure) and linearize the stiffness matrix. Natural frequencies and mode shapes of multi-walled carbon nanotubes are reported using this method [30]. Other researchers have also used the linearize stiffness matrix and studied free vibration of multi-walled carbon nanotubes [31].

This technique is also used to study the mechanical and vibrational characteristics of multi-layered graphene sheets. Georgantzinos et al. [32, 33] used truss elements with nonlinear material properties to simulate van der Waals interactions and studied mechanical characteristics of multi-layered graphene sheets. Nonlinear terms are also considered in other articles by Georgantzinos et al. [34]. Chandra et al. studied free vibration of double-layered graphene sheets with the lattice structure approach [35]. Initial distance between carbon atoms is used in above studies to find the stiffness properties of the truss element used to simulate the van der Waals interactions. Considering the full nonlinear stiffness in above studies limit their applications and increase computational costs and odds of divergence significantly.

This paper is aimed to address the vibrational behaviour of multi-layered graphene sheets based on the well-accepted lattice structure method [19]. This structural approach is considered for simulating each layer of the multi-layered graphene sheet. In order to eliminate the computational costs mentioned above and avoid the nonlinearity of the stiffness matrix, a new technique is considered here to address the nonlinearity of van der Waals forces. Instead of converting van der Waals forces to stiffness properties, van der Waals interactions are considered as nonlinear force components in the load vector here. In the second section of the paper, this method is explained thoroughly. A modified version of Newmark's integration method is presented for the forced vibrational analysis of the abovementioned nonlinear system. This method is also described in detail in the second chapter. In order to study the vibrational characteristics of multi-layered graphene sheets, the structure of the multi-layered graphene sheet is excited by a step load for short duration of time and the structural response is being analyzed. Fast Fourier transformation is being applied on the transient time-response to find the frequency spectrum and contribution of individual mode shapes in the overall response. Results show that the method is a promising way of modelling van der Waals interactions and vibrational analysis of multi-layered graphene sheets. This method is found to be relatively efficient and fast. Scrupulous discussions are presented in section four on the affects of van der Waals forces on the structural stiffness of the multi-layered graphene sheets.

6.2. Governing equation and the solution

In this section, the governing matrix equation of motion is briefly described. For this, each layer of the multi-layered graphene sheet is treated as a plane lattice structure wherein the carbon atoms are placed on the vertices of hexagonal cells. The nuclei are assumed as nodes with concentrated mass m_c of a carbon atom. The covalent bond between two adjacent carbon atoms is modeled as a three-dimensional frame element which forms the side of a hexagonal cell. The element length is the distance between the carbon nuclei which is also equal to the side of the hexagon. The axial, bending and torsional stiffness properties are obtained by considering circular cross section. The mechanical and geometric properties have been reported in the literature [22, 24] and are used later by many to study the static and vibration analyses of single-walled carbon nanotubes and graphene sheets [19, 28].

A diagonal mass matrix \mathbf{M}_g is thus formed for each layer of the graphite structure. Similarly, the stiffness matrix \mathbf{K}_g is built for each layer in three stages; first mass and stiffness matrix of each frame element are calculated in the frame element's local coordinate system, then matrices are transformed into the global coordinate system, and finally assembled. The graphite layers are identical and hence their mass and stiffness matrices are individually the same. Utilising this condition, it becomes very simple to write the mass and stiffness matrices of the graphite structure in the following form.

$$\mathbf{M} = \begin{bmatrix} [\mathbf{M}_g] & & & [0] \\ & [\mathbf{M}_g] & & \\ & & \ddots & \\ & & & [0] \end{bmatrix} \text{ and } \mathbf{K} = \begin{bmatrix} [\mathbf{K}_g] & & & [0] \\ & [\mathbf{K}_g] & & \\ & & \ddots & \\ & & & [0] \end{bmatrix} \quad (6.1)$$

It is obvious here that the layers are totally detached with each layer having its own nodes, degrees of freedom, etc. But from the physics of this structure, it is known that the layers are connected by means of the van der Waals forces in the form of nonlinear interaction. These forces are seen in either attraction or repulsion modes and obtained from the well-accepted Lennard-Jones 6-12 potential function.

$$U(r) = 4\varepsilon \left[\left(\frac{\sigma}{r} \right)^{12} - \left(\frac{\sigma}{r} \right)^6 \right] \quad (6.2)$$

Here, r is the distance between interacting atoms, $\sigma = 0.34$ nm and $\varepsilon = 3.8655 \times 10^{-13}$ N nm. Eq. (6.2) is differentiated with respect to distance r to obtain the van der Waals force between two carbon atoms.

$$F(r) = -\frac{d}{dr}U(r) = \left(\frac{24\varepsilon}{\sigma} \right) \left[2 \left(\frac{\sigma}{r} \right)^{13} - \left(\frac{\sigma}{r} \right)^7 \right] \quad (6.3)$$

Li and Chou [29] have suggested space truss elements with nonlinear material properties to simulate the van der Waals interactions between two carbon atoms. Truss elements are replicating the compressive and tensile nature of the van der Waals forces. They found the nonlinear stiffness of each truss element by calculating the first derivative of van der Waals force with respect to r . Stiffness matrices of all truss elements then are transformed to the global coordinate system and assembled to form the stiffness matrix associated with van der Waals interactions \mathbf{K}_{vdW} . Hence, the equation of motion without the damping can be written as follows.

$$\mathbf{M} \ddot{\mathbf{x}}(t) + [\mathbf{K} + \mathbf{K}_{vdW}] \mathbf{x}(t) = \mathbf{F}(t) \quad (6.4)$$

This brings in nonlinearity in the stiffness matrix and computationally complicates the problem to a great significance, because the stiffness matrix has to be updated and inverted at each iteration step in the solution procedure. In order to avoid nonlinearity in the stiffness matrix, the van der Waals interactions in the present study are applied directly to the relevant nodes. Thus, the force vector can be said to have two components: externally applied mechanical forces ($\mathbf{F}_{ext.}$) and internal interactions (\mathbf{F}_{vdW}) respectively. Ideally, the van der Waals forces exist between every pair of carbon atoms considered in the model. But, as the distance between atoms increases, the magnitude of the force diminishes rapidly. Therefore, Eq. (6.3) is used to calculate the van der Waals forces only if the carbon atoms of the adjacent layers in the model are separated by less than 2.5σ [29]. In this computational scheme, only the force vector \mathbf{F}_{vdW} remains nonlinear by being

dependent upon the inter-atomic distance vector \mathbf{x} . Eq. (6.4) now is rewritten as: $\mathbf{M} \ddot{\mathbf{x}}(t) + \mathbf{K} \mathbf{x}(t) = \mathbf{F}(t, \mathbf{x}(t))$. The composition of this equation is described as follows. The mass matrix \mathbf{M} is diagonal and the stiffness matrix \mathbf{K} is linear elastic. They are assembled and operated upon only in the initial phase of the solution procedure. The force vector expressed by $\mathbf{F}(t, \mathbf{x}(t)) = \mathbf{F}_{ext.}(t) + \mathbf{F}_{vdW}(\mathbf{x}(t))$ has two components.

In other words, in the present study, all nonlinear terms are transferred to the right hand side of the equation of motion and the left hand side is fully linear. Since the load vector is displacement dependent, a numerical solution algorithm based on the Newmark's direct integration method [36] is developed to handle the nonlinearity. The equation of motion at the $(i+1)^{\text{th}}$ time step is:

$$\mathbf{M} \ddot{\mathbf{x}}_{i+1} + \mathbf{K} \mathbf{x}_{i+1} = \mathbf{F}_{i+1} \quad (6.5)$$

Displacement at the $(i+1)^{\text{th}}$ time step is approximated in terms of the displacement, velocity, and acceleration of the previous time step by the Taylor expansion as $\mathbf{x}_{i+1} = \mathbf{x}_i + \dot{\mathbf{x}}_i \Delta t + \frac{1}{2} \ddot{\mathbf{x}}_i^{(\gamma)} (\Delta t)^2$ where $\ddot{\mathbf{x}}_i^{(\gamma)}$ is an implicit approximation of acceleration in the i^{th} time step: $\ddot{\mathbf{x}}_i^{(\gamma)} = (1 - \gamma) \ddot{\mathbf{x}}_i + \gamma \ddot{\mathbf{x}}_{i+1}$. Acceleration term $\ddot{\mathbf{x}}_{i+1}$ is replaced in the above Eq. (6.5) to obtain the following.

$$(\mathbf{K} + c_0 \mathbf{M}) \mathbf{x}_{i+1} = \mathbf{F}_{i+1} + \mathbf{M}(c_0 \mathbf{x}_i + c_1 \dot{\mathbf{x}}_i + c_2 \ddot{\mathbf{x}}_i) \quad (6.6)$$

where $c_0 = 2/(\gamma \Delta t^2)$, $c_1 = 2/(\gamma \Delta t)$ and $c_2 = -1 + 1/\gamma$. Eq. (6.6) is further written by:

$$\mathbf{x}_{i+1} = [\mathbf{K} + c_0 \mathbf{M}]^{-1} \{ \mathbf{F}_{i+1} + \mathbf{M}(c_0 \mathbf{x}_i + c_1 \dot{\mathbf{x}}_i + c_2 \ddot{\mathbf{x}}_i) \} \quad (6.7)$$

Here, matrix $[\mathbf{K} + c_0 \mathbf{M}]$ is assembled in global form and then inverted for repeated use in the solution procedure which begins with the initialized displacement $\mathbf{x}(t)$ and its time derivative $\dot{\mathbf{x}}(t)$ and proceeds successively with assumed parameter γ and time step Δt . The initial acceleration $\ddot{\mathbf{x}}(t)$ is generation from Eq. (6.5). In the present study, the damping is not considered as there is not much available on the damping of carbon

nanostructures. The right hand side of Eq. (6.7) has matrices and vectors like $\mathbf{K}, \mathbf{M}, \mathbf{x}, \dot{\mathbf{x}}$ and $\ddot{\mathbf{x}}$ which are known at the i^{th} time step. But, the force vector \mathbf{F}_{i+1} at the $(i + 1)^{\text{th}}$ time step has external and van der Waals components. Here, the external part is known at all time steps and can be evaluated easily. However, the van der Waals component includes displacement \mathbf{x}_{i+1} which is yet to be found. It is obtained iteratively using displacement, velocity and acceleration vectors from the previous time step. Using this secondary iteration, van der Waals forces are calculated precisely in each time step. This approach ensures the evaluation of nonlinear nature of van der Waals forces throughout the numerical solution. Acceleration and velocity at the $(i+1)^{\text{th}}$ time step are found successively using the Taylor expansion as: $\ddot{\mathbf{x}}_{i+1} = c_0 (\mathbf{x}_{i+1} - \mathbf{x}_i) - c_1 \dot{\mathbf{x}}_i - c_2 \ddot{\mathbf{x}}_i$ and $\dot{\mathbf{x}}_{i+1} = \dot{\mathbf{x}}_i + [(1 - \delta)\ddot{\mathbf{x}}_i + \delta \ddot{\mathbf{x}}_{i+1}]\Delta t$ respectively. δ is a constant parameter. An in-house finite element code is developed in C++ environment to produce the geometry, generate matrices and vectors and solve the governing nonlinear equation. All computing is performed on the computational facilities of SHARCNET. In this simulations, prescribed values of 1.6 and 1.5 are considered for γ and δ respectively to ensure the stability of the solution algorithm [36].

6.3. Numerical results for a double-layered graphene sheet and discussions

The equation of motion and its solution by the modified Newmark's direct integration method as described above are applied to a $3.69 \text{ nm} \times 3.69 \text{ nm}$ square double-layered graphene sheet in this study. Each layer in this numerical model is the true copy of the other and consists of 558 carbon atoms which are packed together to form a flat honeycomb structure as shown in Fig. 6.1. Nucleus of each carbon atom is taken as a node with six degrees of freedom. In this manner, there are 1116 nodes in all and the model has 6696 degrees of freedom which is also the order of each of the stiffness and mass matrices. Two different boundary conditions are considered for the transverse (out-of-plane) case. These are: all simply supported and all clamped edges. All edges are

clamped in the case of the in-plane vibration. A gap of 0.34 nm between the two layers is used in the following computations [29]. The primary objective of this numerical

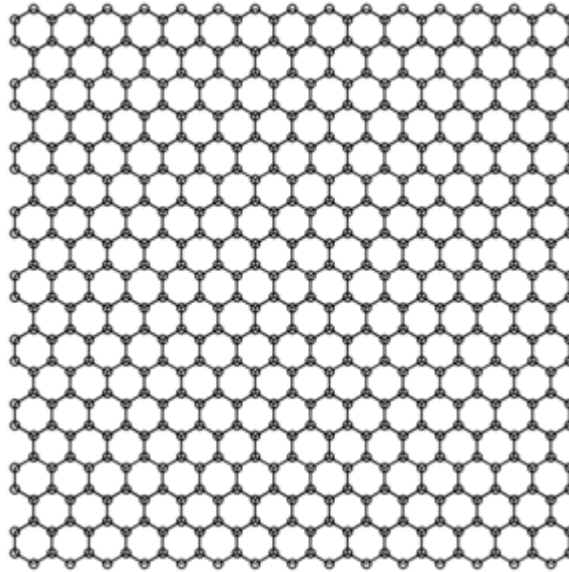


Fig. 6.1 Geometry of one layer of the 3.69 nm \times 3.69 nm double-layered graphene sheet

Table 6.1 Natural frequencies of single-layered graphene sheet

Mode Number	Out-of-plane Natural Frequencies (THz)		In-plane Natural Frequencies (THz)
	SSSS Condition	CCCC Condition	CCCC Condition
1	0.1652	0.2923	3.5022
2	0.4091	0.5905	3.5038
3	0.4094	0.6004	4.5805
4	0.6588	0.8769	5.2204
5	0.8121	1.0562	5.7719
6	0.8124	1.0800	6.2826
7	1.0650	1.3266	6.2983
8	1.0660	1.3425	6.3362
9	1.3734	1.6810	7.0768
10	1.3739	1.7192	7.1612

investigation include: to find the frequency distribution of the double-layered graphene sheet, to obtain understanding of the interaction between the layers due to van der Waals forces, and finally to assess the efficiency and accuracy of the proposed methodology.

Before getting into the vibrational analyses of the double-layered graphene sheet, the first ten bending (out-of-plane) and extensional (in-plane) modes of vibration of a $3.69 \text{ nm} \times 3.69 \text{ nm}$ square single-layered graphene sheet are calculated by the lattice structure method [19] and reported in Table 6.1. As expected, frequencies in bending modes of the simply supported case are significantly lower than the corresponding frequencies of the clamped boundary condition. The value of the fundamental frequency of the in-plane vibration is more than twenty times that of the simply supported case.

Since there is no mechanical connectivity between the two layers which are only bonded by the nonlinear van der Waals forces, no free vibration analysis can be performed due to this nonlinearity. Therefore, in order to investigate the effects of the van der Waals forces on the frequency pattern of this two layer system, the forced vibration analysis is performed and reported in this section. Equal transverse step load is applied to all unsupported nodes on the top layer of the graphene sheet. The magnitude and duration of the load used in the calculation are 5 pN and 10 ps respectively. Vibration of the top layer is the result of both the external step load and van der Waals interactions, while the bottom layer responds only to the van der Waals forces. Fig. 6.2 shows the displacement time-histories of the centrally located nodal points at the top and bottom layers of the simply supported double-layered graphene sheet by dashed and solid lines respectively. The response at the top layer is seen to have larger amplitude than the bottom layer, but the frequency distributions of the two are more or less the same. The top layer is subjected at a given time by externally applied and van der Waals forces. The bottom layer is excited only by the relatively weak van der Waals force and hence its amplitude of vibration is expected to be smaller than the top layer. From each of the displacement time-histories in Fig. 6.2, it is observed that high frequency waves are riding a low frequency wave-form corresponding to the fundamental mode. To unravel it, the fast Fourier transformations of the time histories are computed to capture the frequency distributions which are found to be identical for the top and bottom layers. Hence, fast

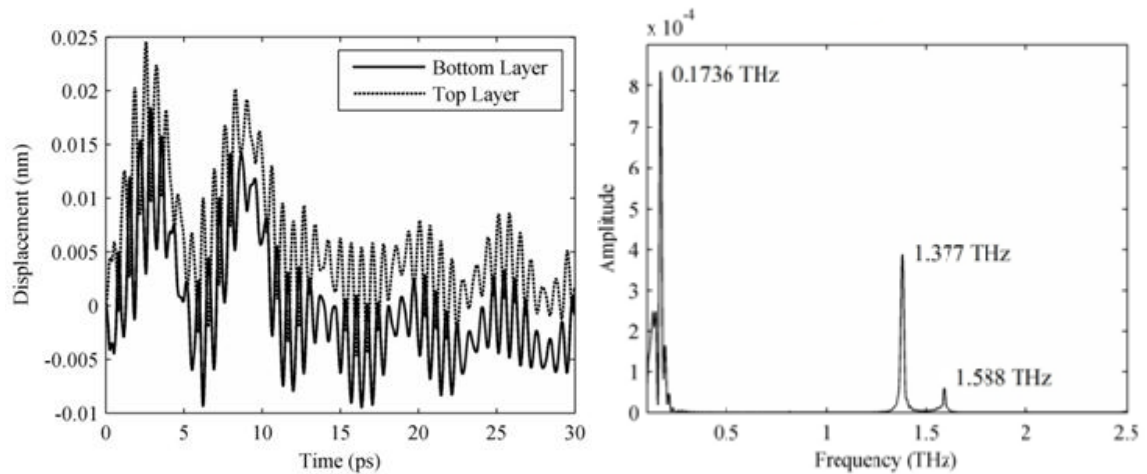


Fig. 6.2 Time history and fast Fourier transform plot of two nodes at the centre of the bottom and top layers of the double-layered simply supported graphene sheets in transverse vibration

Fourier transformation for the top layer case is plotted only in Fig. 6.2 in which three distinct peaks are observed at 0.1736 THz, 1.377 THz and 1.588 THz respectively. The first peak occurs at a frequency which is about 5% higher than the fundamental bending frequency (0.1652 THz) of the simply supported single-layered graphene sheet (Table 6.1). Similarly, the second peak occurs at very high frequency in the neighbourhood of modes 9 and 10 modes and the third at modes 12 and 13. No peak is observed between the 0.5-1.4 THz range in this Fourier spectrum. Still this range is examined very minutely and a very weak peak is noted at 0.8135 THz which is within the computational margin of modes 5 and 6. Mode 1 and the vibrational mode pairs 5-6, 9-10, and 12-13 are all symmetrical about both x and y axes through the centre of graphene sheet. This assures correctness of the trend the results have, i.e. when the geometry, loading and boundary conditions are all symmetrical about both axes, only such symmetrical modes are expected to contribute in producing the transient response.

Next, the transverse vibration of the double-layered graphene sheet with clamped edges is studied. Time-histories and fast Fourier transformation plots are found as seen in Fig. 6.3. In this case also, the dashed line represents response at the top central point and the solid line at the corresponding point on the bottom layer. There are three peaks that are visible in the fast Fourier transformation spectrum occurring at 0.2889 THz, 1.4 THz,

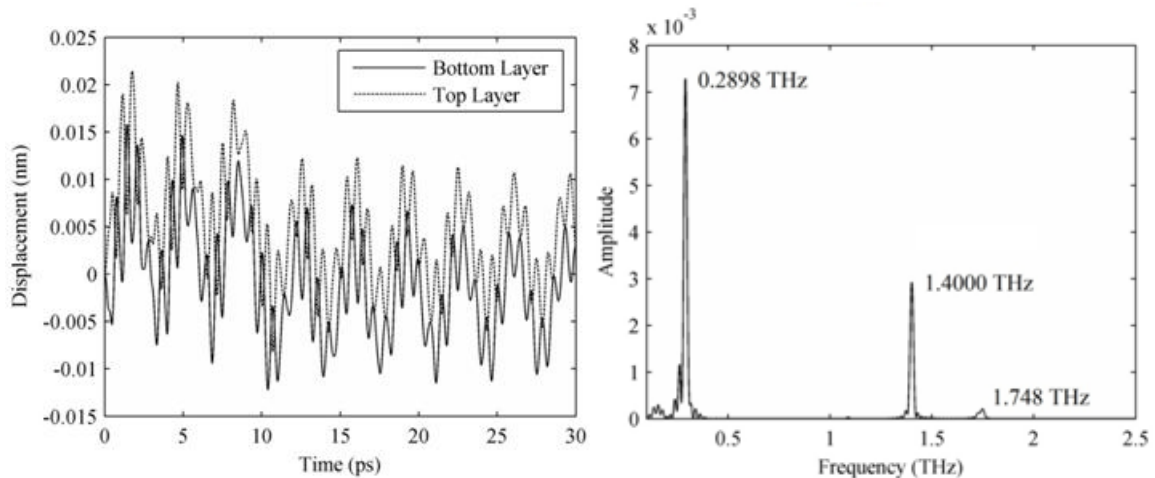


Fig. 6.3 Time history and fast Fourier transform plot of two nodes at the centre of the bottom and top layers of the double-layered clamped graphene sheets in transverse vibration

and 1.748 THz respectively. First peak falls within 1.2% of the first natural frequency 0.2923 THz of the clamped single-layered graphene sheet, while the second between the 8th and 9th natural modes (Table 6.1). The third peak is found at frequency slightly higher than the 10th natural frequency. In the overall sense, the fundamental bending frequency of the single-layered graphene sheet dominates the out-of-plane response of the double-layered graphene sheet cause by external and nonlinear van der Waals forces.

Vibration of double-layered graphene sheet has been reported by others [3, 4, 35] where nonlinear van der Waals force directly derived from the Lennard-Jones 6–12 potential function. But due to severe complexity involved in dealing with this nonlinear form of van der Waals force, they all linearized it in their solution methods. Explicit formulae have been reported for predicting the natural frequencies of double-layered graphene sheet based on the classical plate bending theory and linear approximation of the van der Waals forces in the literature [3, 4]. Using these formulae with the mechanical properties of the graphene sheet as given by $\rho = 2250 \text{ Kg m}^{-3}$, $\nu = 0.16$ and $E_b = 0.112 \text{ TPa}$ [18], the first two frequencies are found to be 0.1616 and 2.6872 THz respectively. The first value 0.1616 THz is very comparable with the fundamental frequency 0.1652 THz of a simply supported single-layered graphene sheet, but the second

frequency which according to them [3] is the direct effect of the van der Waals interaction, is approximately twice the 10th natural frequency (Table 6.1). Recently Chandra et al. [35] studied double-layered graphene strips by the atomistic finite element approach and modelled van der Waals force by truss element. Using the procedure suggested in ref. [35], the present two layered lattice structure model subject to simply supported and clamped boundary conditions is analyzed. The fundamental frequencies are found to be 0.068 THz and 0.126 THz which are significantly lower than 0.1736 THz and 0.2898 THz as shown in Fig. 6.2 respectively for the two cases. From the present study using nonlinearity in the van der Waals forces without any simplification, it is found that results show very reasonable pattern. For example, the suddenly applied load on a linear elastic structure produces response time history which is a result of the superposition of the normal modes of vibration in the frequency spectrum, peaks at the case dependent natural modes are observed. In the nonlinear case, the transient response is very similar to the linear type. The frequency distribution is also very similar. The difference is that the positions of the resonant peaks are slightly shifted from the corresponding linear peaks.

The in-plane vibration of the same model of the double-layered graphene sheet is also studied with the clamped edge condition. Again, all nodes on the top layer are excited by an in-plane step load of equal magnitude in both x and y directions. The transient response at the centre of the top layer in x direction and its fast Fourier transformation are plotted as shown in Fig. 6.4. Only one peak very close to the first in-plane natural frequency of the clamped single-layered graphene sheet is visible in the fast Fourier transformation plot. Response of the corresponding point on the bottom layer has also been examined, but it is found to have negligible magnitude as compared to that of the top layer. Its further examination reveals nearly the same oscillatory pattern and hence, is not included in this paper. This shows that there is a negligible transfer of the in-plane van der Waals forces from the top layer to the bottom. This can be explained as follows. If the van der Waals forces on a carbon atom at the bottom layer are resolved, the in-plane components of the van der Waals forces are balanced due to symmetric nature of the placement of the carbon atom on the top layer and hence the effects of van der Waals forces are neutralized. Also, the overall in-plane stiffness of graphene as can be seen from the in-

plane frequencies in Table 6.1 is extremely high, in-plane deflection is expected to be small and hence very low magnitude van der Waals forces will be produced.

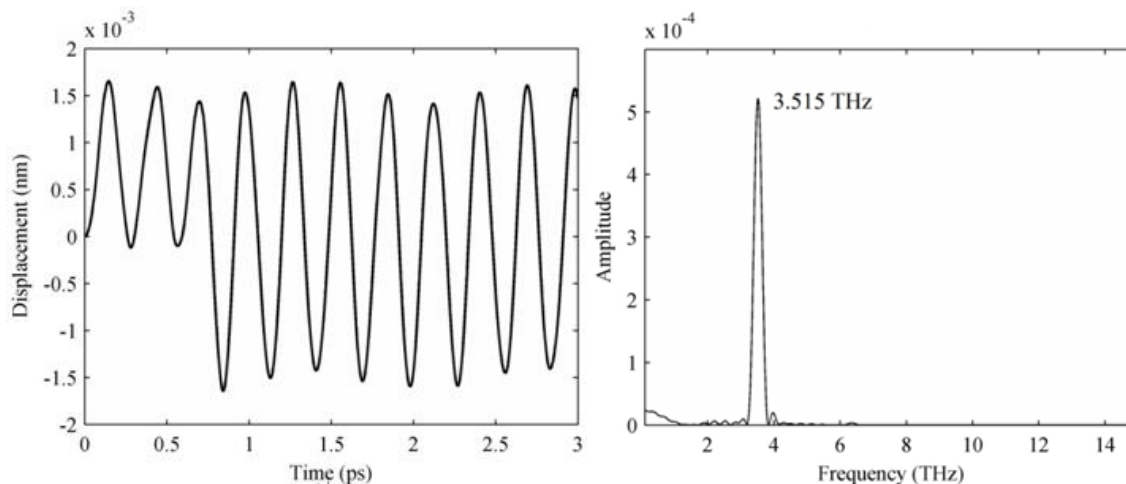


Fig. 6.4 Time history and fast Fourier transform plot of a node at the centre of the top layer of the double-layered clamped graphene sheets in in-plane vibration

6.4. Concluding remark

The lattice structure approach is used for the investigation of the vibrational behaviour of double-layered graphene sheets. In the present method, the highly nonlinear van der Waals interactions directly derived from Lennard-Jones 6–12 potential function without simplification are used. The van der Waals forces are directly applied to the nodal points of each layer and the stiffness matrix is kept linear. Since the combined mass and stiffness matrices are inverted only once during the iteration, the computational rigor is significantly reduced. In the solution algorithm, the Newmark's direct integration method is modified accordingly to solve the nonlinear governing equation. The present method is capable of modelling the nonlinear forced vibration of multi-layered graphene sheets under bending and in-plane modes with different boundary conditions. In the transverse vibration, multi-layered graphene sheet essentially vibrates with the fundamental frequency of the single-layered graphene sheet of the same size and boundary conditions. Effects of significantly weak van der Waals forces are seen at the higher natural

frequencies through the fast Fourier transformation plot of the response. The nonlinearity alters the frequency spectrum in a similar manner as the large scale structures. The peaks at higher frequencies show little dependency on the boundary conditions. In contrast to transverse vibration, van der Waals forces do not have any substantial role in in-plane vibration. Layers are vibrating horizontally with the in-plane natural frequency of the single-layered graphene sheet of the same size and boundary condition.

Acknowledgement

This research has been made possible by the Shared Hierarchical Academic Research Computing Network (SHARCNET: <http://www.sharcnet.ca>) facilities.

References

- [1] Jenkins, G. M., Williamson, G. K., and Barnett, J., 1964, "The role of crystal structure in determining the mechanical properties of graphite," *Carbon*, 1(3), p. 361.
- [2] Enoki, T., Suzuki, M., and Endo, M., 2003, *Graphite intercalation compounds and applications*, Oxford University Press, New York.
- [3] He, X. Q., Kitipornchai, S., and Liew, K. M., 2005, "Resonance analysis of multi-layered graphene sheets used as nanoscale resonators," *Nanotechnology*, 16, pp. 2086–2091.
- [4] Kitipornchai, S., He, X. Q., and Liew, K. M., 2005, "Continuum model for the vibration of multilayered graphene sheets," *Physical Review B - Condensed Matter and Materials Physics*, 72(7).
- [5] Liew, K. M., He, X. Q., and Kitipornchai, S., 2006, "Predicting nanovibration of multi-layered graphene sheets embedded in an elastic matrix," *Acta Materialia*, 54, pp. 4229–4236.
- [6] Behfar, K., and Naghdabadi, R., 2005, "Nanoscale vibrational analysis of a multi-layered graphene sheet embedded in an elastic medium," *Composites Science and Technology*, 65, pp. 1159–1164.
- [7] Wang, J., He, X., Kitipornchai, S., and Zhang, H., 2011, "Geometrical nonlinear free vibration of multi-layered graphene sheets," *Journal of Physics D: Applied Physics*, 44, p. 135401.

- [8] Pradhan, S. C., and Phadikar, J. K., 2009, "Nonlocal elasticity theory for vibration of nanoplates," *Journal of Sound and Vibration*, 325(1-2), pp. 206-223.
- [9] Murmu, T., and Pradhan, S. C., 2009, "Vibration analysis of nano-single-layered graphene sheets embedded in elastic medium based on nonlocal elasticity theory," *Journal of Applied Physics*, 105(6).
- [10] Pradhan, S. C., and Sahu, B., 2010, "Vibration of single layer graphene sheet based on nonlocal elasticity and higher order shear deformation theory," *Journal of Computational and Theoretical Nanoscience*, 7(6), pp. 1042-1050.
- [11] Pradhan, S. C., and Phadikar, J. K., 2009, "Small scale effect on vibration of embedded multilayered graphene sheets based on nonlocal continuum models," *Physics Letters, Section A: General, Atomic and Solid State Physics*, 373(11), pp. 1062-1069.
- [12] Ansari, R., Sahmani, S., and Arash, B., 2010, "Nonlocal plate model for free vibrations of single-layered graphene sheets," *Physics Letters, Section A: General, Atomic and Solid State Physics*, 375(1), pp. 53-62.
- [13] Jomehzadeh, E., and Saidi, A. R., 2011, "A study on large amplitude vibration of multilayered graphene sheets," *Computational Material Science*, 50(3), pp. 1043-1051.
- [14] Arash, B., and Wang, Q., 2011, "Vibration of single- and double-layered graphene sheets," *Journal of Nanotechnology in Engineering and Medicine*, 2(1), p. 011012.
- [15] Pradhan, S. C., and Kumar, A., 2011, "Vibration analysis of orthotropic graphene sheets using nonlocal elasticity theory and differential quadrature method," *Composite Structures*, 93(2), pp. 774-779.
- [16] Pradhan, S. C., and Kumar, A., 2010, "Vibration analysis of orthotropic graphene sheets embedded in Pasternak elastic medium using nonlocal elasticity theory and differential quadrature method," *Computational Materials Science*, 50(1), pp. 239-245.
- [17] Ansari, R., Arash, B., and Rouhi, H., 2011, "Vibration characteristics of embedded multi-layered graphene sheets with different boundary conditions via nonlocal elasticity," *Composite Structures*, 93(9), pp. 2419-2429.
- [18] Ansari, R., Rajabiehfard, R., and Arash, B., 2010, "Nonlocal finite element model for vibrations of embedded multi-layered graphene sheets " *Computational Materials Science*, 49(4), pp. 831-838
- [19] Arghavan, S., and Singh, A. V., 2011, "Atomic lattice structure and continuum plate theories for the vibrational characteristics of graphenes," *Journal of Applied Physics*, 110(8).
- [20] Chowdhury, R., Adhikari, S., Scarpa, F., and Friswell, M. I., 2011, "Transverse vibration of single-layer graphene sheets," *Journal of Physics D: Applied Physics*, 44(20).

- [21] Nakajima, T., and Shintani, K., 2011, "Controlling out-of-plane deformations of graphene nanobridges," *Physica Status Solidi (B) Basic Research*, 248(12), pp. 2839-2847.
- [22] Li, C., and Chou, T. W., 2003, "A structural mechanics approach for the analysis of carbon nanotubes," *International Journal of Solids and Structures*, 40, pp. 2487–2499.
- [23] Singh, A. V., and Arghavan, S., 2010, "Vibrations of Carbon Nanoscale Structures: A Critical Review," *Computational Technology Reviews*, 1, pp. 281-314.
- [24] Cornell, W. D., Cieplak, P., Bayly, C. I., Gould, I. R., Merz Jr, K. M., Ferguson, D. M., Spellmeyer, D. C., Fox, T., Caldwell, J. W., and Kollman, P. A., 1995, "A second generation force field for the simulation of proteins, nucleic acids, and organic molecules," *Journal of the American Chemical Society*, 117(19), pp. 5179-5197.
- [25] Li, C., and Chou, T. W., 2003, "Single-walled carbon nanotubes as ultrahigh frequency nanomechanical resonators," *Physical Review B*, 68.
- [26] Arghavan, S., and Singh, A. V., 2011, "On the vibrations of single-walled carbon nanotubes," *Journal of Sound and Vibration* 330(13), pp. 3102-3122.
- [27] Sakhaee-Pour, A., Ahmadian, M. T., and Naghdabadi, R., 2008, "Vibrational analysis of single-layered graphene sheets," *Nanotechnology*, 19(8), p. 085702.
- [28] Arghavan, S., and Singh, A. V., 2011, "Free Vibration of Single Layer Graphene Sheets: Lattice Structure Versus Continuum Plate Theories," *Journal of Nanotechnology in Engineering and Medicine*, 2(3), pp. 031005-031006.
- [29] Li, C., and Chou, T. W., 2003, "Elastic moduli of multi-walled carbon nanotubes and the effect of van der Waals forces," *Composites Science and Technology*, 63, pp. 1517–1524.
- [30] Li, C., and Chou, T. W., 2004, "Vibrational behaviors of multiwalled-carbon-nanotube-based nanomechanical resonators," *Applied Physics Letters*, 84(1), pp. 121-123.
- [31] Fan, C. W., Liu, Y. Y., and Hwu, C., 2009, "Finite element simulation for estimating the mechanical properties of multi-walled carbon nanotubes," *Applied Physics A*, 95, pp. 819–831.
- [32] Georgantzinos, S. K., Giannopoulos, G. I., and Anifantis, N. K., 2010, "Numerical investigation of elastic mechanical properties of graphene structures," *Materials and Design*, 31(10), pp. 4646-4654.
- [33] Giannopoulos, G. I., Liosatos, I. A., and Moukanidis, A. K., 2011, "Parametric study of elastic mechanical properties of graphene nanoribbons by a new structural mechanics approach," *Physica E: Low-Dimensional Systems and Nanostructures*, 44(1), pp. 124-134.

- [34] Georgantzinos, S. K., Giannopoulos, G. I., Katsareas, D. E., Kakavas, P. A., and Anifantis, N. K., 2011, "Size-dependent non-linear mechanical properties of graphene nanoribbons," *Computational Materials Science*, 50(7), pp. 2057-2062.
- [35] Chandra, Y., Chowdhury, R., Scarpa, F., and Adhikaricor, S., 2011, "Vibrational characteristics of bilayer graphene sheets," *Thin Solid Films*, 519(18), pp. 6026-6032.
- [36] Bathe, K. J., and Wilson, E. L., 1976, *Numerical methods in finite element analysis*, Prentice Hall Inc., New Jersey.

CHAPTER 7

Conclusions, Contributions and Future Works

7.1. Introduction

Studying mechanical properties of carbon nano-structures is the focus of this thesis. These structures have attracted huge amount of attentions because of their exceptional physical, chemical, mechanical, optical and electrical characteristics and continues to do so. The lattice structure approach based on finite element method is considered to be as accurate as molecular dynamic techniques and used in this thesis to study the mechanical and vibrational behaviors of carbon nano-structures. Preserving the simplicity, this method is able to simulate the stiffness of graphitic structures very accurately and has outstanding advantages over other analytical and numerical methods used in the literature.

Several well liked methods which are being used in the literature frequently for such studies of nano-structures are introduced in the second chapter of this thesis. Molecular dynamic procedures having roots in quantum physics are used extensively by physicists to investigate the behaviors of individual and/or interacting nano-structures. These trials have originated from empirical and theoretical force-fields that describe the interactions between two particles. Even though such practices are able to simulate the behaviors of nano-structures very precisely, they come with huge computational costs. Researchers can not apply these methods to structures with more than a couple of hundred particles, even if networked super computers with very efficient parallel processing algorithms are used. In a successful run in such computational environment, they are able to process

only for a few nano seconds. These limitations push researches, especially engineers, to find simpler ways to deal with the problem.

Quite a lot of classic continuous models such as Euler-Bernoulli and Timoshenko beam theories and plates and shell structures are recommended by researchers for simulating the behaviors of nano-structures. Simplicity, availability of closed form solutions and ease of deriving and modifying formulations are the most dominant motivating factors for using these methods by researchers. However, the fact of neglecting the effects of atomic structures and simplifying the solution by dropping significant factors are the main shortfalls of these techniques. Moreover, lack of a systematic way of finding the equivalent mechanical properties raises questions over the accuracy of the results. Very few articles can be found that attempt to compare results of these simplified theories with accurate molecular dynamic methods. Even applying nonlocal elasticity theorems and unrealistic equivalent thickness do not help to improve the results and hence, a wide gap is seen between molecular dynamic and continuous methods.

The lattice structure method which is introduced and developed in 2000's has many advantages over all of the above mentioned methods without shortfalls and deficits. This finite element based approach uses the precise atomic arrangement of the graphitic structures, models the covalent bonds and van der Waals interactions accurately and is very fast and efficient. The method has been explained comprehensively in the second chapter of this thesis and used in chapter three to six to study the mechanical properties and vibrational characteristics of single-walled carbon nanotubes and single and double-layered graphene sheets. In each case, the structure was modeled accordingly and appropriate analyses are performed to study the complicated behaviors of these nano-structures.

7.2. Conclusions

In chapter three of this thesis, single-walled carbon nanotubes are studied. Zigzag and armchair structures are considered and effects of different combinations of boundary

conditions are investigated. Static analysis as well as free and forced vibrational analyses is explored. Presented below is a list of main conclusions of this chapter:

- Static analysis of different sizes and atomic structures of single-walled carbon nanotubes shows that zigzag structure has generally higher Young's modulus of elasticity than the armchair case. In both cases, it is near 1 TPa.
- From the free vibration analysis, it is found that bending, torsional and extensional modes appear together in all cases. Different types are identified by the mode shapes. Modes with deformations along the cross section are also observed.
- While bending, torsional, extensional and cross sectional waved modes are decoupled in zigzag tubes, modes show coupled trend in armchair tubes because of weaker cross sectional stiffness than the zigzag tubes.
- Forced vibration analyses of same tubes are also performed and frequency spectra are calculated by FFT and plotted for each case. Based on the specific loading condition in each case, corresponding natural frequencies are obtained. Results are in perfect match with free vibration analysis. Forced vibration is recommended as an easy and straightforward method to identify different categories of mode shapes.

In chapters four and five, attempts are made to find equivalent Young's modulus of single-layered graphenes using the static analyses. Two different loading conditions are applied. Consequently, two different values are reported for in-plane and out-of-plane Young's modulus. These values are later used in plane-stress and plate theories to model the behaviors of graphenes. Below is a list of conclusions that are made in this chapter:

- Static analysis of rectangular single-layered graphenes of different sizes and boundary conditions provides two values of Young's modulus for in-plane and out-of-plane modes. They are 1.03 and 0.112 TPa respectively.

- Densities of different sizes of graphene sheets are calculated. It is found that density converges to 2250 Kg.m^{-3} as the size of the sheet increases.
- Using these values of Young's moduli along with realistic thickness of 0.34 nm and Poisson ratio of 0.16 in plate theory and plane-stress problems respectively, natural frequencies and modes shapes of rectangular sheets are obtained.
- In-plane and out-of-plane mode of vibrations are found to be completely decoupled.
- Results are compared with lattice structure method for different boundary conditions and for higher modes of vibration for rectangular sheets. Natural frequencies matched perfectly even for very high modes of vibration.
- As the size of the graphene sheet increases, results become closer and closer to the lattice structure method.
- Skewed and circular graphene sheets are also studied to show the effectiveness of the Young's moduli obtained from rectangular sheets. Results are impressive and verify the correctness and effectiveness of the proposed properties.

In chapter six, modeling of the van der Waals interactions between two layers of carbon atoms is investigated. Instead of modeling these forces using the nonlinear truss elements as done by other researchers, here a new technique has been introduced. The van der Waals interactions are modeled as force components in the load vector with complete nonlinear effects. This method turned out to be much faster and has less complication compared to the previous methods proposed by others. A modified direct integration method is introduced to solve the forced vibration problem. In-plane and out-of-plane forced vibrations are studied and frequency spectra are obtained. Author draws the following conclusions from this chapter.

- Very fast and efficient procedure is obtained for modeling the van der Waals interactions by placing them as force components in the load vector.

- Newmark's direct integration method is modified accordingly in order to address the nonlinearity of the load vector.
- In-plane and out-of-plane vibration of double-layered graphene sheets are studied. Results show the existence of peaks at higher frequencies in the frequency spectra of out-of-plane vibration in addition to the natural frequencies of the single layer graphene. These peaks are fairly close to the natural frequencies of single-layered graphene sheets of same size and boundary conditions.
- Van der Waals forces cancel the effects of each other in the in-plane condition due to the symmetry. These interactions do not affect the in-plane vibration of double-layered graphenes. Each layer vibrates independently with its own natural frequencies.

7.3. Contributions

The following points summarize the main contributions made in the thesis:

- After a comprehensive literature review, systematic shortfalls and advantageous of each modeling technique are distinguished.
- In-house codes are developed in C++ environment to generate complex geometry of carbon nano-structures and to solve various algorithms of static analyses and free and forced vibrations.
- Different categories of mode shapes are identified and plotted for zigzag and armchair atomic structures.
- Forced vibration method is applied and different categories of mode shapes based on the loading condition are identified.
- Dependency of vibrational and mechanical characteristics of single-walled carbon nanotubes on their atomic structure is extensively studied and shown.

- Mechanical properties of single-layered graphene sheets are obtained and systematic procedures are provided for modeling graphenes by continuous field theories.
- An efficient and straightforward technique is provided for modeling the van der Waals interactions. These are directly derived from the Lennard Jones 6-12 potential function and directly used without simplifications.
- Newmark's direct integration method is modified to accommodate the complex nonlinear force vector in the equation of motion.
- In-plane and out-of-plane vibrational characteristics of single and double-layered graphene sheets are studied in detail.

To this end, all the objectives set in the beginning of this research study have been met. However, the complicated area of nano-structures has the potential of much deeper research and still many unsolved issues that need special attention, exist. In the next section, some of the major areas of future research is suggested.

7.4. Future works

The author believes that the lattice structure method which is used in this thesis can be applied with confidence to study the mechanical and vibrational behaviors of nano-composites. Either carbon nanotubes or graphene sheets have been used as high strength fibers in nano-composites during the recent years. Nonlinear interactions between resin and fibers in composite structures can be modeled using techniques proposed in this thesis and hopefully some sort of trends and relations can be developed for mechanical properties and vibrational characteristics of nano-composites.

Moreover, other structural problems such as buckling of the tubes and sheets and post-buckling behaviors can be analyzed using the lattice structure method and applicability of the equivalent plate model recommended in this thesis can be verified. Since two values are reported here for in-plane and out-of-plane behaviors of graphenes, simulation of

post-buckling behaviors of graphene sheets using the continuous theories might be challenging and leads to counter-intuitive results.

Since beam theories are favorable models for representing carbon nanotubes' behaviors, other interesting research topic for possible future works might deal with finding equivalent Young's modulus of the beam in the bending load condition. According to the author's literature reviews, researchers mostly use static extensional analyses to find equivalent mechanical properties of the beam structure. However, as it is shown in this thesis, bending and extensional properties of nano-structures might be quite different. This study might lead to very novel results which simplify the complicated behaviors of carbon nanotubes.

As shown in this thesis, graphene sheets tend to behave like a continuous field when their mechanical and vibrational characteristics are studied. In this thesis, author reported two different Young's moduli values and use of plane stress and plate theories are recommended for simulating in-plane and out-of-plane behaviors of graphenes. Despite the simplicity of this method, the fact of reporting two different Young's moduli for a single structure is still unfavorable. Author strongly believes that by considering polynomial, Bezier or NURBS displacement fields, one simpler element can be introduced in finite element method that includes all properties of the graphene in a single stiffness matrix while reduces number of degrees of freedom significantly.

APPENDIX

This thesis is written in integrated format and each chapter is a standalone article. Papers are published in technical journals. Permissions have been granted to the author to include the articles in this thesis. Copyright permissions are brought in this appendix.

A.1. Permission for chapter 2: Vibration of carbon nanoscale structures: a critical review

A version of this chapter is published in the Computational Technology Reviews as: Singh, A. V., and Arghavan, S., 2010, "Vibration of carbon nanoscale structures: a critical review," Computational Technology Reviews, 1, pp. 281-314.

Dear Sir

Permission is granted for you to reproduce parts of this paper in your thesis provided you make appropriate acknowledgement to the original paper:

A.V. Singh, S. Arghavan, "Vibrations of Carbon Nanoscale Structures: A Critical Review", Computational Technology Reviews, vol. 1, pp. 281-314, 2010.
doi:10.4203/ctr.1.10

Best wishes with the defence of your thesis.

Kind regards

A.2. Permission for chapter 3: On the vibrations of single-walled carbon nanotubes

A version of this chapter is published in the Journal of Sounds and Vibration as: Arghavan, S., and Singh, A. V., 2011, "On the vibrations of single-walled carbon nanotubes," Journal of Sounds and Vibration, 330(13), pp. 3102-3122.

This is a License Agreement between Sina Arghavan ("You") and Elsevier ("Elsevier"). The license consists of your order details, the terms and conditions provided by Elsevier, and the payment terms and conditions.

License Number	2843790255785
License date	Feb 07, 2012
Licensed content publisher	Elsevier
Licensed content publication	Journal of Sound and Vibration
Licensed content title	On the vibrations of single-walled carbon nanotubes
Licensed content author	S. Arghavan,A.V. Singh
Licensed content date	20 June 2011
Licensed content volume number	330
Licensed content issue number	13
Number of pages	21
Type of Use	reuse in a thesis/dissertation
Portion	full article
Format	both print and electronic
Are you the author of this Elsevier article?	Yes
Will you be translating?	No
Order reference number	None
Title of your thesis/dissertation	Vibration of Carbon Nano-Structures
Expected completion date	Apr 2012
Estimated size (number of pages)	140
Elsevier VAT number	GB 494 6272 12
Permissions price	0.00 USD
VAT/Local Sales Tax	0.0 USD / 0.0 GBP
Total	0.00 USD

A.3. Permission for chapter 4: Mechanical properties and vibrational characteristics of graphenes

A version of this chapter is published in the Journal of Applied Physics as: Arghavan, S., and Singh, A. V., 2011, "Atomic lattice structure and continuum plate theories for the vibrational characteristics of graphenes," Journal of Applied Physics, 110(8).

Dear Dr. Arghavan:

Thank you for requesting permission to reproduce material from American Institute of Physics publications.

Permission is granted – subject to the conditions outlined below – for the following:

J. Appl. Phys. 110, 084308 (2011)

To be used in the following manner:

Included as part of your thesis.

1. The American Institute of Physics grants you non-exclusive world rights in all languages and media.
2. This permission extends to all subsequent and future editions of the new work.
3. The following copyright notice must appear with the material (please fill in the information indicated by capital letters): "Reprinted with permission from [FULL CITATION]. Copyright [PUBLICATION YEAR], American Institute of Physics."
Full citation format is as follows: Author names, journal title, Vol. #, Page #, (Year of publication).
For an article, the copyright notice must be printed on the first page of the article or book chapter. For figures, photographs, covers, or tables, the notice may appear with the material, in a footnote, or in the reference list.
4. This permission does not apply to any materials credited to sources other than the copyright holder.

Please let us know if you have any questions.

Sincerely,

A.4. Permission for chapter 5: Free vibration of single-layered graphene sheets: lattice structure versus continuum plate theories

A version of this chapter is published in the Journal of Nanotechnology in Engineering and Medicine as: Arghavan, S., and Singh, A. V., 2011, "Free vibration of single layer graphene sheets: lattice structure versus continuum plate theories," Journal of Nanotechnology in Engineering and Medicine, 2(3).

Dear Mr. Arghavan,

It is our pleasure to grant you permission to use ASME paper "Free Vibration of Single Layer Graphene Sheets: Lattice Structure Versus Continuum Plate Theories," by S. Arghavan and A. V. Singh, Journal of Nanotechnology in Engineering and Medicine, Volume 2, 2011, cited in your letter for inclusion in a publication entitled Vibration of Carbon Nano-Structures to be published by Library and Archives Canada and ProQuest/UMI.

As is customary, we ask that you ensure full acknowledgment of this material, the author(s), source and ASME as original publisher on all printed copies being distributed.

Many thanks for your interest in ASME publications.

Sincerely,

CURRICULUM VITAE

Name	Sina Arghavan
Place of Birth	Shiraz, Iran
Year of Birth	1984
Degrees	Shiraz University Shiraz, Iran 2002-2006 Bachelor of Science
	Shiraz University Shiraz, Iran 2006-2008 Master of Science
	The University of Western Ontario London ON, Canada 2008-2012 Doctor of Philosophy

Publications:

Arghavan, S., and Singh, A. V., 2012, "Nonlinear vibration of multi-layered graphene sheets," *Journal of Physics D: Applied Physics*, Submitted.

Arghavan, S., and Singh, A. V., 2011, "Free vibration of single layer graphene sheets: lattice structure versus continuum plate theories," *Journal of Nanotechnology in Engineering and Medicine*, 2(3).

Arghavan, S., and Singh, A. V., 2011, "Atomic lattice structure and continuum plate theories for the vibrational characteristics of graphenes," *Journal of Applied Physics*, 110(8).

Arghavan, S., and Singh, A. V., 2011, "On the vibrations of single-walled carbon nanotubes," *Journal of Sounds and Vibration*, 330(13), pp. 3102-3122.

Singh, A. V., and Arghavan, S., 2010, "Vibrations of carbon nanoscale structures: a critical review," *Computational Technology Review*, 1, pp. 281-314.

Doostfatemeh, A., Hematiyan, M. R., and Arghavan, S., 2009, "Closed-form approximate formulas for torsional analysis of hollow tubes with straight and circular edges," *Journal of Mechanic*, 25(4), pp. 401-409.

Arghavan, S., and Hematiyan, M. R., 2009, "Torsion of functionally graded hollow tubes," *European Journal of Mechanics - A/Solids*, 28(3), pp. 551-559.